Elsevier Editorial System(tm) for Marine Geology
Manuscript Draft

Manuscript Number: MARGO5079R1

Title: Approaching the seismogenic source of the Calabria 8 September 1905 earthquake: New geophysical, geological and biochemical data from the S. Eufemia Gulf (S Italy)

Article Type: Research Paper

Keywords: seismogenic source, earthquake, seismotectonics, prokaryotes, Calabrian Arc

Corresponding Author: Dr. Maria Filomena Loreto, Ph.D.

Corresponding Author's Institution: Institute of Marine Sciences - CNR

First Author: Maria F Loreto, Ph.D.

Order of Authors: Maria F Loreto, Ph.D.; Maria F Loreto, Ph.D.; Umberto Fracassi, Ph.D.; Annalisa Franzo, Dr.; Paola Del Negro, Dr.; Fabrizio Zgur, Ph.D.

Approaching the ~~potential~~ seismogenic source of the Calabria 8 September 1905 earthquake: New geophysical, geological and biochemical data from the S. Eufemia Gulf (S Italy)

Maria Filomena Loreto[1,2,*], Umberto Fracassi[3], Annalisa Franzo[2,4], Paola Del Negro[2], Fabrizio Zgur[2] and Lorenzo Facchin[2]

[1] Istituto di Scienze Marine – Consiglio Nazionale delle Ricerche, U.O.S. Bologna, Via Gobetti 101, 40129 Bologna, Italy

[2] Istituto Nazionale di Oceanografia e di Geofisica Sperimentale, Borgo Grotta Gigante 42/C, 34010 Sgonico (TS), Italy

[3] Istituto Nazionale di Geofisica e Vulcanologia, Via di Vigna Murata 605, 00143 Roma, Italy

[4] Dipartimento di Science della Vita, Università degli Studi di Trieste, 34127, Trieste, Italy

* Corresponding author: filomena.loreto@bo.ismar.cnr.it; +390516398878; ISMAR-CNR Via Gobetti 101 - 40129 Bologna.

Abstract

Recognizing the seismogenic source of major historical earthquakes, particularly when these have occurred offshore, is a long-standing issue across the Mediterranean Sea and elsewhere. The destructive ~~The~~ earthquake (M ~7) that struck western Calabria (southern Italy) ~~occurred~~ on the night of 8 September 1905 is one such case ~~is one of the strongest events that ever affected western Calabria. . This event caused 557 casualties, more than 2000 injured, and left about 300,000 people homeless. The mainshock was followed by a feeble tsunami and hundreds of aftershocks. During the last 15 years,~~ having various authors ~~proposed hypotheses~~proposed a ~~for a~~ seismogenic source~~s~~ ~~causative of the 1905 earthquake~~, with apparently diverse hypotheses and without ~~an~~ achieving a ~~unequivocal~~unique solution. ~~To study the active tectonics of the region and t~~To gain novel~~n~~ insight into ~~a potential seismogenic source responsible~~the crustal volume where ~~for the 1905~~~~this event~~the

1905 earthquake took place and to seek a more robust solution for the seismogenic source associated with this destructive event, we carried out a well-targeted multidisciplinary survey within the Gulf of S. Eufemia (SE Tyrrhenian Sea), ~~(summer 2010) in the frame of the ISTEGE project, using the R/V OGS *Explora*. The acquired dataset consists of~~collecting geophysical data, oceanographic~~al~~ measurements, and biological, chemical and sedimentary samples.

~~The analysis of the geophysical data~~ We identified ~~(330 km of MultiChannel Seismic, 2223 km of sub-bottom Chirp profiles, and 2231 km^2 of high resolution morpho-bathymetric data) allowed the identification of some main morpho-structural features characterizing the sedimentary basin hosted within the S. Eufemia Gulf. The~~ three main tectonic ~~structures~~features ~~shaping~~ affecting the sedimentary basin in the Gulf of S. Eufemia~~, and its sedimentary bodies are~~: 1) a NE-SW striking, ca. 13-km-long, normal fault,~~n~~ here named S. Eufemia Fault~~E-dipping large-normal fault, N31° oriented~~; 2) a WNW-~~trending~~ striking polyphased fault system; and 3) a likely E-W trending lineament~~-fault with dip-slip motion~~. Among these, the ~~large~~ normal fault shows evidence of activity~~, as~~ witnessed by the deformed recent sediments~~,~~ and by ~~the~~ its ~~lineament due to consistent~~ seabed rupture ~~observed on the seafloor~~ along which, locally, fluid~~s~~ leakage occurs. ~~Finally,~~ Features in agreement with the ~~evidence of probable geothermal activity is reflected by the~~ anomalous distribution of prokaryotic abundance and biopolymeric C content, resulted from the shallow sediments analyses~~, whereas no such evidence comes from water temperature analysis (CTD measurements)~~.

The ~~various~~ numerous seismogenic sources proposed in the literature during the past 15 years make up a composite framework of this sector of western Calabria, ~~and can b~~that we ~~reviewed~~ tested against a) ~~in the light of~~ the geological evidence ~~arising~~ from the newly acquired ~~multidisciplinary~~ dataset, and b) the ~~against~~ regional seismotectonic models. Such assessment ~~with surprising results~~allows us to propose the NE-SW striking normal fault as the most probable candidate for the seismogenic source of the 1905 earthquake. Re-appraising ~~such~~ a major historical earthquake~~s~~ as the 1905 one ~~one located within poorly explored submarine areas, promisingly~~

Formatted: Not Highlight

enhances the seismotectonic picture of western Calabria. ~~A comprehensive~~Further understanding of the region and better ~~robust constraining of th~~constraining the location of the ~~e~~ seismogenic source ~~of the 1905 earthquake~~ may ~~arise from an~~be attained through integrated interpretation of our data together with a) on-land field evidence, and b) seismological modeling.

Keywords: seismogenic source, earthquake, seismotectonics, prokaryotes, Calabrian Arc

1. Introduction

Calabria is one of the Italian regions ~~showing~~ with ~~a very high seismicity rate (Fig. 1; Gasparini et al., 1982; Castello et al., 2006; Calò et al., 2012),~~ ~~major~~the largest concentration of seismic moment release (Fig. 1; Gasparini et al., 1982; Westaway, 1992; Castello et al., 2006; Calò et al., 2012~~Westaway, 1992~~), and highest probability of occurrence of major earthquakes (Rotondi, 2010), mainly located between two main shear zones, the Tindari Fault ~~(TF),~~ to the south-west, and the Cirò-Benevento Fault ~~(CBF) Zones (Fig. 1)~~ to the north. Most earthquakes affecting ~~the~~ Calabria and its western offshore~~n Arc~~ are characterized by a normal fault plane solution (D'Agostino and Selvaggi, 2004; Vannucci and Gasperini, 2004), ~~describing~~ confined within a continuous extensional belt parallel to the Calabrian Arc.

The earthquake that struck western Calabria on the night of 8 September 1905 is ~~can be considered as~~ one of the strongest events ~~of~~ in the Italian catalogue (M_w up to 7.5, according to Michelini et al., 2006)~~.~~ ~~-~~ b~~B~~esides the 28 December 1908 earthquake (M_w 7.1), that struck southern Calabria and the ~~the~~ Messina Straits, ~~the 1905 event is one of the catastrophic earthquakes (M_w > 6.5) that, together with~~ and the numerous ones occurred ~~during 1638 and 1783~~in the 17th and 18th century, that severely ~~devastated~~ hit large parts of the ~~Calabria~~ region ~~-~~(Postpischl, 1985; Boschi et al., 2000; Guidoboni et al., 2007). The 1905~~is~~ earthquake caused 557 ~~victims~~ deaths (Baratta,

Formatted: Font: 11 pt

Formatted: Superscript

Formatted: Superscript

1906), most of them around the Capo Vaticano ~~Promontory~~promontory, with the highest intensity values (Mercalli-Cancani-Sieberg = XI) recorded between the towns of Tropea, to the west, and Vibo Valentia, to the east (Fig. 2; Tiberti et al., 2006). ~~This earthquake injured more than 2000 people, and left 300,000 inhabitants homeless (Boschi et al., 2000; Guidoboni et al., 2007).~~ Historical documents reported ~~S~~several triggered ground failures~~environmental effects were recorded in coeval sources, including ground effects~~ (landslides, rock falls and lateral spreads), hydrological changes (stream-flow variations, liquefaction, rise of water temperature and turbidity), and earthquake "*lights*" and "*sounds*" (Guidoboni et al., 2007; Tertulliani and Cucci, 2008, 2009). Finally, a tsunami, ~~if~~ albeit modest, was reported by contemporary observers both in the open sea and along the coast of the ~~Sant'Eufemia (~~S. Eufemia~~, hereafter)~~ Gulf ~~(SE Tyrrhenian Sea)~~ (see blue small waves in Fig. 2), with few meters of maximum run-up and sea flooding in some beaches up to 30 m (Tinti and Maramai, 1996 and references therein; Guidoboni and Ebel, 2009; NGDC/WDC, 2012).~~-~~

Although this earthquake ~~can be~~ is ~~considered~~ one of the most catastrophic ones recorded in the region, ~~its age and the~~ poor documentation resulting from this early 20th century ~~earthquake~~event has ~~have long~~ caused it to go relatively overlooked and not fully ~~constrained~~ understood in terms of magnitude and epicentral location. Uncertain M estimates, particularly when so diverging among each other, and dubious location, especially when the latter is at sea, make earthquake assessment all the more problematic. Together with the underlying geology, these are among the primary ingredients to search the seismogenic source (i.e., the causative fault) of a damaging earthquake, to ultimately enhance the seismic hazard pattern of a given region. ~~-~~To address these issues and to ~~accrue~~ build on the knowledge ~~concerning~~ of the seismotectonic framework and the seismogenic potential of ~~the~~ western Calabria~~region~~, we performed a well-targeted multidisciplinary survey during the summer of 2010 in the S. Eufemia Gulf (gray transparent square in Fig. 1) aboard the R/V OGS-*Explora*. ~~The new acquired multidisciplinary dataset provided us with promising, unexpected results.~~ Biological and geochemical data, collected

Formatted: Superscript

Formatted: Font: Italic

to detect hydrothermal activity of potential seismotectonic relevance, ~~Combining~~ and ~~the~~ evidence stemming from the analysis of geophysical data (m~~M~~ulti~~c~~C~~h~~annel s~~S~~eismic - MCS~~)~~, sub-bottom ~~Chirp~~ profiles - Chirp and~~,~~ high resolution morpho-bathymetry) ~~and biological and geochemical data,~~ allowed us ~~we here~~to propose a ~~solution for a potential seismogenic~~ causative source ~~causative of~~for the 1905 earthquake, while reappraising previously proposed solutions in the light of the new geological evidence.

2. Geological and seismotectonic framework

2.1 Geological Setting

~~Our study area, the~~ The S. Eufemia Gulf~~,~~ lies between the Calabrian Arc and the SE Tyrrhenian Basin ~~and the Calabrian arc~~ (Fig. 1), which ~~. The Tyrrhenian Basin~~ is the~~a~~ Neogene back-arc basin ~~formed west~~ of the Apennines subduction system ~~of the Apennines thrust belt~~ (Patacca et al., 1990, 1993, 2004, and references therein). Subduction migrated eastward from the Tortonian to Early Pliocene, and south-eastward from the Late Pliocene to Early Pleistocene (Patacca et al., 1990; Sartori, 2003). ~~Interaction between the migrating system and the buoyant lithosphere of the Apulian and Pelagian foreland caused: 1) the slow-down of subduction along the central Apennines, and 2) the switching direction in the opening of the back-arc basin (Argnani and Savelli, 1999; Sartori, 2003).~~

The Calabrian arc (Fig. 1) is an independent arcuate continental block (~~Calabria-Peloritani Terrane;~~ Bonardi et al., 2001) that bridges the NW-SE trending southern Apennines with the SSW-NNE ~~-~~trending Apennines in Sicily. Several authors have considered the Calabrian arc as an uprooted fragment of the Alpine belt (e.g., Amodio-Morelli et al., 1976; Malinverno and Ryan, 1986; v~~V~~an Dijk et al., 2000 and references therein). Its arcuate shape can be attributed to the diachronous collision of the Apennine chain with the Apulian foreland, to the north, and ~~of the~~with

Formatted: Not Highlight

the ~~Pelagian~~ Hyblean foreland~~block~~, to the south (Malinverno and Ryan, 1986; v~~V~~an Dijk et al., 2000). ~~These p~~~~Processes~~Such collision also controlled (1~~i~~) the clockwise rotation~~s~~ of Sicily and Calabria, (~~ii~~2) the counter-clockwise rotation of the southern Apennines (Cifelli et al., 2007), that ceased at the end of the Pleistocene ~~in Calabria ceased during the end of the Pleistocene~~ (Mattei et al., 2007), and (~~iii~~3) the intense fragmentation of the Calabrian Arc in NW-SE strik~~trend~~ing blocks (Knott and Turco, 1991; v~~V~~an Dijk, 1991, 1992; Del Ben et al., 2008; Barone at al., 2008). Since the M~~m~~iddle ~~-~~Pleistocene, the Calabrian Arc experienced rapid uplift of up to ~~about~~ ca. 1 mm/y (Westaway, 1993; Bordoni and Valensise, 1998; Anzidei et al., 2012) and a ESE-trending forearc advancement, ~~of the forearc~~ shown by GPS data (D'Agostino et al., 2011; Devoti et al., 2011). Uplift was in part accommodated ~~locally by repeated displacement along the~~ by major ~~active, mainly~~ normal faults (Monaco and Tortorici, 2000; Catalano et al., 2003), frequently bounded by NW-SE strik~~trend~~ing shear zones (Fig. 1; van Dijk, 1991; Tansi et al., 2007). ~~GPS vectors show a ESE forearc advancement (D'Agostino et al., 2011; Devoti et al., 2011).~~

The ~~S. Eufemia~~sedimentary ~~sub~~ basin~~,~~ hosted by the S. Eufemia Gulf ~~corresponding to the southern part of the large Paola Basin (Fig. 2),~~ is bounded by the Capo Vaticano ~~Promontory~~promontory to the south, by the Calabrian ~~Arc~~ landmass to the east, and by the steep submarine slope ~~that leaves room~~extending to the Marsili abyssal plain to the west (~~see~~ Figs. 1 and 2). The S. Eufemia ~~sub~~ basin is filled by a ca. 2~~-~~km~~-~~thick, Plio-Quaternary ~~sedimentary~~ sequence, overlying intensely deformed Miocene units (Argnani and Trincardi, 1993; Milia et al., 2009; Loreto et al., 2012). ~~Within t~~The S. Eufemia ~~and the Paola~~ slope basin~~s, considered by~~ (~~-~~Argnani and Trincardi; ~~(~~1993) ~~as slope basins,~~ include~~s~~ several turbiditic, large mass-failure and drape deposits~~-~~ (Trincardi et al.,~~:~~1995). Finally, Milia et al. (2009) identified a sub-vertical fault system showing a polyphased history, ~~(including fault inversion)~~ coeval with the early N-S extensional phase~~, that gave rise to the Paola basin and the S. Eufemia sub-basin.~~

2.2 Seismogenic source models of the 1905 earthquake

Formatted: Not Highlight

Formatted: Not Highlight

Formatted: Highlight

Numerous epicentral locations and M_w estimates of the 8 September 1905 earthquake have been proposed in the literature. According to Rizzo (1906), Boschi et al. (2000), and Guidoboni et al. (2007), the epicenter of the ~~1905~~ earthquake was onshore (Fig. 2), whereas ~~locations by~~ Riuscetti and Schick (1975), Camassi and Stucchi (1997), Michelini et al. (2006), and a recent macroseismic ~~one~~ study by Rovida et al. (2011) all place the epicenter offshore (Fig. 2). Assigned ~~M~~magnitudes ~~values~~ range from instrumental estimates ~~at 7.3 (Mulargia et al., 1984) and~~ of~~at~~ M 7.0 (Martini and Scarpa, 1982) and M 7.5 (Michelini et al., 2006), to the macroseismic ones ~~at~~ of M 6.7 (Guidoboni et al., 2007), M 7.0 (Gruppo di Lavoro CPTI04, 2004; Rovida et al., 2011) and M 7.1 (Postpischl, 1985).

Over the ~~last~~ past 15 years, various researchers hypothesized a possible~~tential~~ seismogenic source responsible for the 1905 earthquake (see Table 1, Fig. 3~~2~~). ~~Perhaps~~ Peruzza et al. (1997) ~~the first attempt to~~ presented the first~~a~~ seismotectonic model for ~~some of~~ the largest Calabrian earthquakes ~~was that of Peruzza et al. (1997), . These authors~~ proposinged a segmentation model ~~and~~ with large normal faults sub-parallel to the extensional axis of ~~the~~ western Calabria~~n arc~~. ~~Source models included key parameters and, f~~For the 1905 earthquake case, ~~Peruzza et al. (1997)~~these authors ~~proposed~~ maintained an E-dipping, NNE-SSW ~~trending~~ striking source (PE in Fig. 3), ~~, onland yet along shore, using~~based on an onshore epicenter. Monaco and Tortorici (2000) presented a seismotectonic model of the Calabrian Arc and eastern Sicily and proposed causative faults for key destructive earthquakes. For the 1905 event ~~(Fig. 2)~~, these authors ~~proposed~~ hypothesized the Capo Vaticano Fault, a NW-dipping, NE-SW strik~~trend~~ing normal fault (MT in Fig. 3), ~~along the NE shore of the Capo Vaticano Promontory, using~~with an offshore epicenter.

Valensise and Pantosti (2001b) presented a regional seismogenic source model and proposed a ~~large~~40-km-long, SE-dipping, NE ~~SW~~ striking~~trending~~ normal fault ~~affecting~~ near the edge of the S. Eufemia Gulf (VP in Fig. 3), ~~and extending on land~~the northern sector of the Capo Vaticano Promontory and the S. Eufemia Plain. Searching for an explanatory source of the tsunami ~~caused~~ associated with~~by~~ the 1905 earthquake, Piatanesi and Tinti (2002) ~~took into account and~~

parameterized the Capo Vaticano and the Vibo Valentia faults (Monaco and Tortorici, 2000), two NW-dipping, NE-SW ~~oriented~~ striking normal faults ~~proposed by Monaco and Tortorici (2000) that~~ straddling~~affect~~ the northern shore of the Capo Vaticano promontory and the internal sector of the gulf ~~and the shore of the Capo Vaticano Promontory~~ (CV and VV in Fig. ~~2~~3; Table 1). Finally, Cucci and Tertulliani (2006; 2010) suggested the Coccorino Fault, a ~~large~~ 29-km-long S-dipping, WNW-ESE ~~trending~~ striking normal fault ~~affecting the southern sector of~~~~in~~affecting the southern sector of the Capo Vaticano ~~Promontory~~promontory and the northern ~~portion of the~~ Gioia Tauro Plain (CT in Fig. ~~2~~3).

3. ~~Acquired d~~Data and Methods

3.1 Geophysical data

~~The present study is based on MultiChannel Seismic (MCS), very high resolution seismic data (Chirp profiles) morpho bathymetric, biological, chemical, and oceanographic data (Fig. 4).~~ Nine ~~MCS~~ multichannel seismic profiles, organized in a tight grid (thin yellow lines in Fig. 4)~~,~~ were acquired using a 1500~~ -~~m~~ -~~long streamer cable, with a 120~~ -~~channels array and a 12.5 m trace interval. The energy source consisted of two GI-guns with a total volume of 8 liters sho~~o~~ting every 25 m~~,~~, ~~and the~~with a resulting seismic coverage ~~is~~ of 30 for each investigated depth point. ~~During the acquisition low cut (3 Hz) and high cut (anti alias) filters were applied.~~ The seismic data were processed following a standard procedure, in order to get post-stack time migrated seismic sections~~;~~ ~~SRME technique was applied to improve signal quality and to attenuate the multiple signal~~. More details about acquisition parameters and processing performed to improve Signal/Noise ratio can be found in Loreto et al. (2012).

More than 2200 km of s~~S~~ub~~ -~~b~~B~~ottom ~~Chirp~~ p~~P~~rofiles (Chirp) were acquired using a Benthos CAP-6600, consisting of 16 keel mounted transducers~~ keel mounted~~. Sweep ranges between 2 and 7 kHz, with the resulting configuraton ensuring a full ocean depth investigation.

Chirp data image in detail the ~~shallower~~ uppermost section of the sedimentary cover ~~from the seafloor to~~down to a ~~maximum~~ca. ~~depth of~~ 75 m depth, assuming a constant ~~sound speed of about~~ 1550 m/s sound speed within the shallowest sediments.

The high resolution morpho-bathymetric map (Fig. 4) was obtained using two hull mounted m~~M~~ultib~~B~~eam echosounders, ~~(MBES):~~ a Reson Seabat 8111 (100 kHz) , ~~,~~and ~~a Reson Seabat~~ 8150 (12 k~~K~~Hz). We employed ~~T~~the Seabat 8111 up to 400 m depth ~~, reaching the maximum swath width~~ (maximum swath width of 7.4 times the water depth), ~~) and working in less than 150 m of water, was used in waters up to 400 m deep. On the other hand,~~ the Seabat 8150~~, used within~~for water depth ~~greater~~ >~~than~~ 500 m~~, has a~~ (maximum swath width of 4.5 times the water depth), and both echosounders for the 400-500 m depth range. ~~Finally,~~ The data were processed to remove spikes due to navigation system problems and/or to the acquisition system.

3.2 Chemical, ~~B~~biological and ~~O~~oceanographic data

We collected 12 biological samples (white triangles in Figs. 4), at the top of gravity cores using a sterile spoon and frozen at -20 °C, and performed 10 CTD (Conductivity-Temperature-Depth) profile measurements in the sector near the tectonic features recognized in the multichannel data. ~~loser to the area of maximum damage caused by the 1905 earthquake (white triangles in Fig. 4). Small quantities of sediment, taken at the seafloor, were sampled at the top of the 12 gravity cores.~~ These samples were used to evaluate prokaryotic abundance, and to perform Total Carbon (TC), Total Nitrogen (TN), and Total Organic Carbon (TOC) chemical analyses. ~~On board, sediment samples were collected using a sterile spoon and immediately frozen at -20 °C.~~

For ~~Total Carbon (~~TC~~)~~, ~~Total Nitrogen (~~TN~~)~~ and ~~Total Organic Carbon (~~TOC~~)~~ analyses, triplicate sub-samples of homogenized and freeze-dried sediment (< 250 µm) were weighed directly in capsules (5x9 mm). Before the TOC determination, sub-samples were treated with increasing concentrations of HCl (0.1N and 1N) to remove carbonates, following the procedure by Nieuwenhuize et al. (1994). Carbon and nitrogen were determined using a CHNO-S elemental

analyzer according to the methods of Pella and Colombo (1973) and Sharp (1974). Sub-samples of homogenized sediment were freeze-dried and processed to determine carbohydrates, lipids, and proteins following the procedure described by Cibic et al. (2008). The sum of carbohydrates, lipids and proteins carbon was referred to as Biopolymeric Carbon (BPC).

Prokaryotic abundance was determined using the centrifugation method by Ravenschlag et al. (2000) and a modified protocol by Lunau et al. (2005). Sediment samples were diluted to a final concentration of 1:110 and filtered on black Nuclepore polycarbonate 0.2-µm-pore-size filters. Filters were mounted on microscope slides, stained with a SYBR Green I-mounting medium Mowiol solution (1:15) and counted by epifluorescence microscopy (LEICA DM2500) at 1000 X magnification under a blue filter set (BP 450-490 nm, BA 515). A minimum of 300 cells were accounted for each filter in at least 40 randomly selected fields.

The CTD measurements are done using the sSea-bBird eElectronics (SBE) 911plus system with sensors mounted on the Carousel SBE32 frame with 12 Niskin bottles. The We measured parameters are: Pressure (db), ; Conductivity (mS/cm); Temperature (°C); Oxygen (uA0); Fluorescence (ug/l); and optical backscatter, with a 10^{-3} accuracy. Lacking a high accuracy altimeter, the last measurement was done at about ca. 10 m from the seafloor to avoid problems of interaction with the seafloor morphology.

4. Results

4.1 Morphological Morpho-bathymetric features

The Our high resolution morpho-bathymetric map data of the S. Eufemia Gulf (Fig. 4) allowed us to identify some mainkey elementsfeatures: 1) a large submarine Angitola canyon, –already knownshown by Argnani and Trincardi (1988) as Angitola Channel (Gamberi and Marani, 2004), characterized in the internal near-shore part of the gulf by an unusually straight trend, ca. ENE-WSW oriented for about 20 km, and in the external distal part by a meandering trend; 2) a NW-SE

oriented morpho-structural high (hereafter: MS-High) ~~located~~ offshore the town of Tropea, recognized as the seaward prolongation of the Capo Vaticano ~~p~~promontory, ~~and~~ surrounded by several slide scars (Loreto et al., 2012). However, ~~A~~ a more detailed analysis (Fig. 5) allowed us to identify other noteworthy ~~morphological~~ features, ~~located~~ between the northern internal slope of the gulf and the Angitola Channel, ~~like incisions and~~such as small slides or slumps (see white thick arrows) and a ~~an evident~~prominent N31°~~E~~-trending, 3-m-high, ~~and~~ 8-km-long ~~morphological escarpment~~scarp. ~~Among the towns of Lamezia Terme and Briatico, the seafloor is affected by this morphological escarpment trending N31°~~ well visible across the 150-m ~~, as also highlighted by~~ contour line ~~at 150 m~~ (i.e., the shelf break; see inset in Fig. 5).

4.2 Tectonic features

~~The analysis of the multichannel seismic data allowed us to map new interesting tectonic features.~~

Seismic profile GSE10-05, NE-SW oriented (Fig. 4), shows a thick and well stratified sedimentary sequence ~~laying at the top of~~overlying a poorly reflective and poorly stratified ~~one~~ sequence (Fig. 6). Based on previous works (Argnani & Trincardi, 1993; Trincardi et al., 1995; Milia et al., 2009; Pepe et al., 2010) and on evidence from ~~deep~~ the Marisa industrial well ~~information~~(Figs. 4 and 7; ~~, Marisa well (Fig. 7) included in the open access~~ VI.D.E.PI. Project, (www.videpi.com), the ~~sedimentary~~ imaged sequence ~~can be constrained as~~probably is the Plio-Quaternary basin infill deposited on top of the Miocene, which correspond to the Messinian units. ~~The~~ Data from the Marisa well ~~information~~ lack~~s~~ the upper part from Pleistocene to present that could be associated with the uppermost, condensed ~~sediment~~ layer. ~~The Pliocene formation is composed mainly by silty claystones with local sandy intercalations laying in angular unconformity on top of the Messinian deposits. The Messinian top is covered by a thin layer of evaporites underlain by a thick conglomerates layer.~~ The boundary between the Miocene and Pliocene generates a strong acoustic contrast, due to lithology, seismically associated with a high amplitude horizon, ~~that~~ here ~~we call~~ defined Top Horizon.

The southern levee of the Angitola Channel (~~see~~ SL; Fig. 6~~, Box~~) shows a ~~morphological~~ scarp ~~about~~ 200 ms high~~,~~ ~~and corresponding~~ i.e. ~~to about~~ 150 m, assuming a fixed seismic water velocity of 1500 m/s. Sediments next to the levee show gentle folding (see black thick arrow) involving only the well-stratified Plio-Quaternary sequence~~, never affecting~~ leaving the Top Horizon undisturbed. Combined with these elements, t~~T~~he ~~morphological~~ straight trend of the Angitola Channel ~~(i.e., the straight trend) combined with these elements~~ leads us to hypothesize that a shallow ca. E-W striking fault (see AF? in Fig. 6, box and inset), with a likely ~~dip~~strike-slip motion, ~~probably controls~~ passively controls the edge of the channel ~~trend~~ (Loreto et al., 2012).

Plio-Quaternary sediments of the central basin (Fig. 6) are deformed by two gentle ~~and~~ wide anticlines, the main one controlled~~bounded~~ by the compressional phase of a SW-dipping fault ~~southwest-ward dipping~~. ~~The amount of deformation~~ Folding decreases with depth and~~-~~ fades out at mid-sequence ~~up to the null point~~ (see black dot). The underlying~~. Below the null point,~~ sediments thicken ~~forming~~ into a syn-rift sequence ~~deposited during~~ controlled by the extensional phase ~~activity~~ of the bordering fault. Assuming a constant seismic velocity of 2200 m/s for Plio-Quaternary sediments (Pepe et al., 2010; Marisa well ~~by VIDEPI project~~), we ~~calculated~~ estimate ~~an offset at~~ that the Top Horizon ~~of~~ is offset ca. 350 m ~~along a fault plane 58° SWS dipping~~ (see Trc num 61~~0~~50 in Fig. 6). We interpret such deformational style as due to a N93° striking Polyphased Fault (from here on, PF) and 58° SSW-dipping (Fig. 6, inset), visible in ~~Similar deformations are well identifiable only within~~ two seismic profiles (GSE10_04A and GSE10_05)~~, allowing us to define a major Polyphased Fault, N93° oriented and, based on the available data, 10 km long.~~ Up~~-~~ward, contraction~~al~~ ~~deformation~~ abruptly stops below a thick and chaotic body perching in stratigraphic unconformity (dotted line~~;) above the folded sediments (~~Fig. 8). ~~No sign of fault activity~~There is no evidence of surface rupture, such as a ~~morphological escarpment~~scarp~~,~~ ~~is identifiable at~~on the seafloor (Fig. 8, left), confirming that ~~this polyphased fault~~PF~~s~~ ~~system~~ is ~~fossilized,~~ sealed by the upper section of the Plio-Quaternary deposits.

The analysis of the E-W-striking GSE10_07 seismic profile (Figs. 4 and 9) allowed us to identify two main features: 1) ~~the incisions of the~~ the Angitola Channel~~, also here~~ characterized by steep and deep levees, to the west; and 2) a normal fault ~~affecting~~ extending through the whole imaged sedimen~~t~~nary ~~stack~~succession, to the east ~~including the Plio-Quaternary sequence and the Miocene units~~ (Fig. 9, Box). Discontinuities and deformations ~~affecting~~ of the Plio-Quaternary sediments, expressed as ~~the~~ gentle folds ~~at~~ in the foot-wall (thick white arrows) and small drag folds (thick black arrow) ~~at~~ in the hanging-wall ~~(Fig. 9, Box)~~, can be recognized within older ~~(deeper)~~ and recent sediments (Fig. 9, Box). ~~Moreover, t~~These folded and faulted recent deposits are well imaged on ~~the~~ Chirp profile CH_39 (Fig. 10B), acquired north of seismic profile GSE10_07, that crosses the ~~morphological escarpment well shown~~notable scarp on the high~~-~~-resolution morpho-bathymetric ~~map~~ data (Fig 5). Northward over the seafloor scarp zone, the discontinuities and deformations affect the shallow deposits without reaching the seafloor (see chirp profile CH_52 in Fig. 10C); farther north, the deformation of the recent sediments strongly decreases and only a weak, structurally-controlled offset is detectable (see chirp profile CH_71 in Fig. 10D). ~~-~~Combining evidence from all geophysical ~~observations~~ data (MCS, C~~c~~hirps, and bathymetry ~~data~~), we mapped a N31° trending ~~normal fault~~, 38° ESE-dipping, ca. 13-km-long normal fault ~~whose fault plane~~ rupturing~~res~~ the seafloor for about 8 km along strike (Figs. 9, Box and 10).

Assuming a constant seismic velocity of 2200 m/s for Plio-Quaternary sediments, the normal fault, that here we call~~ed~~ S. Eufemia Fault (Fig. 10), offsets the upper Miocene ~~unit~~ top ~~of ca.~~ about 460 m ~~and plunges southeast-ward with an estimated 38° angle~~. ~~The vertical offset along this fault and~~ Using ~~the commonly accepted~~ fault scaling relationships by ~~(Kanamori and Anderson, 1975;~~ Walsh and Watterson (1988~~;Wells and Coppersmith, 1994~~) to compute fault length from cumulative offset, we ~~lead us to believe~~ estimate that the S. Eufemia Fault length ranges from 20 to 30 km, ~~is~~ much longer than ~~the length we could assess from the~~ the 13 km we measured on the ~~seismic~~ geophysical ~~grid~~ data (see Fig 10). ~~The coastline and shallow waters posed evident geographical constraints to the extents of the seagoing survey. We measured the maximum~~

~~displacement caused by this fault,~~In other words, the S. Eufemia Fault credibly propagates along-strike toward the mainland, to the north-east and to the south-west. ~~Based on analytical relationships by Walsh and Watterson (1988) that derive ranges of expected fault lengths from cumulative displacement, we tentatively estimate a 25 km length for the S. Eufemia Fault (see Fig 10, left).~~ Considering an estimated median fault length of 25 km, and based on formulations by Wells and Coppersmith (1994) and by Kanamori and Anderson (1975), we estimate a M_w ranging from 6.5 to 6.8, respectively (Table 2) - the latter being directly influenced by the amount of slip per event. Based on data from comparable Italian earthquakes with normal faulting mechanism, like the 1908 Messina-Reggio Calabria one (Valensise, 1988; Amoruso et al., 2002; Pino et al., 2009), we infer 2 m to be a credible slip amount, which therefore leads us to tentatively adopt ~~a~~ M_w 6.8 ~~M_w~~ for this fault.

Formatted: Indent: First line: 0 cm

4.3 Chemical and biological analyses

The stations (St.) sampled ~~(see white triangles in Fig. 11)~~ for chemical and biological parameters in the sediments ~~are~~ can be grouped into three transects (see white triangles in Figs. 4 and 11), with inshore-offshore direction and located a) north (N Tran. in Fig. 11), b) along (AC Tran. in Fig. 11), and c) south (S tran. in Fig. 11) of the Angitola channel. ~~The "northern" transect (water depth between 202 m and 425 m) includes St. 1, 11 and 12; the "Angitola channel" transect (water depth from 268 m to 548 m) includes St. form 2N to 7; the "southern" transect (water depth between 111 and 181 m) includes St. 8, 9 and 10.~~ Water temperature close to the sea-bottom was almost constant in all stations and ~~varying~~ varied in a range of 13.97 °C (St. 3) - 14.18 °C (St. 12).

~~In this study,~~The results of both chemical and biological parameters are reported in Table 3. TN, TC and TOC did not show any evident difference~~s~~ among stations, except for the southern transect, along which we observed a small decreasing gradient from inshore to offshore. ~~Moreover, the highest values of TN, TC and TOC were measured at the shallowest station, i.e. St. 8. In~~

~~general, TN content ranged from 0.66 ± 0.01 mg N g^{-1} (St. 10) to 0.89 ± 0.04 mg N g^{-1} (St. 8). TC varied from 18.21 ± 0.04 mg C g^{-1} (St. 5) to 21.16 ± 0.08 mg C g^{-1} (St. 8) while the organic fraction of carbon (TOC) from 6.19 ± 0.12 mg C g^{-1} (St. 12) to 8.20 ± 0.09 mg C g^{-1} (St. 8).~~

~~According to the biological analysis, p~~Proteins were the main constituent of the BPC, followed by lipids and carbohydrates (Fig. 12, left). Their values ~~Protein content~~ did not change remarkably among stations ~~since with the~~it ~~ranged from 888 ± 18 µg C g_{dry}^{-1} (St. 12) to 1113 ± 28 µg C g_{dry}^{-1} (St. 8). An~~ exception ~~is represented by~~of ~~St. 7, showing~~ characterised by the highest proteins content ~~value~~ (1623 ± 25 µg C g_{dry}^{-1}; Table 3). The other components of the BPC (~~L~~lipids, CHO-H_2O and CHO-EDTA) showed a slightly higher variability~~, particularly along the Angitola channel. Along the southern transect, a decrease of lipids, from 626 ± 78 µg C g_{dry}^{-1} (St.8) to 229 ± 24 µg C g_{dry}^{-1} (St. 10), was measured as depth increased. Colloidal carbohydrates (CHO-H2O) are characterized by a high variability~~ and no evident pattern was detected (Fig. 12, left). ~~The lowest contents were measured a~~Along the Angitola channel, ~~(14 ± 1 µg C g_{dry}^{-1} at St. 4 and St. 5), whereas maximum content was found at St. 8 (55 ± 2 µg C g_{dry}^{-1}). C~~carbohydrates extracted in EDTA were ~~varied from a minimum of 61 ± 6 µg C g_{dry}^{-1} (St. 10) to a maximum of 218 ± 12 µg C g_{dry}^{-1} (St. 2), with~~ higher than in the other stations (Table 3). ~~values along the "Angitola channel" transect (Fig. 12, left).~~

Prokaryotic abundance~~s~~ in the sediment showed a great variability among stations, particularly along the Angitola channel (Fig. 12, right). The lowest ~~prokaryotic value~~density was measured at St. 11 (0.70 ± 0.05 10^8 cells g_{dry}^{-1}), whereas the maximum at St. 7 (2.94 ± 0.38 10^8 cells g_{dry}^{-1}). A strong variability was also observed along the northern sector, where a strong increase of the prokaryotic abundance was recognized at St. 12.

4.4 Physical parameters of CTD measurements

CTD profiles were analyzed focusing on the temperature close to the bottom of each profile, i.e. looking for signals of geothermal activity~~ies~~. The standard deviation evaluated for each profile at its

Formatted: Subscript

bottom and 5 m above gives no evident anomalous signal – thus ~~they sit~~ranging within the variability ~~range~~ of a significant statistical test. The lack of variability in temperature detection close the seafloor could be partially justified by the distance of the CTD measurement~~,~~ from the seafloor (at least 10 m).

5. Discussions

The aim of this paper is to contribute with sub-surface offshore data and interpretations to ~~: a) tackle some seismotectonic issues of this sector of the Calabrian Arc, and b) the~~ identify~~ication~~ ~~of~~ the ~~potential~~ possible seismogenic source of the 8 September 1905 earthquake, contributing to better constrain its location and M_w, using a unique approach.~~, which despite several studies and methodologies already applied in the literature, remains a debated earthquake – from its very epicentral location and M_w.~~

Formatted: Subscript

Evidence from MCS data analysis (Figs. 6 and 9~~4~~) allowed us to identify ~~mainly~~ three faults that ~~affect~~ deform ~~sediments~~ the deposits of the S. ~~ant'~~Eufemia ~~sub~~ basin~~, that are~~: 1) the Angitola Fault (~~AF;~~ Fig. 6, Box); 2) the~~a~~ Polyphased Fault ~~(PF) confined~~ in the central part of the gulf (Fig. 6); and 3) ~~a major normal fault,~~ the S. Eufemia Fault (Fig. 9).

The Angitola fault~~F~~ is ~~characterized~~ identifiable by ~~the~~ its tectonic control ~~it exerts~~ on the straight trend of ~~the internal segment of~~ the Angitola Channel, and by the steep and deep levees associated with a ~~bathymetric offset higher than~~ >~~–~~150 m bathymetric offset (Fig. 6, Box). ~~Nevertheless, d~~Deformation rapidly decreases with depth and fades out before reaching the ~~undisturbed~~ Messinian top (Fig. 6). AF, therefore, is a shallow (if long) structural feature with no basin-wide tectonic role.~~ This allows us to consider AF as a local structure, possibly resulting from the geometry of the basin development. All these elements show that AF~~showing that it has ~~bears neither role~~ nor causative relationship with the 1905 earthquake or any earthquake at all.

The Polyphased FaultPF is characterized by the main fault that strongly affectsdeforms the deeper sedimentary stack and the Messinian top, clearly showing positive inversion features likely accompanied by oblique motion (Fig. 6). In the shallower stack, thise PF system fault shows is associated with anticlines folds, and deformation is accommodated along several sub-parallel secondary faults buried below a thick layer of chaotic sediments body (Fig. 8). This fault system is long-lived, well organized through the pre-Messinian sequence and has had clearly affected a broad regionthe central part of the S. Eufemia basin. Its spatial extents lend an intuitive hint at the tectonic fabric of this sector of the back-arc basin. However, it PF is sealeddoes not extend through by the upper part of the Plio-Quaternary deposits, likely Pleistocene in age, and therefore has thus making it incompatible with anyno present-day tectonic activity. As Like with the AF Angitola Fault case above, no relationship can be established between the Polyphased Fault PF and the 1905 earthquake.

The third fault, S. Eufemia Fault, is an active major normal fault, sub-parallel to the large normal faults that control the basins known in the western Calabrian mainland , such as the (i.e., the Mesima and the Gioia Tauro bBasins). Its dip-slip kinematics appears to have been consistent at least since the late Miocene times up today, as confirmed shown by the MCS profiles for the full sedimentary stack (Fig. 9, Box) and by Chirp data for its shallower section (Fig. 10). The S. Eufemia Fault is in agreementproperly oriented with (1i) fault plane solutions derived for the other earthquakes that have occurred offshore to the NW of our study area (Mulargia et al., 1984), and (ii2) current extensional tectonics that interacts with regional uplift of the western Calabrian Arc (Westaway, 1993; Bordoni and Valensise, 1998; Monaco and Tortorici, 2000; Catalano et al., 2003; Pizzino et al., 2004; Ferranti et al., 2007). Moreover, our high resolution morpho-bathymetric data highlighted a straightthis fault shows a, 8 km long and up to 3 m high morphological escarpmentscarp (Fig. 5) associated with the cut-off of the fault plane rupture, located near shore. Such scarp occurs close to (1) the maximum damage area of the 1905 earthquake, and to (2) the coastal strip between Vibo Marina and Tropea, inundated by the tsunami associated with the 1905

earthquake (Guidoboni et al., 2007; Fig. 2). ~~close to.~~ Although such seafloor rupture may not necessarily be the direct trigger of the tsunami associated with this event, ~~—~~ ~~a feature~~ ~~which makes this rupture~~it is ~~-~~possibly ~~consistent in agreement~~ a favorable factor ~~with~~(NGDC/WDC, 2012) ~~the occurrence of the recorded tsunami~~. ~~The discontinuities and folding affecting very recent sediments imaged in the Chirp profile (Fig. 10, right) confirm this hypothesis, bridging the gap between low and very high resolution seismic reflection data (Fig. 9, Box).~~

~~A further proof of the~~ Biological data analysis provides some indications about the recent activity of the S. Eufemia Fault in terms of seafloor heterogeneity and fluids circulation~~can also be provided by the biological data analysis. The variability of biopolymeric C content, influenced by channels and water currents, and the prokaryotic abundance in the studied area also supplies indications about the seafloor heterogeneity~~, which ~~can~~ could be associated with the fluid ~~escape~~ up-welling ~~features at the seafloor~~from deep sediments. The presence of active faulting could influence the water currents at a local scale, favoring the accumulation of organic matter at the seafloor (Danovaro et al., 2010 and references therein). Data from s~~S~~hallower stations ~~could be~~show ~~characterized by~~ more labile compounds (Danovaro, et al., 1998)~~,~~ as colloidal carbohydrates, which promote microbial activities, thus supporting high abundances as those observed at St. 7 and St. 8 (Fig. 12, left; de Brouwer and Stal, 2001). On the other hand, moving offshore along the Angitola channel, ~~the presence of~~the labile compounds probably decrease~~s~~ due to preferential~~ably~~ use~~d~~ by prokaryotes. Although available, the prokaryotic community could be less supported by the refractory organic fraction, harder to degrade, and this could partially explain the limited ~~prokaryotic concentrations~~ abundances at the offshore stations. An exception is represented by St. 4, characterized by high prokaryotic ~~abundance~~ density not supported by the high biopolymeric C content (Fig. 12). ~~Such~~ This anomaly could be explained considering that St. 4 is located at the border of the Angitola channel (Figs. 4 and 11), ~~from~~ along which water enriched by organic matter can flow.

Formatted: English (U.S.)

Formatted: English (U.S.)

Along the southern transect, the high ~~chemical~~ organic content ~~values along the stations and depth of sampling~~at St. 8 suggests ~~allow us to infer that~~the presence of ~~the~~ ~~fluids and gases escape at the seafloor~~ up-welling fluids, which could represent an alternative source~~s~~ of carbon and energy for the microbial ~~activity~~community. ~~As a consequence,~~ Prokaryotes ~~concentration of microbes~~ with particular metabolisms (as chemiosynthetic ones) could ~~rise~~ in fact be enhanced and their proliferation could support the other trophic levels~~,~~ explaining ~~in~~ partially the high biopolymeric ~~BP~~C ~~content~~ values observed ~~detected~~ (Fig. 12, left). Even if not supported by the low organic matter content, ~~Moreover,~~also the high prokaryotic abundance ~~detected in~~at St. 12 (Fig. 12, right), located along the seafloor trace of the S. Eufemia Fault (Figs. 4 and 10, left), could be explained in part by the presence of deep fluids, not necessarily warm, up-welling along the fault plane, which act as a source of carbon ~~and the low biopolymeric C content~~ (Fig. 12, left) ~~could be partially explained by the presence of deep fluids, up-welling along the fault plane, acting as source of carbon~~. Such hypothesis is in agreement with the small fluid escape detected on the Chirp profile (Fig. 10B~~, right~~).

~~Thus, the prokariotic abundance detected at St. 12 could indicate hydrothermal fluid activity – if modest – along the S. Eufemia Fault.~~

~~As per the geometrical parameters of the S. Eufemia Fault, the seismic grid acquisition restricted by the physiography of the Gulf did not allow us to constrain the real lateral extents of the S. Eufemia Fault. Its length measured on the morpho bathymetric data (8 km; Fig. 10, left) is tentatively estimated to be 25 km *sensu* Walsh and Watterson (1988); it is therefore associated with a M_w ranging from 6.5 to 6.8, based on formulations by Wells and Coppersmith (1994) and by Kanamori and Anderson (1975; Table 2) respectively. The latter estimate is directly influenced by the amount of slip per event. Based on data from comparable Italian earthquakes with normal faulting mechanism like the 1908 Messina Reggio Calabria one (Valensise, 1988; Amoruso et al., 2002), we infer 2 m to be a credible slip amount, which therefore leads us to tentatively adopt a 6.8 M_w.~~

Concerning the geometrical parameters of the S. Eufemia Fault, its measured~~A seafloor rupture associated with the S. Eufemia Fault only~~length of only 13~~8~~ km (Fig. 10A) and its total displacement of 460 m ~~long (Fig. 10, left) does not prevent~~lead us ~~a fault with the displacement we measured~~ to ~~be~~ infer a (much) longer fault~~than its outcropping rupture~~, at least for two simple reasons:

~~-~~a) a stratigraphic one: the ~~northeasterly~~ southwesterly strand of the S. Eufemia fault is ~~closer~~ buried below the Angitola channel system that completely masks any fault deformation clues~~to the sediment supply of the coastline, i.e. it may lie confined below recent sediments (sedimentation rate may be higher than displacement rate)~~; and

b) a tectonic one: all field and experimental observation of normal faults consistently show decreasing throw towards fault tips (for a reference: Ramsay and Huber, 1987), as suggested by the decreasing deformation toward the northeast (Figs. 10B, C, and D).

~~If we consider the~~From the macroseismic M_w estimates~~d~~ ~~M_w derived from macroseismic data~~ ranging between 6.7 and 7.0 (Gruppo di Lavoro CPTI04, 2004; Guidoboni et al., 2007; Rovida et al., 2011), the expected fault length derived using empirical relationships by Wells and Coppersmith (1994) and Kanamori and Anderson (1975) ~~would~~ should ~~be~~ exceed our estimated 25~~30~~ km ~~or more~~, as ~~confirmed~~ suggested by field evidence for other ~~major~~ Italian earthquakes of the same M_w range (~~for a summary: see Basili et al., 2008 and references therein~~see: Ward and Valensise, 1989; Pantosti and Valensise, 1990; Burrato and Valensise, 2008; Pino et al., 2009). It would, however, be close to the 20 to 30 km range inferred using Walsh and Watterson (1988) formulations (see em20 and em30 in Fig. 13A). On the other hand, instrumental estimates ranging from M 7.0~~3~~ ~~by~~ (Mulargia et al.,~~:~~ ~~(~~1984) to M 7.5 ~~by~~ (Michelini et al.,~~:~~ ~~(~~2006) require up to a >>50 km expected fault length~~ by the same empirical relationships~~. Given the epicentral locations proposed by these authors and by Riuscetti and Schick (1975), such fault sh~~w~~ould ~~be~~ lie entirely ~~located~~ offshore, west of Capo Vaticano.~~ Regardless of its physical and geometrical constraints, such hypothetic fault should be associated~~ causing ~~with a~~ longer-wave and~~,~~ long-term imprint on

the geology ~~and the landscape of~~offshore central Calabria, to-date ~~neither inferred~~ not~~r~~ recognized on data.

Based on the current set of knowledge and on the geological ~~constraints~~ evidence ~~highlighted by~~ in our data, we prefer a conservative approach, considering 6.8 to 7.0 as a fairly reliable estimate range (Fig. 13; Table 2). In fact, it is certainly true that poorly located moderate-size earthquakes ~~with dubious location may show~~are associated with uncertain M_w estimates, especially when ~~such~~ a novel location can be constrained offshore by geological means (see an example in Fracassi et al., 2012).

Finally, although our data cover only the marine sector of the S. Eufemia Gulf, they fall in a broader seismotectonic context (Fig. 13) and shed some light on ~~comparisons,~~ possible contradictions ~~and roles~~ among the various seismogenic faults / source models previously proposed ~~by previous authors~~, so different ~~among~~ from one another (Fig. 3, Table 1).

In chronological order, length (22 km) and dip direction (SE) of PE ~~, the seismogenic source by~~(~~-~~Peruzza et al.; ~~(~~1997)~~, lies outside the physical range of our survey, being essentially onland. However, size (22 km long) and dip direction (SE) is~~ are consistent with our data, thus making PE an interesting source model, although lying ~~–~~essentially onland.~~also because it derives from a regional segmentation model.~~ MT~~, derived from a fault in a regional interpretive model of the Calabrian Arc by~~ (Monaco and Tortorici; ~~(~~2000)~~,~~ dips to the NW and lies in part within our survey's boundaries but is not shown on our data~~ – possibly due to the geometry of the acquisition grid within and nearby the S. Eufemia Gulf~~. Therefore, MT ~~Such negative evidence, however, can only suggest that MT~~ is not likely to affect the inner Gulf, while it could affect the NW flank of the Capo Vaticano ~~Promontory~~promontory, and ~~. However, due to its location and dip direction, MT~~ would belong to an entirely distinct fault system~~ from that including SE dipping structures~~. VP~~,~~ ~~based on a regional model by~~ (Valensise and Pantosti; ~~(~~2001b)~~,~~ is the longest ~~one~~ possible source in the literature (40 km). Our data show no evidence of this source, which however is interestingly sub-parallel to the S. Eufemia Fault, with same dip direction, like PE.

Formatted: Indent: First line: 1.25 cm

~~Using data by Monaco and Tortorici (2000), Piatanesi and Tinti (2002) proposed two possible solutions for their tsunami inversion: CV and VV.~~ CV (Piatanesi and Tinti, 2002) is essentially MT, although dipping at very high angle; given its location, same considerations done for MT apply for CV. VV (Piatanesi and Tinti, 2002), ~~another very~~ a ~~high angle~~ NW-dipping high-angle normal fault, lies outside our survey's boundaries~~, nearby the city of Vibo Valentia,~~ and we therefore cannot ~~ascertain~~ verify its geometry and role~~, if any~~. However, since its rupture would occur onland, one would likely need to invoke other nearby phenomena to account for the tsunami, such as large submarine slides ~~or slumps~~, which our marine data do not show. We therefore doubt that VV can be considered as a viable seismogenic source for the 1905 earthquake. On the other hand, MT/CV's location and geometry seems to conflict with the S. Eufemia Fault, for which we gathered positive evidence from our data.

~~The most recent source model,~~ CT (~~is based on a model by~~ Cucci and Tertulliani, ~~;~~ (2010)~~,~~ is located ~~whose location~~ away from the area of maximum damage of the 1905 earthquake, along a regional transverse structure~~, and size, similar to that of MT, lead us to compare its role and hierarchy with MT/CV and, ultimately, with the S. Eufemia Fault.~~ Maximum damage is expected to occur in and near the hanging-wall of CT, which however is not the case here (major damage is located way north of CT's foot-wall). Therefore, while we clearly have no geological data to discuss CT, we doubt it can be associated with the 1905 earthquake. ~~On the other hand, MT/CV's location and geometry seems to conflict with the S. Eufemia Fault, for which we gathered positive evidence from our data.~~

Based on the above considerations, we believe that the S. Eufemia Fault redraws the seismotectonic understanding of this sector of western Calabria (Fig. 13), and that it proves to be a credible candidate as a ~~potential~~ seismogenic source model for the 1905 earthquake.

6. Conclusions

Uncertain epicentral location and M estimate of large historical earthquakes that have occurred at sea yet caused major damage on-land often hamper the correct understanding of such destructive events.

In a region such as Calabria, with its numerous seismic crises and puzzling catastrophic earthquakes that have occurred in a relatively narrow landmass, identifying the likely seismogenic source that could be associated with the 8 September 1905 ~~earthquake~~ event is of key relevance to correctly evaluate the seismogenic potential of this area and its seismic hazard. To contribute to this ~~purpose~~goal, we present a multidisciplinary study that brings together evidence from our ~~new multidisciplinary survey~~data to ~~with open seismological issues of this area. Our data highlighted new geological and geo-biological features that~~ shed new light on the seismo-tectonics of ~~the S. Eufemia Gulf~~central-western Calabria.

Our geophysical data allowed us to identify three tectonic features ~~affecting~~ in the Gulf: 1) ~~a likely~~the Angitola Fault, ~~affecting~~ which deforms only shallower sediments; 2) ~~the~~a Polyphased Fault system, currently buried below a thick chaotic body~~, affecting the upper part of Miocene units and deeper part of Plio-Quaternary deposits, buried below a thick chaotic layer~~; and 3) ~~the~~a N31°-striking ~~normal~~ S. Eufemia normal F~~f~~ault, rupturing the shallow deposits for ~~-~~13~~-~~ km along-strike, ~~N31° oriented~~ that dips to the southeast and extends through~~, SE-dipping, rupturing~~ the whole sedimentary stack up to the seabed~~., located offshore between the towns of Briatico and Lamezia Terme.~~ Among these structures, the ~~normal~~ S. Eufemia ~~f~~Fault is the only active one and compatible with ~~shows several elements that strongly agree with most of~~ the 1905 earthquake required features, ~~like~~ i.e.; ~~a~~1) expected fault size ~~compatible~~ suitable ~~with~~ for the macroseismic M_w range, 2~~b~~) a 8-km-long seabed rupture~~-~~, corresponding to the up-ward prolongation of the fault plane, compatible with the ~~recorded~~ occurrence of a tsunami, ~~and~~ 3~~c~~) location ~~compatible~~ fitting ~~with~~ the distribution of the maximum damage area, and 4) geometry in agreement with the regional seismotectonic model of the Calabria block. In light of these factors, we maintain that the S. Eufemia Fault ~~a~~is the most credible seismogenic source for the 1905 earthquake, also against the critical review of source

Formatted: Normal, Justified, Line spacing: Double

Formatted: None

Formatted: Not Highlight

Formatted: Not Highlight

Formatted: Font: (Default) Times New Roman, 12 pt

Formatted: Not Highlight

Formatted: Not Highlight

Formatted: Not Highlight

Formatted: Not Highlight

Formatted: Not Highlight

Formatted: Not Highlight

models proposed in the literature. ~~The normal fault, here called S. Eufemia Fault, ruptures the seafloor as revealed by the 8 km long morphological escarpment, corresponding to the cut-off of the fault plane.~~

~~A critical review of previous seismogenic source models allowed us to compare and contrast characteristics and constraints of these models against the S. Eufemia Fault.~~

Recent activity of the S. Eufemia Fault is also witnessed by ~~i) discontinuities and deformation affecting shallow sediments in the overburden, and ii)~~ the ~~likely~~ fluid escapes detected close to the seafloor. Such evidence is also confirmed by the high Prokaryotes abundance and biopolymeric C content distribution that we tentatively explain with deep fluids, locally up-welling along the fault plane, acting as source of carbon.

Despite the undersized length of the ~~seafloor~~ rupture associated with the S. Eufemia Fault, cumulative displacement indicates that this fault is likely at least as long as the basin itself and spans along-strike the whole Gulf - possibly beyond into the mainland. Geomorphological survey, drainage basin evolution and displacement modeling are the premier tools of another on-going study to test our hypothesis against field and regional evidence, to understand ~~i)~~ how this major tectonic feature falls within the fault network ~~that~~ described in previous studies ~~depicted., and ii) what is the seismotectonic model that best fits onshore-to-offshore geological evidence, fault hierarchy and kinematic relationships.~~

Captions:

Figure 1 - A) Structural sketch ~~map~~ of the Southern Apennines and Calabrian Arc, simplified by Catalano and Sulli (2006) and v~~V~~an Dijk et al. (2000); slip vectors ~~derived~~ from D'Agostino and Selvaggi (2004). Shaded relief modified ~~by~~ © Google Earth, using data by SIO, NOAA, U.S, Navy, NGA, and GEBCO. Small red dots represent M_w>3 instrumental earthquakes recorded since 2000 up to date, ~~day with M_w>3~~ from INGV Seismic Bulletin (ISIDe ~~Working Group (INGV, 201;0),~~

Formatted: Not Highlight
Formatted: Not Highlight
Formatted: Not Highlight
Formatted: Not Highlight
Formatted: Not Highlight
Formatted: Not Highlight
Formatted: Not Highlight

~~Italian Seismological Instrumental and parametric database:~~ http://iside.rm.ingv.it~~).~~ ~~GTB = Gioia Tauro Basin; PB = Paola Basin; CPT = Calabrian Peloritan Terranes; SM = Sila Massif;~~ SM = Strait of Messina~~,~~ ~~ME = Malta Escarpment;~~ TF = Tindari Fault; CBF = Cirò-Benevento Fault~~,~~ ~~The transparent gray box includes the S. Eufemia Gulf.~~

Figure 2 - Morpho-bathymetric map of the stud~~y~~ied area~~,~~ ~~derived by~~(from NOAA satellite data ~~(~~http://topex.ucsd.edu/WWW_html/mar_topo.html; contour interval: 50 m), showing intensities distribution (Mercalli-Cancani-Sieberg scale) caused by the 1905 earthquake and the ~~the main~~hypothetical ~~s~~seismogenic faults associated with it in the literature ~~the 1905 event~~: 1) Capo Vaticano Fault (Monaco and Tortorici, 2000); 2) Vibo Valentia Fault (Piatanesi and Tinti, 2002); 3) Coccorino Fault Zone (Cucci and Tertulliani, 2006~~; Cucci and Tertulliani~~, 2010); 4) Angitola Fault (Peruzza et al., 1997; Valensise and Pantosti, 2001a); 5) Angitola Fault (Valensis~~t~~e and Pantosti, 2001b). Notice that the highest damage was reported on the northern flank of the Capo Vaticano Promontory. ~~The~~ Y~~y~~ellow stars indicate~~d~~ the 1905 ~~earthquake~~ epicentral locations proposed by (S1) Riuscetti and Schick (1975), (S2) Camassi and Stucchi (1997), (S3) Boschi et al. (2000) and Guidoboni et al. (2007), (S4) Rizzo (1906), and (S5) Michelini et al. (2006). ~~Br. = Briatico.~~ Blue waves indicate the tsunami effects recorded by contemporary observers (data from Tinti and Maramai, 1996).

Figure 3 ~~–~~ ~~Possible S~~s~~S~~ource models ~~causative~~ of the 8 September 1905 earthquake derived ~~available in the literature~~from ~~published sources~~the literature, based on seismogenic faults in Fig. 2 (data in Tab. 1). Inset 1: conceptual model of geometry and parameters. Inset 2: list of ~~ID~~s ~~identify~~source models ~~are listed~~and associated studies ~~within the inset 2.~~ ~~taken from the following papers: PE: Peruzza et al. (1997); VP, Valensise and Pantosti (2001b); MT = Monaco and Tortorici (2000); CV, Capo Vaticano Fault, in Monaco and Tortorici (2000),~~

Formatted: English (U.S.)
Formatted: English (U.S.)
Formatted: English (U.S.)
Formatted: Italian (Italy)
Formatted: Italian (Italy)
Formatted: Italian (Italy)
Formatted: Italian (Italy)
Formatted: Italian (Italy)
Formatted: Italian (Italy)
Field Code Changed
Formatted: Italian (Italy)
Formatted: Italian (Italy)
Formatted: Italian (Italy)
Formatted: Italian (Italy)
Formatted: English (U.S.)
Formatted: Font: Not Bold
Formatted: Italian (Italy)
Formatted: Italian (Italy)

~~parameters by Piatanesi and Tinti (2002); VV = Vibo Valentia Fault, in Monaco and Tortorici, 2000), parameters by Piatanesi and Tinti (2002); CT, Cucci and Tertulliani (2010). Inset: visual representation of source geometry model and parameters.~~

Formatted: Italian (Italy)

Formatted: English (U.S.)

Figure 4 - Image of the high ~~-~~resolution morpho-bathymetric map. Thin yellow lines indicate the newly-acquired seismic dataset; white triangles show locations of the oceanographic and geo-biological measurements; the blue circle show location of the industrial Marisa well. The ~~two~~ seismic profiles described later ~~on are indicated~~are shown by thick yellow lines. Grey shade: mainland

Figure 5 - High resolution morpho-bathymetric map, with a detail (inset). The white dashed line underlines the Angitola Channel (AC) trend; thick white arrows highlight the several minor incisions and slide. LMT = ~~,~~ = Lametia Terme; Br. = ~~,~~ = Briatico.

Figure 6 – Time migrated seismic profile GSE10_05 located in the central part of the S. Eufemia Gulf; ~~hypothesized~~ interpreted faults are indicated with dashed black lines~~,~~; ~~within the~~ Box (left)~~,~~: the likely dip-slip fault affecting the Angitola channel is indicated as AF ? = Angitola Fault; the ~~null~~ point where fault offsets is null (null point) is indicated with a black dot; SL indicates the southern levee. Inset: bathymetric map showing a sketch of the two faults location.

Figure 7 - Marisa well plotted on the nearest seismic profile, GSE10_02 (location in Fig. 4), running parallel to the ~~morphological escarpment~~fault plane.

Figure 8 – Left: high resolution morpho-bathymetry of the area surrounding the Polyphased Fault (thick red line). ~~On the r~~Right:~~,~~ a detail of the upper part of the Ppolyphased Ffault system ~~affecting~~ deforming the central part of the S. Eufemia sedimentary b~~B~~asin (Fig. 6). ~~On the left, the high resolution morpho-bathymetry of the area surrounding the polyphased fault (thick red line).~~

Figure 9 - Time migrated seismic profile GSE10-07 located close to the continental shelf (see location in Fig. 4~~2~~). Faults are shown as dashed black lines; AC = Angitola Channel; ~~P-Q Dep. indicates the Plio-Quaternary deposits are;~~ white thick arrows indicate gentle folds, while the black one indicates the drag fold. Inset: bathymetric map showing a sketch of the normal fault location.

Figure 10 - ~~Left:~~ A) h~~H~~igh resolution morpho-bathymetric map showing the location of the S. Eufemia Fault, ~~which~~ includinges the segment recognized on the ~~seismic~~ geophysical data (thick black line encircled by a thin rectangle around the seafloor rupture) and the one derived from analytical relationships (dashed black line). ~~Right~~B)~~:~~ ~~P~~part of Chirp profile 39 crossing the outcropping ~~out~~ fault plane. C) part of Chirp profile 52 crossing the fault plane and shallow sediments deformation. D) part of Chirp profile 71 crossing the fault plane deforming shallow sediments without reaching the seafloor.

Figure 11 - Location map of biological samples (white triangles), whose analysis results are listed in table 3. N tran. = Northern transect; AC tran. = Angitola Channel transect; S tran. = Southern transect.

Figure 12 – Left: Biopolymeric C content and its composition measured at the twelve stations, grouped in the three transects ~~(left)~~. The arrows indicate the near shore to offshore direction~~: from inshore to offshore~~. CHO-EDTA = carbohydrates extracted in EDTA; CHO-H2O = colloidal carbohydrates. ~~On the r~~Right:~~,~~ prokaryotic abundances measured at the twelve stations grouped in

Formatted: Font: Not Bold

Formatted: Font: Not Bold

Formatted: Font: Not Bold

the three transects. The arrows indicate the near shore to offshore direction~~: from inshore to offshore~~.

Figure 13 – A) sketch map including the Sant'Eufemia Fault (thick red box) seismogenic source ~~model~~ against: a) source models based on causative faults ~~causative~~ of the 8 September 1905 earthquake available in the literature (see Fig. 2 and 3; Table 1), and b) Individual Seismogenic Sources from DISS 3.1.1 (DISS Working Group, 2010). The length of the two end members (em20 and em30) derived from the Walsh and Watterson (1988) empirical relationship (20 and 30 km fault length, respectively). Notice that em30 reaches into the mainland beyond the Gulf's extents. Among em20 and em30, we adopted a conservative median length of 25 km. ~~We adopted a conservative fault length (and, therefore, M_w: 6.8) of 25 km using analytical relationships by Walsh and Watterson (1988)~~. See parameters and explanations in Table 2. B) morpho-structural map combining the satellite-derived bathymetry (http://topex.ucsd.edu/WWW_html/mar_topo.html; contour interval: 50 m) and the main on-land faults (modified after Monaco and Tortorici, 2000; Pizzino et al., 2004; Tansi et al., 2007) and the offshore faults identified on our geophysical dataset. ~~Inset: visual representation of source geometry model and parameters.~~

Formatted: Font: Not Bold

Formatted: Font: Not Bold

Formatted: Font: Not Bold

Formatted: No underline

Table 1 - Parameters for the source models causative of the 8 September 1905 earthquake available in the literature (see also Fig. 2).

IDs identify models taken from the following papers: PE = ~~:~~ Peruzza et al. (1997); VP = Valensise and Pantosti (2001b); MT = Monaco and Tortorici (2000); CV = Capo Vaticano Fault, in Monaco and Tortorici (2000), parameters by Piatanesi and Tinti (2002); VV = Vibo Valentia Fault, in Monaco and Tortorici~~,~~ (2000), parameters by Piatanesi and Tinti (2002); CT = Cucci and Tertulliani (2010). Note that source model parameters were available only for Peruzza et al. (1997) and for Piatanesi and Tinti (2002), while in most cases L (Length) was deduced from mapped fault trace; we computed W (Width) and the remaining parameters using empirical and analytical relationships.

TD and BD are top and bottom depth, respectively; Sl is slip; M_w (W&C) and M_w (K&A) are computed using formulations by Wells and Coppersmith (1994) and Kanamori and Anderson (1975), respectively.

Table 2 - Parameters for the source model deduced from the SE (S. Eufemia) Fault. First and second row list the two end-members (20 and 30 km legnth, respectively); third row lists the source with the median length (25 km), that we adopted in this study.

ID identifies~~y~~ the source model. TD and BD are top and bottom depth, respectively; Sl is Slip; M_w (W&C) and M_w (K&A) are computed using formulations by Wells and Coppersmith (1994) and Kanamori and Anderson (1975), respectively. L is Length inferred using cumulative displacement of the Miocene reflector, *sensu* Walsh and Watterson (1988); W is Width computed using empirical and analytical relationships. Dip is constrained using averaged Vp velocity and adjacent wells.

Table 3 - Values and standard deviation (SD) of the chemical and biological parameters. TN = Total Nitrogen; TC = Total Carbon; TOC = Total Organic Carbon; CHO-H_2O = colloidal carbohydrates; CHO-EDTA = carbohydrates extracted in EDTA.

Formatted: Font: Bold

Formatted: Justified

Formatted: English (U.K.)

Acknowledgements

We wish to thank OGS that supported the acquisition of the multidisciplinary dataset in the frame of the ISTEGE (Indagine Sismotettonica del TErremoto dell'8 Settembre 1905 (Mw 7.4) nel Golfo di Sant'Eufemia - offshore tirrenico calabrese) project. Special thanks are due to Drs. Vedrana Kovacevic and Giampiero Cossarini (OGS) who performed the temperature (CTD) data analysis, and to Drs. Gianluca Valensise and Salvatore Barba (INGV), ~~the Dr.~~ and Dario Civile (OGS) for the fruitful ~~interesting~~ scientific discussions. Finally, we wish to thank the R/V *OGS-Explora* technicians' team. Remarks by two anonymous referees and the Editor greatly enhanced this

Formatted: Font: (Default) Times New Roman, Not Bold

Formatted: Font: (Default) Times New Roman

Formatted: No underline

Formatted: Font: Italic

manuscript. Seismic data interpretation was managed using the Kingdom software (IHS, Global Inc.). This paper is ISMAR-CNR contribution.

Formatted: Font: (Default) Arial, Do not check spelling or grammar

References

Amodio-Morelli, L., Bonardi, G., Colonna, V., Dietrich, D., Giunta, G., Ippolito, F., Liguori, V., Lorenzoni, P., Paglionico, A., Perrone, V., Piccarreta, G., Russo, M., Scandone, P., Zanettin-Lorenzoni, E., and Zuppetta, A., 1976. L'Arco Calabro-Peloritano nell'orogene Appenninico-Maghrebide. Memorie della Società Geologica Italiana~~Mem. Soc. Geol. It.,~~ 17, 1-60.

Amoruso, A., Crescentini, L., and Scarpa R., 2002. Source parameters of the 1908 Messina Straits, Italy, earthquake from geodetic and seismic data. Journal of Geophysical Research: Solid Earth 107, B4. doi: 10.1029/2001JB000434.

Formatted: English (U.S.)

~~Amoruso ……?~~

Formatted: Highlight

Anzidei, M., ~~F.~~ Antonioli, F., ~~A.~~ Benini, A., ~~A.~~ Gervasi, A., and ~~I.~~ Guerra, I., 2012. Evidence of vertical tectonic uplift at Briatico (Calabria, Italy) inferred from Roman age maritime archaeological indicatore. Quaternary International~~Quatern. Internat.,~~ doi: 10.1016/j.quaint.2012.01.019.

Formatted: Font: Not Italic

Argnani, A., and~~&~~ Trincardi, F., 1988. Paola slope basin: evidence of regional contraction on the eastern Tyrrhenian margin. Memorie della Società Geologica Italiana 44, 93-105.

Formatted: Indent: Left: 0 cm, Hanging: 0.95 cm, Space Before: 0 pt

Formatted: Italian (Italy)

~~Argnani A. and Savelli C., 1999. Cenozoic volcanism and tectonics in the southern Tyrrhenian sea: space-time distribution and geodynamic significance. J of Geod., 27, 398-321~~

Formatted: Font: Not Italic, Italian (Italy)

Formatted: Italian (Italy)

Argnani, A., and Trincardi, F, 1993. Growth of a slope ridge and its control on sedimentation: Paola slope basin (eastern Tyrrenian margin). ~~Intern. Ass. Sedimentol.~~ Special~~.~~ Publications~~s~~~~.~~ International Association of Sedimentology~~,~~ 20, 467-480.

Formatted: Font: Not Italic, Italian (Italy)

Formatted: Italian (Italy)

Formatted: English (U.S.)

Baratta, M., 1906. Il grande terremoto calabro dell'8 settembre 1905. Atti della Societa Toscana di Scienze Naturali, Memorie, 22~~Atti Soc. Toscana di Sc. Nat., XXII, 57-80~~.

Barone, M., Dominici, R., Muto, F., Critelli, S., 2008. Detrital modes in a Late Miocene wedge-top basin, northeastern Calabria, Italy: compositional record of wedge-top partitioning. Journal of Sedimentary Research~~J. Sediment. Res.,~~ 78, 693–711.

Basili, R., Valensise, G., Vannoli, P., Burrato, P., Fracassi, U., Mariano, S. and Tiberti, M.M., 2008. The Database of Individual Seismogenic Sources (DISS), version 3: summarizing 20 years of research on Italy's earthquake geology, Tectonophysics~~,~~ 453, 1/4, 20-43. doi: 10.1016/j.tecto.2007.04.014.

Bonardi, G., Cavazza, W., Perrone, V., and Rossi, S., 2001. Calabria-Peloritani Terrane and Northern Ionian Sea. In: Martini L.P., Vai G.B. (Eds.), Anatomy of an Orogen: the Apennines and adjacent Mediterranean Basins. Kluwer Academic~~.~~ Publication~~,~~ 287-306.

Bordoni, P., and G. Valensise, 1998. Deformation of the 125 ka marine terrace in Italy: tectonic implications. In: I. Stewart e C. Vita Finzi (eds.), Late Quaternary coastal tectonics, Geological Society Special Publications~~,~~ 146, 71-110.

Boschi, E., Guidoboni, E., Ferrari, G., Mariotti, D., Valensise, G., Gasperini, P. (Eds.), 2000. Catalogue of strong Italian earthquakes from 461 B.C. to 1997~~,~~ Annali ~~di~~ Geofi~~phy~~sica~~.~~ 43, with CD-Rom, 259 p.

Burrato, P., and Valensise, G. 2008. Rise and fall of a hypothesized seismic gap: source complexity in the Mw 7.0 16 December 1857 Southern Italy earthquake. Bulletin of the Seismological Society of America 98, 1, 139-148. doi: 10.1785/0120070094.

Calò, M., Dorbath, C., Luzio, D., Rotolo, S.G., and D'Anna, G., 2012. Seismic velocity structures of southern Italy from tomographic imaging of the Ionian slab and petrological inferences. Geophysical~~.~~ Jo~~r~~urnal~~.~~ International~~,~~ doi: 10.1111/j.1365-246X.2012.05647.x.

Formatted: Font: Not Italic, Italian (Italy)

Formatted: Italian (Italy)

Formatted: Font: Not Italic, Italian (Italy)

Formatted: English (U.S.)

Formatted: English (U.S.)

Formatted: Italian (Italy)

Camassi, R., and Stucchi, M., 1997. NT4.1.1, un catalogo prametrico di terremoti di area italiana al di sopra della soglia del danno – Gr. Naz. Difesa dai Terremoti, RAapp. Interno, Milano, 95 pp.

Castello, B., Selvaggi, G., Chiarabba, C., and Amato, A., 2006. CSI Catalogo della sismicità italiana 1981-2002, versione 1.1, INGV-CNT, Roma, http://csi.rm.ingv.it/.

Catalano, S., G. De Guidi, C. Monaco, G. Tortorici, and L. Tortorici, 2003. Long-term behavior of the late Quaternary normal faults in the Straits of Messina area (Calabrian arc): structural and morphological constraints., Quaternary International Quat. Int., 101-102, 81-91.

Catalano, R., and Sulli, A., 2006. Crustal image of the Ionian basin and accretionary wedge. Bollettino di Geofisica Teorica e Applicata,, 47, 3, 343-374.

Cibic, T., Acquavita, A., Aleffi, F., Bettoso, N., Blasutto, O., De Vittor, C., Falconi, C., Falomo, J., Faresi, L., Predonzani, S., Tamberlich, F., Fonda Umani, S., 2008. Integrated approach to sediment pollution: A case study in the Gulf of Trieste. Marine Ppollution bBulletin Mar. Pollut. Bull. 56, 1650-1667.

Cifelli, F., M. Mattei, M., and F. Rossetti, F., 2007. Tectonic evolution of arcuate mountain belts on top of a retreating subduction slab: The example of the Calabrian Arc., J.ournal of Geophys.ical Research,, 112, B09101, doi: 10.1029/2006JB004848.

Cucci, L., and Tertulliani, A., 2006. I terrazzi marini nell'area di Capo Vaticano (arco calabro): solo un record di sollevamento regionale o anche di deformazione cosismica? Il Quaternario, Ital. J. Quatern. Sc., 19, 89-101.

Cucci, L., and Tertulliani, A., 2010. The Capo Vaticano (Calabria) coastal terraces and the 1905 M7 earthquake: the geomorphological segnature of the regional uplift and coseismic slip in southern Italy. Terra Nova, 22, (5), 378-389. doi: 10.1111/j.1365-3121.2010.00961.x.

D'Agostino, N., E. D'Anastasio, E., A. Gervasi, A., I. Guerra, I., M. R. Nedimović, M.R., L. Seeber, L., and M. Steckler, M., 2011. Forearc extension and slow rollback of the Calabrian Arc from

Formatted: English (U.S.)
Formatted: English (U.S.)
Formatted: Font: Not Italic
Formatted: English (U.S.)
Formatted: Font: Not Italic
Formatted: Font: Not Italic
Formatted: Font: Not Italic
Formatted: English (U.S.)
Formatted: English (U.S.)
Formatted: English (U.S.)
Formatted: English (U.S.)
Formatted: English (U.S.)
Formatted: English (U.S.)
Formatted: English (U.S.)
Formatted: English (U.S.)
Formatted: English (U.S.)
Formatted: English (U.S.)
Formatted: Italian (Italy)
Formatted: Italian (Italy)
Formatted: Italian (Italy)
Formatted: Italian (Italy)
Formatted: Italian (Italy)
Formatted: Italian (Italy)
Formatted: Italian (Italy)

GPS measurements., Geophysical. Research. Letters., 38, L17304, doi: 10.1029/2011GL048270

D'Agostino, N., and Selvaggi, G., 2004. Crustal motion along the Eurasia-Nubia plate boundary in the Calabrian Arc and Sicily and active extension in the Messina Straits from GPS measurements. Journal of. Geophysical. Research., 109, B11402, doi:10.1029/2004JB002998.

Danovaro, R., Company, J.B., Corinaldesi, C., D'Onghia, G., Galil, B., Gambi, C., Gooday, A.J., Lampadariou, N., Luna, G.M., Morigi, C., Olu, K., Polymenakou, P., Ramirez-Llodra, E., Sabbatini, A., Sardà, F., Sibuet, M., Tselepides, A., 2010. Deep-sea biodiversity in the Mediterranean Sea: the known, the unknown, and the unknowable. PLoS ONE, 5, 8, e11832: 1-25. doi: 10.1371/journal.pone.0011832.

Danovaro, R., Marrale, D., Della Croce, N., Dell'Anno, A., Fabiano, M., 1998. Heterotrophic nanoflagellates, bacteria and labile organic compounds in continental shelf and deep-sea sediments of the eastern Mediterranean. Microbial eEcology 35 (3-4), 244-255.

De Brouwer, J.F., and Stal, L.J., 2001. Short-term dynamics in microphytobenthos distribution and associated extrecelluler carbohydrates in surface sediments of an intertidal mudflat. Marine Ecology Progress SeriesMar. Ecol. Prog. Ser., 218, 33-44.

Del Ben, A., Barnaba, C., Taboga, A., 2008. Strike-slip systems as the main tectonic features in the Plio-Quaternary kinematics of the Calabrian Arc. Marine. Geophysical. Res.earch, 29, 1–12, doi: 10.1007/s11001-007-9041-6.

Devoti, R., Esposito, A., Pietrantonio, G., Pisani, A.R., Riguzzi, F., 2011. Evidence of large scale deformation patterns from GPS data in the Italian subduction boundary. Earth and Planetary Science Letters 311 (3–4), 230-241, doi: 10.1016/j.epsl.2011.09.034.

DISS Working Group, 2010. Database of Individual Seismogenic Sources (DISS), Version 3.1.1: A compilation of potential sources for earthquakes larger than M 5.5 in Italy and surrounding areas. http://diss.rm.ingv.it/diss/, © INGV 2010 - Istituto Nazionale di Geofisica e Vulcanologia - All rights reserved.

Formatted: Indent: Left: 0 cm, Hanging: 0.95 cm

Formatted: Italian (Italy)

Formatted: English (U.S.)

Formatted: Italian (Italy)

Ferranti, L., C. Monaco, C., F. Antonioli, F., L. Maschio, L., S. Kershaw, S. and V. Verrubbi, V., 2007. The contribution of regional uplift and coseismic slip to the vertical crustal motion in the Messina Straits, southern Italy: evidence from raised Late Holocene shorelines. Journal of Geophysical Research, 112, B06401, doi: 10.1029/2006JB004473.

Fracassi, U., Di Bucci, D., Ridente, D., Trincardi, F., and Valensise, G., 2012. Recasting Historical Earthquakes in Coastal Areas (Gargano ~~Promontory~~Promontory, Italy): Insights From Marine Paleoseismology, ~~Bull. Seismol. Soc. Am.,~~ Bulletin of the Seismological Society of America 102, 1, 1-17. doi: 10.1785/0120110001.

~~Gamberi F. and Marani M.P., 2004. Deep sea depositional systems of the Tyrrhenian Basin. In: Marani M.P., Gamberi F. and Bonatti E. (eds), From Seafloor to Deep Mantle: Architecture of the Tyrrhenian Backarc Basin, Memorie Descrittive Carta Geologica d'Italia, LXIV, pp. 127-146.~~

Gasparini, C., Iannacone, G., Scandone, P., and Scarpa, R., 1982. Seismotectonics of the Calabrian Arc. Tectonophysics, 82, 267–286.

Gruppo di Lavoro CPTI, 2004. Catalogo Parametrico dei Terremoti Italiani, versione 2004 (CPTI04). INGV, Bologna, http://emidius.mi.ingv.it/CPTI/.

Guidoboni, E., and J. E. Ebel, 2009. Earthquakes and Tsunamis in the Past, Cambridge Univ. Press, Cambridge, 590 p.

Guidoboni, E., G. Ferrari, G., D. Mariotti, D., A. Comastri, A., G. Tarabusi, G., and G. Valensise, G., 2007. CFTI4Med, Catalogue of Strong Earthquakes in Italy (461 B.C.-1997) and Mediterranean Area (760 B.C.-1500). INGV-SGA. Available from http://storing.ingv.it/cfti4med/.

Kanamori, H., and Anderson, D.L. ~~Anderson~~, 1975. Theoretical basis of some empirical relations in seismology. ~~Bull. Seismol. Soc. Am.,~~ Bulletin of the Seismological Society of America 65, 5, 1073-1095.

Formatted: English (U.S.)
Formatted: English (U.S.)
Formatted: English (U.S.)
Formatted: English (U.S.)
Formatted: English (U.S.)
Formatted: Italian (Italy)
Formatted: Indent: Left: 0 cm, Hanging: 0.95 cm
Formatted: Italian (Italy)
Formatted: Font: Not Italic

Knott, S.D., and E. Turco, 1991. Late Cenozoic kinematics of the Calabrian arc, southern Italy, Tectonics, 10 (6), 1164-1172.

Loreto, M.-F., Zgur, F., Facchin, L., Fracassi, U., Pettenati, F., Tomini, I., Burca, M., Diviacco, P., Sauli, C., Cossarini, G., De Vittor, C., Sandron, D., and the Explora technicians team, 2012. In Search of New Imaging For Historical Earthquakes: A New Geophysical Survey Offshore Western Calabria (Southern Tyrrhenian Sea, Italy), Bollettino di Geofisica Teoreorica e Applicata, 53. doi: 10.4430/bgta0046.

Lunau, M., Lemke, A., Walther, K., Martens-Habbena, W., Simon, M., 2005. An improved method for counting bacteria from sediments and turbid environments by epifluorescence microscopy. Environmental Microbiology 7, (7), 961-968.

Malinverno, A., and Ryan, W.B.F., 1986. Extension in the Tyrrhenian Sea and shortening in the Apennines as result of arc migration driven by sinking of the lithosphere. Tectonics, 5, 227-245.

Martini, M., and Scarpa, R., 1982. Italian earthquakes since 1900. Proc. E. Fermi Summer School in Geophysics, Varenna, Springer-Verlag.

Mattei, M., F. Cifelli, and N. D'Agostino, 2007. The evolution of the Calabria Arc: Evidence from paleomagnetic and GPS observations, Earth Planet. Sci. Lett., Earth and Planetary Science Letters 263, 259–274. doi: 10.1016/j.epsl.2007.08.034.

Michelini, A., Lomax A., Nardi A., and Rossi A., 2006. La localizzazione del terremoto della Calabria dell'8 settembre 1905 da dati strumentali. In: Guerra I. and Savaglio A. (eds.), "8 settembre 1905, terremoto in Calabria", Università della Calabria, 225-240.

Milia, A., Turco, E., Pierantoni, P.P., and Schettino, A., 2009. Four-dimensional tectono-stratigraphic evolution of the Southern peri-Tyrrhenian Basins (Margin of Calabria, Italy). Tectonophysics 476, 41-56. doi: 10.1016/j.tecto.2009.02.030

Monaco, C., and Tortorici, L., 2000. Active faulting in the Calabrian arc and eastern Sicily. Journal of Geodynamics, 29, 407-424.

Formatted: Not Highlight

Formatted: English (U.S.)

Formatted: Font: Not Italic

Formatted: English (U.S.)

Formatted: English (U.S.)

Formatted: English (U.S.)

Formatted: English (U.S.)

Mulargia, F., Balsi, P., Achilli, V., Broccio, F., 1984. Recent crustal deformaitons and tectonics of the Messina Strait area. ~~Geophys. J. R. Astr. Soc.,~~ Geophysical Journal International 76, 369-386.

National Geophysical Data Center / World Data Center (NGDC/WDC), 2012. Global Historical Tsunami Database, Boulder, CO, USA, available at http://www.ngdc.noaa.gov/hazard/tsu_db.shtml

Nieuwenhuize, J., Maas, Y.E.M., Middelburg, J.J., 1994. Rapid analysis of organic carbon and nitrogen in particulate materials. Marine~~.~~ Chemistry~~.~~ 45, 217-224.

Pantosti, D., and Valensise, G., 1990. Faulting mechanism and complexity of the 23 November, 1980, Campania-Lucania earthquake inferred form surface observations. Journal of Geophysical Research 95, B10, 15319-15341.

Patacca, F., Sartori, R., Scandone, P., 1990. Tyrrhenian basin and Apenninic arcs: kinematic relations since Late Tortonian times. Memorie~~.~~ Soc~~.~~ ietà Geol~~.~~ogica Ital~~.~~iana~~,~~ 45, 425–451.

Patacca, F., Sartori, R., Scandone, P., 1993. Tyrrhenian basin and Apennines. Kinematic evolution and related dynamic constraints. In: Boschi, E., Mantovani, E., Morelli, A. (Eds.), Recent Evolution and Seismicity of the Mediterranean Region. Kluwer Academic Publishers, Dordrecht, Netherlands, pp. 161–171.

Patacca, E., Scandone, P., 2004. The Plio-Pleistocene thrust belt – foredeep system in the Southern Apennines and Sicily (Italy). In: Crescenti, U., D'Offizi, S., Merlini, S., Lacchi, L. (Eds.), Geology of Italy. Soc. Geol. It., Roma, 93-129.

Pella, E. and Colombo, B., 1973. Study of carbon, hydrogen and nitrogen determination by combustion-gas chromatography. Microchimica~~.~~ Acta 5, 697-719.

Pepe, F., Sulli, A., Bertotti, G., and Cella, F., 2010~~,~~ Architecture and Neogene to Recent evolution of the western Calabrian continental margin: An upper plate perspective to the Ionian subduction system, central Mediterranean. Tectonics~~,~~ 29, TC3007. doi: 10.1029/2009TC002599.

Formatted: English (U.S.)

Formatted: Font: Not Italic

Formatted: Italian (Italy)

Formatted: Italian (Italy)

Formatted: Italian (Italy)

Peruzza, L., Pantosti, D., Slejko, D., Valensise, G., 1997. Testing a new hybrid approach to seismic hazard assessment: an application to the Calabrian Arc (Southern Italy). Naturala. Hazardsz., 14, 113-126.

Piatanesi, A., and Tinti, S., 2002. Numerical modelling of the September 8, 1905 Calabrian (southern Italy) tsunami. Geophysical. Journal. International., 150, 271-284. doi: 10.1046/j.1365-246X.2002.01700.x.

Pino, N.A., Piatanesi A., Valensise G., and Boschi E., 2009. The 28 December 1908 Messina Straits Earthquake (Mw 7.1): A Great Earthquake throughout a Century of Seismology. Seismological Research Letters 80, 2, 243-259. doi: 10.1785/gssrl.80.2.243.

Pizzino, L., P. Burrato, P., F. Quattrocchi, F., and G. Valensise, G., 2004. Geochemical signatures of large active faults: the example of the 5 February 1783, Calabrian earthquake (southern Italy). J.ournal of Seismology., spec. vol., 8, 3, 363-380. doi: 10.1023/B:JOSE.0000038455.56343.e7.

Postpischl, D., 1985. Catalogo dei terremoti italiani dall'anno 1000 al 1980. Consiglio Nazionale delle Ricerche, Progetto Finalizzato Geodinamica, Graficoop, Bologna, 239 pp.

Ramsay, J.G., and Huber, M.I., 1987. The techniques of modern structural geology. Vol. 2: Folds and Fractures, Academic Press, London, 700 p.

Ravenschlag, K., Sahm, K., Knoblauch, C., Jørgensen, B.B., and Amann, R., 2000. Community structure, cellular rRNA content and activity of sulfate-reducing bacteria in marine arctic sediments. Applied. and Environmental. Microbiology. 66(8), 3592-3602.

Riuscetti, M., and Schick, R., 1975. Earthquakes and tectonics in Southern Italy. Bollettino di. Geofisica. Teorica e. Applicata., 17, 59-78.

Rizzo, G.B., 1906. Sulla velocità di propagazione delle onde sismiche del terremoto della Calabria del giorno 8 Settembre 1905. C. Clausen Ed., 46 pp. Mem. R. Accad. Scienze, Torino, 1905-1906, s. II, Tom. LVII.

Formatted: English (U.S.)
Formatted: English (U.S.)
Formatted: English (U.S.)
Formatted: English (U.S.)
Formatted: Italian (Italy)
Formatted: English (U.S.)
Formatted: English (U.S.)
Formatted: English (U.S.)
Formatted: Indent: Left: 0 cm, Hanging: 0.95 cm
Formatted: English (U.S.)

Rotondi, R., 2010. Bayesian nonparametric inference for earthquake recurrence time distributions in different tectonic regimes. Journal of Geophysical Research: Solid Earth ~~(1978–2012),~~ 115, B01302. doi: 10.1029/2008JB006272.~~(B1),~~

Rovida, A., Camassi, R., Gasperini, P., Stucchi, M. (eds.), 2011. CPTI11, the 2011 version of the Parametric Catalogue of Italian Earthquakes. Milano, Bologna, http://emidius.mi.ingv.it/CPTI.

Sartori, R., 2003. The Tyrrhenian back-arc basin and subduction of the Ionian lithospere. Episodes, 26, 3, 217-221.

~~Sharp, J.H., 1974. Improved analysis for "particulate" organic carbon and nitrogen from seawater. Limnol. Oceanogr., 19, 984-989.~~

Sharp, J.H., 1974. Improved analysis for" particulate" organic carbon and nitrogen from seawater. Limnology and Oceanography, 984-989.

Tansi, C., Muto, F., Critelli, S., and Iovine, G., 2007. Neogene-Quaternary strike-slip tectonics in the central Calabrian Arc (southern Italy). Journal of Geodynamics 43 (3), 393-414.

Tinti, S., and Maramai, A., 1996. Catalogue of tsunamis generated in Italy and in Côte d'Azur, France: a step towards a unified catalogue of tsunamis in Europe. Annali di Geofisica, XXXIX, 6, 1253-1299.

Tertulliani, A., and Cucci, L., 2008. Fenomeni associati al terremoto della Calabria del 1905. Quaderni di Geosifica, ISSN 1590-2595, No. 60.

Tertulliani, A., and Cucci, L., 2009. Clues to the identification of a seismogenic source from environmental effects: the case of the 1905 Calabria (Southern Italy) earthquake. Natural Hazards Earth System Sci., 9, 1787-1803, doi: 10.5194/nhess-9-1787-2009.

Tiberti, M.M., Fracassi, U., and Valensise, G., 2006, Il quadro sismotettonico del grande terremoto del 1905, in: Guerra I. and Savaglio A. (eds.), "8 Settembre 1905: Terremoto in Calabria", Università della Calabria, 181-205.

Formatted: Font: Not Italic
Formatted: Font: Not Italic
Formatted: English (U.S.)
Formatted: Indent: Left: 0 cm, Hanging: 0.95 cm
Formatted: Font: Not Italic
Formatted: Italian (Italy)
Formatted: Italian (Italy)
Formatted: English (U.S.)
Formatted: English (U.S.)
Formatted: Indent: Left: 0 cm, Hanging: 0.95 cm
Formatted: English (U.S.)

Trincardi, F., Corregiari, A., Field, M.E., and Normark, W.R., 1995. Turbidite deposition from multiple sources: Quaternary Paola Basin (eastern Tyrrenian Sea). Journal of Sedimentary Research, 65, 469-483.

Valensise, G., 1988. Low angle normal faulting during the 1908, Messina, earthquake revealed by geodetic data analysis (abstract), Eos Trans., AGU, 69(44), F1433, Fall Meet. Suppl.

Valensise, G., and D. Pantosti, 2001a. Seismogenic faulting, moment release patterns and seismic hazard along the central and southern Apennines and the Calabrian arc. In: G. B. Vai and I. P. Martini (Eds.), Anatomy of an orogen: the Apennines and adjacent Mediterranean basins. Kluwer Academic Publishers, Dordrecht, 2001, 495-512.

Valensise, G., and Pantosti, D., 2001b. The investigation of potential earthquake sources in peninsular Italy: A review. Journal of Seismology, 5, 3, 287-306, doi: 10.1023/A:1011463223440.

van Dijk, J.P., 1991. Basin dynamics and sequence stratigraphy in the Calabrian Arc Central Mediterranean); records and pathways of the Crotone Basin. Geologie en Mijnbouw Geol. Mijnbouw, 70, 187-201.

van Dijk, J.P., 1992. Late Neogene Fore-arc Basin Evolution in the Calabrian Arc (Central Mediterranean); Tectonic Sequence Stratigraphy and Dynamic Geohistory. With Special Reference to the Geology of Central Calabria. Geologica Ultraiectina Geol. Ultraiect., 92, 288 pp.

van Dijk, J.P., Bello, M., Brancaleoni, G.P., Cantarella, G., Costa, V., Frixa, A., Golfetto, F., Merlini, S., Riva, M., Toricelli, S., Toscano, C., and Zerilli, A., 2000. A new structural model for the northern sector of the Calabrian Arc. Tectonophysics, 324, 267-320.

Vannucci, G., and Gasperini, G., 2004. The new release of the Database of Earthquake Mechanisms of the Mediterranean Area (EMMA version 2). Annals of Geophysics, 47, 1, with CD-Rom.

Formatted: Font: Not Italic

Formatted: English (U.S.)

VIDEPI, 2012. Visibilità dei dati afferenti all'attività di esplorazione petrolifera in Italia. © 2009-2012, Progetto ViDEPI - Ministero dello Sviluppo Economico UNMIG - Società Geologica Italiana - Assomineraria, http://www.videpi.com.

Walsh, J.J., and Watterson, J., 1988. Analysis of the relationship between displacements and dimensions of faults. Journal of Structural Geology, 10, 3, 239-247.

Ward, S.N., and Valensise, G., 1989. Fault parameters and slip distribution of the 1915, Avezzano, Italy earthquake derived from geodetic observations. Bulletin of the Seismological Society of America 79, 690-710.

Wells, D., and Coppersmith, K., 1994. New empirical relationship among magnitude, rupture length, rupture width, rupture area and surface displacement. Bullettin of Seismological Society of America, 84, 974-1002, 1994.

Westaway, R., 1992. Seismic moment summation for historical earthquakes in Italy: tectonic implications. Journal of Geophysical ResearchJ. Geophy. Res., 97, 15.437-15.464

Westaway, R., 1993. Quaternary uplift of Southern Italy. Journal of Geophysical Research, 98, (B12), 741-772.

***Highlights (for review)**

- We analysed a multidisciplinary data set to identify the source of the 1905 earthquake
- Our data reveals a NE-trending SE-dipping normal fault (S. Eufemia Fault) displacing modern sediments
- Prokaryotes abundance distribution agree with fluid up-welling along the fault
- We evaluate previous seismogenic source models for the 1905 event in light of this new data
- kinematics , orientation and location of the S. Eufemia Fault satisfies the historical record of the 1905 earthquake required features

Approaching the seismogenic source of the Calabria 8 September 1905 earthquake: New geophysical, geological and biochemical data from the S. Eufemia Gulf (S Italy)

Maria Filomena Loreto[1,2,*], Umberto Fracassi[3], Annalisa Franzo[2,4], Paola Del Negro[2], Fabrizio Zgur[2] and Lorenzo Facchin[2]

[1] Istituto di Scienze Marine – Consiglio Nazionale delle Ricerche, U.O.S. Bologna, Via Gobetti 101, 40129 Bologna, Italy

[2] Istituto Nazionale di Oceanografia e di Geofisica Sperimentale, Borgo Grotta Gigante 42/C, 34010 Sgonico (TS), Italy

[3] Istituto Nazionale di Geofisica e Vulcanologia, Via di Vigna Murata 605, 00143 Roma, Italy

[4] Dipartimento di Science della Vita, Università degli Studi di Trieste, 34127, Trieste, Italy

* Corresponding author: filomena.loreto@bo.ismar.cnr.it; +390516398878; ISMAR-CNR Via Gobetti 101 - 40129 Bologna.

Abstract

Recognizing the seismogenic source of major historical earthquakes, particularly when these have occurred offshore, is a long-standing issue across the Mediterranean Sea and elsewhere. The destructive earthquake (M ~7) that struck western Calabria (southern Italy) on the night of 8 September 1905 is one such case. having various authors proposed a seismogenic source, with apparently diverse hypotheses and without achieving a unique solution. To gain novel insight into the crustal volume where the 1905 earthquake took place and to seek a more robust solution for the seismogenic source associated with this destructive event, we carried out a well-targeted multidisciplinary survey within the Gulf of S. Eufemia (SE Tyrrhenian Sea), collecting geophysical data, oceanographic measurements, and biological, chemical and sedimentary samples.

We identified three main tectonic features affecting the sedimentary basin in the Gulf of S.

Eufemia : 1) a NE-SW striking, ca. 13-km-long, normal fault, here named S. Eufemia Fault; 2) a WNW-striking polyphased fault system; and 3) a likely E-W trending lineament. Among these, the normal fault shows evidence of activity witnessed by the deformed recent sediments and by its seabed rupture along which, locally, fluid leakage occurs. Features in agreement with the anomalous distribution of prokaryotic abundance and biopolymeric C content, resulted from the shallow sediments analyses.

The numerous seismogenic sources proposed in the literature during the past 15 years make up a composite framework of this sector of western Calabria, that we tested against a) the geological evidence from the newly acquired dataset, and b) the regional seismotectonic models. Such assessment allows us to propose the NE-SW striking normal fault as the most probable candidate for the seismogenic source of the 1905 earthquake. Re-appraising a major historical earthquake as the 1905 one enhances the seismotectonic picture of western Calabria. Further understanding of the region and better constraining the location of the seismogenic source may be attained through integrated interpretation of our data together with a) on-land field evidence, and b) seismological modeling.

Keywords: seismogenic source, earthquake, seismotectonics, prokaryotes, Calabrian Arc

1. Introduction

Calabria is one of the Italian regions with the largest concentration of seismic moment release (Fig. 1; Gasparini et al., 1982; Westaway, 1992; Castello et al., 2006; Calò et al., 2012) and highest probability of occurrence of major earthquakes (Rotondi, 2010), mainly located between two main shear zones, the Tindari Fault to the south-west, and the Cirò-Benevento Fault to the north. Most earthquakes affecting Calabria and its western offshore are characterized by a normal fault plane

53 solution (D'Agostino and Selvaggi, 2004; Vannucci and Gasperini, 2004), confined within a
54 continuous extensional belt parallel to the Calabrian Arc.

55 The earthquake that struck western Calabria on the night of 8 September 1905 is one of the
56 strongest events in the Italian catalogue (M_w up to 7.5, according to Michelini et al., 2006), besides
57 the 28 December 1908 earthquake (M_w 7.1), that struck southern Calabria and the Messina Straits,
58 and the numerous ones occurred in the 17th and 18th century, that severely hit large parts of the
59 region (Postpischl, 1985; Boschi et al., 2000; Guidoboni et al., 2007). The 1905 earthquake caused
60 557 deaths (Baratta, 1906), most of them around the Capo Vaticano promontory, with the highest
61 intensity values (Mercalli-Cancani-Sieberg = XI) recorded between the towns of Tropea, to the
62 west, and Vibo Valentia, to the east (Fig. 2; Tiberti et al., 2006). Historical documents reported
63 several triggered ground failures (landslides, rock falls and lateral spreads), hydrological changes
64 (stream-flow variations, liquefaction, rise of water temperature and turbidity), and earthquake
65 "*lights*" and "*sounds*" (Guidoboni et al., 2007; Tertulliani and Cucci, 2008, 2009). Finally, a
66 tsunami, albeit modest, was reported by contemporary observers both in the open sea and along the
67 coast of the S. Eufemia Gulf (see blue small waves in Fig. 2), with few meters of maximum run-up
68 and sea flooding in some beaches up to 30 m (Tinti and Maramai, 1996 and references therein;
69 Guidoboni and Ebel, 2009; NGDC/WDC, 2012).

70 Although this earthquake is one of the most catastrophic ones recorded in the region, poor
71 documentation resulting from this early 20th century event has caused it to go relatively overlooked
72 and not fully understood in terms of magnitude and epicentral location. Uncertain M estimates,
73 particularly when so diverging among each other, and dubious location, especially when the latter is
74 at sea, make earthquake assessment all the more problematic. Together with the underlying
75 geology, these are among the primary ingredients to search the seismogenic source (i.e., the
76 causative fault) of a damaging earthquake, to ultimately enhance the seismic hazard pattern of a
77 given region. To address these issues and to build on the knowledge of the seismotectonic
78 framework and the seismogenic potential of western Calabria, we performed a well-targeted

multidisciplinary survey during the summer of 2010 in the S. Eufemia Gulf (gray transparent square in Fig. 1) aboard the R/V OGS-*Explora*. Biological and geochemical data, collected to detect hydrothermal activity of potential seismotectonic relevance, and evidence stemming from the analysis of geophysical data (multichannel seismic - MCS, sub-bottom profiles - Chirp and high resolution morpho-bathymetry) allowed us to propose a causative source for the 1905 earthquake, while reappraising previously proposed solutions in the light of the new geological evidence.

2. Geological and seismotectonic framework

2.1 Geological Setting

The S. Eufemia Gulf lies between the Calabrian Arc and the SE Tyrrhenian Basin (Fig. 1), which is the Neogene back-arc basin of the Apennines subduction system (Patacca et al., 1990, 1993, 2004, and references therein). Subduction migrated eastward from the Tortonian to Early Pliocene, and south-eastward from the Late Pliocene to Early Pleistocene (Patacca et al., 1990; Sartori, 2003).

The Calabrian arc (Fig. 1) is an independent arcuate continental block (Bonardi et al., 2001) that bridges the NW-SE trending southern Apennines with the SSW-NNE trending Apennines in Sicily. Several authors have considered the Calabrian arc as an uprooted fragment of the Alpine belt (e.g., Amodio-Morelli et al., 1976; Malinverno and Ryan, 1986; van Dijk et al., 2000 and references therein). Its arcuate shape can be attributed to the diachronous collision of the Apennine chain with the Apulian foreland, to the north, and with the Hyblean foreland, to the south (Malinverno and Ryan, 1986; van Dijk et al., 2000). Such collision also controlled (1) the clockwise rotation of Sicily and Calabria, (2) the counter-clockwise rotation of the southern Apennines (Cifelli et al., 2007), that ceased at the end of the Pleistocene (Mattei et al., 2007), and (3) the intense fragmentation of the Calabrian Arc in NW-SE striking blocks (Knott and Turco, 1991; van Dijk, 1991, 1992; Del Ben et al., 2008; Barone at al., 2008). Since the Middle Pleistocene, the Calabrian

105 Arc experienced rapid uplift of up to ca. 1 mm/y (Westaway, 1993; Bordoni and Valensise, 1998;
106 Anzidei et al., 2012) and a ESE-trending forearc advancement, shown by GPS data (D'Agostino et
107 al., 2011; Devoti et al., 2011). Uplift was in part accommodated by major normal faults (Monaco
108 and Tortorici, 2000; Catalano et al., 2003), frequently bounded by NW-SE striking shear zones
109 (Fig. 1; van Dijk, 1991; Tansi et al., 2007).

110 The sedimentary basin hosted by the S. Eufemia Gulf is bounded by the Capo Vaticano
111 promontory to the south, by the Calabrian landmass to the east, and by the steep submarine slope
112 extending to the Marsili abyssal plain to the west (Figs. 1 and 2). The S. Eufemia basin is filled by a
113 ca. 2-km-thick, Plio-Quaternary sequence, overlying intensely deformed Miocene units (Argnani
114 and Trincardi, 1993; Milia et al., 2009; Loreto et al., 2012). The S. Eufemia slope basin (Argnani
115 and Trincardi; 1993) includes several turbiditic, large mass-failure and drape deposits (Trincardi et
116 al.,1995). Finally, Milia et al. (2009) identified a sub-vertical fault system showing a polyphased
117 history, coeval with the early N-S extensional phase.

118

119 *2.2 Seismogenic source models of the 1905 earthquake*

120 Numerous epicentral locations and M_w estimates of the 8 September 1905 earthquake have been
121 proposed in the literature. According to Rizzo (1906), Boschi et al. (2000), and Guidoboni et al.
122 (2007), the epicenter of the earthquake was onshore (Fig. 2), whereas Riuscetti and Schick (1975),
123 Camassi and Stucchi (1997), Michelini et al. (2006), and a recent macroseismic study by Rovida et
124 al. (2011) all place the epicenter offshore (Fig. 2). Assigned magnitudes range from instrumental
125 estimates of M 7.0 (Martini and Scarpa, 1982) and M 7.5 (Michelini et al., 2006), to the
126 macroseismic ones of M 6.7 (Guidoboni et al., 2007), M 7.0 (Gruppo di Lavoro CPTI04, 2004;
127 Rovida et al., 2011) and M 7.1 (Postpischl, 1985).

128 Over the past 15 years, various researchers hypothesized a possible seismogenic source
129 responsible for the 1905 earthquake (see Table 1, Fig. 3). Peruzza et al. (1997) presented the first
130 seismotectonic model for the largest Calabrian earthquakes, proposing a segmentation model with

large normal faults sub-parallel to the extensional axis of western Calabria. For the 1905 earthquake case, these authors maintained an E-dipping, NNE-SSW striking source (PE in Fig. 3), based on an onshore epicenter. Monaco and Tortorici (2000) presented a seismotectonic model of the Calabrian Arc and eastern Sicily and proposed causative faults for key destructive earthquakes. For the 1905 event, these authors hypothesized the Capo Vaticano Fault, a NW-dipping, NE-SW striking normal fault (MT in Fig. 3), with an offshore epicenter.

Valensise and Pantosti (2001b) presented a regional seismogenic source model and proposed a 40-km-long, SE-dipping, NE-striking normal fault near the edge of the S. Eufemia Gulf (VP in Fig. 3), and extending on land. Searching for an explanatory source of the tsunami associated with the 1905 earthquake, Piatanesi and Tinti (2002) parameterized the Capo Vaticano and the Vibo Valentia faults (Monaco and Tortorici, 2000), two NW-dipping, NE-SW striking normal faults straddling the northern shore of the Capo Vaticano promontory and the internal sector of the gulf (CV and VV in Fig. 3; Table 1). Finally, Cucci and Tertulliani (2006; 2010) suggested the Coccorino Fault, a 29-km-long S-dipping, WNW-ESE striking normal fault affecting the southern sector of the Capo Vaticano promontory and the northern Gioia Tauro Plain (CT in Fig. 3).

3. Data and Methods

3.1 Geophysical data

Nine multichannel seismic profiles, organized in a tight grid (thin yellow lines in Fig. 4) were acquired using a 1500-m-long streamer cable, with a 120-channels array and a 12.5 m trace interval. The energy source consisted of two GI-guns with a total volume of 8 liters shot every 25 m, with a resulting seismic coverage of 30 for each investigated depth point. The seismic data were processed following a standard procedure, in order to get post-stack time migrated seismic sections. More details about acquisition parameters and processing performed to improve Signal/Noise ratio can be found in Loreto et al. (2012).

More than 2200 km of sub-bottom profiles (Chirp) were acquired using a Benthos CAP-6600, consisting of 16 keel mounted transducers. Sweep ranges between 2 and 7 kHz, with the resulting configuraton ensuring a full ocean depth investigation. Chirp data image in detail the uppermost section of the sedimentary cover down to a ca. 75 m depth, assuming a constant 1550 m/s sound speed within the shallowest sediments.

The high resolution morpho-bathymetric map (Fig. 4) was obtained using two hull mounted multibeam echosounders, a Reson Seabat 8111 (100 kHz) and 8150 (12 kHz). We employed the Seabat 8111 up to 400 m depth (maximum swath width of 7.4 times the water depth), the Seabat 8150 for water depth >500 m (maximum swath width of 4.5 times the water depth), and both echosounders for the 400-500 m depth range. The data were processed to remove spikes due to navigation system problems and/or to the acquisition system.

3.2 Chemical, biological and oceanographic data

We collected 12 biological samples (white triangles in Figs. 4), at the top of gravity cores using a sterile spoon and frozen at -20 °C, and performed 10 CTD (Conductivity-Temperature-Depth) profile measurements in the sector near the tectonic features recognized in the multichannel data. These samples were used to evaluate prokaryotic abundance, and to perform Total Carbon (TC), Total Nitrogen (TN), and Total Organic Carbon (TOC) chemical analyses.

For TC, TN and TOC analyses, triplicate sub-samples of homogenized and freeze-dried sediment (< 250 μm) were weighed directly in capsules (5x9 mm). Before the TOC determination, sub-samples were treated with increasing concentrations of HCl (0.1N and 1N) to remove carbonates, following the procedure by Nieuwenhuize et al. (1994). Carbon and nitrogen were determined using a CHNO-S elemental analyzer according to the methods of Pella and Colombo (1973) and Sharp (1974). Sub-samples of homogenized sediment were freeze-dried and processed to determine carbohydrates, lipids, and proteins following the procedure described by Cibic et al.

(2008). The sum of carbohydrates, lipids and proteins carbon was referred to as Biopolymeric Carbon (BPC).

Prokaryotic abundance was determined using the centrifugation method by Ravenschlag et al. (2000) and a modified protocol by Lunau et al. (2005). Sediment samples were diluted to a final concentration of 1:110 and filtered on black Nuclepore polycarbonate 0.2-µm-pore-size filters. Filters were mounted on microscope slides, stained with a SYBR Green I-mounting medium Mowiol solution (1:15) and counted by epifluorescence microscopy (LEICA DM2500) at 1000 X magnification under a blue filter set (BP 450-490 nm, BA 515). A minimum of 300 cells were accounted for each filter in at least 40 randomly selected fields.

The CTD measurements are done using the sea-bird electronics (SBE) 911plus system with sensors mounted on the Carousel SBE32 frame with 12 Niskin bottles. We measured: Pressure (db), Conductivity (mS/cm), Temperature (°C), Oxygen (uA0), Fluorescence (ug/l), and optical backscatter, with a 10^{-3} accuracy. Lacking a high accuracy altimeter, the last measurement was done at ca. 10 m from the seafloor to avoid problems of interaction with the seafloor morphology.

4. Results

4.1 Morpho-bathymetric features

Our high resolution morpho-bathymetric data (Fig. 4) allowed us to identify some key features: 1) a large submarine Angitola canyon, already shown by Argnani and Trincardi (1988), characterized in the near-shore part of the gulf by an unusually straight trend, ca. ENE-WSW oriented for about 20 km, and in the distal part by a meandering trend; 2) a NW-SE oriented morpho-structural high (hereafter: MS-High) offshore the town of Tropea, recognized as the seaward prolongation of the Capo Vaticano promontory, surrounded by several slide scars (Loreto et al., 2012). However, a more detailed analysis (Fig. 5) allowed us to identify other noteworthy features, between the northern internal slope of the gulf and the Angitola Channel, such as small slides or slumps (see

white thick arrows) and a prominent N31°-trending, 3-m–high, 8–km-long scarp, well visible across the 150-m contour line (i.e., the shelf break; see inset in Fig. 5).

4.2 Tectonic features

Seismic profile GSE10-05, NE-SW oriented (Fig. 4), shows a thick and well stratified sedimentary sequence overlying a poorly reflective and poorly stratified sequence (Fig. 6). Based on previous works (Argnani & Trincardi, 1993; Trincardi et al., 1995; Milia et al., 2009; Pepe et al., 2010) and on evidence from the Marisa industrial well (Figs. 4 and 7; VI.D.E.PI. Project, www.videpi.com), the imaged sequence probably is the Plio-Quaternary basin infill deposited on top of the Miocene, which correspond to the Messinian units. Data from the Marisa well lack the upper part from Pleistocene to present that could be associated with the uppermost, condensed layer. The boundary between the Miocene and Pliocene generates a strong acoustic contrast, due to lithology, seismically associated with a high amplitude horizon, here defined Top Horizon.

The southern levee of the Angitola Channel (SL; Fig. 6) shows a scarp 200 ms high, i.e. 150 m, assuming a fixed seismic water velocity of 1500 m/s. Sediments next to the levee show gentle folding (see black thick arrow) involving only the well-stratified Plio-Quaternary sequence leaving the Top Horizon undisturbed. Combined with these elements, the straight trend of the Angitola Channel leads us to hypothesize that a shallow ca. E-W striking fault (see AF? in Fig. 6, box and inset), with a likely strike-slip motion, passively controls the edge of the channel (Loreto et al., 2012).

Plio-Quaternary sediments of the central basin (Fig. 6) are deformed by two gentle wide anticlines, the main one controlled by the compressional phase of a SW-dipping fault. Folding decreases with depth and fades out at mid-sequence (see black dot). The underlying sediments thicken into a syn-rift sequence controlled by the extensional phase of the bordering fault. Assuming a constant seismic velocity of 2200 m/s for Plio-Quaternary sediments (Pepe et al., 2010; Marisa well), we estimate that the Top Horizon is offset ca. 350 m (see Trc num 6150 in Fig. 6). We

234 interpret such deformational style as due to a N93° striking Polyphased Fault (from here on, PF)
235 and 58° SSW-dipping (Fig. 6, inset), visible in two seismic profiles (GSE10_04A and GSE10_05).
236 Upward, contraction abruptly stops below a thick and chaotic body perching in stratigraphic
237 unconformity (dotted line; Fig. 8). There is no evidence of surface rupture, such as a scarp on the
238 seafloor (Fig. 8, left), confirming that PF is sealed by the upper section of the Plio-Quaternary
239 deposits.

240 The analysis of the E-W-striking GSE10_07 seismic profile (Figs. 4 and 9) allowed us to
241 identify two main features: 1) the Angitola Channel characterized by steep and deep levees, to the
242 west; and 2) a normal fault extending through the whole imaged sedimentary succession, to the east
243 (Fig. 9, Box). Discontinuities and deformations of the Plio-Quaternary sediments, expressed as
244 gentle folds in the foot-wall (thick white arrows) and small drag folds (thick black arrow) in the
245 hanging-wall, can be recognized within older and recent sediments (Fig. 9, Box). These folded and
246 faulted recent deposits are well imaged on Chirp profile CH_39 (Fig. 10B), acquired north of
247 seismic profile GSE10_07, that crosses the notable scarp on the high-resolution morpho-
248 bathymetric data (Fig 5). Northward over the seafloor scarp zone, the discontinuities and
249 deformations affect the shallow deposits without reaching the seafloor (see chirp profile CH_52 in
250 Fig. 10C); farther north, the deformation of the recent sediments strongly decreases and only a
251 weak, structurally-controlled offset is detectable (see chirp profile CH_71 in Fig. 10D). Combining
252 evidence from all geophysical data (MCS, Chirps, and bathymetry), we mapped a N31° trending,
253 38° ESE-dipping, ca. 13-km-long normal fault rupturing the seafloor for about 8 km along strike
254 (Figs. 9, Box and 10).

255 Assuming a constant seismic velocity of 2200 m/s for Plio-Quaternary sediments, the
256 normal fault, that here we call S. Eufemia Fault (Fig. 10), offsets the upper Miocene top about 460
257 m. Using fault scaling relationships by Walsh and Watterson (1988) to compute fault length from
258 cumulative offset, we estimate that the S. Eufemia Fault length ranges from 20 to 30 km, much
259 longer than the 13 km we measured on the geophysical data (see Fig 10). In other words, the S.

Eufemia Fault credibly propagates along-strike toward the mainland, to the north-east and to the south-west. Considering an estimated median fault length of 25 km, and based on formulations by Wells and Coppersmith (1994) and by Kanamori and Anderson (1975), we estimate a M_w ranging from 6.5 to 6.8, respectively (Table 2) - the latter being directly influenced by the amount of slip per event. Based on data from comparable Italian earthquakes with normal faulting mechanism, like the 1908 Messina-Reggio Calabria one (Valensise, 1988; Amoruso et al., 2002; Pino et al., 2009), we infer 2 m to be a credible slip amount, which therefore leads us to tentatively adopt M_w 6.8 for this fault.

4.3 Chemical and biological analyses

The stations (St.) sampled . for chemical and biological parameters in the sediments can be grouped into three transects (see white triangles in Figs. 4 and 11), with inshore-offshore direction and located a) north (N Tran. in Fig. 11), b) along (AC Tran. in Fig. 11), and c) south (S tran. in Fig. 11) of the Angitola channel. Water temperature close to the sea-bottom was almost constant in all stations and varied in a range of 13.97 °C (St. 3) - 14.18 °C (St. 12).

The results of both chemical and biological parameters are reported in Table 3. TN, TC and TOC did not show any evident difference among stations, except for the southern transect, along which we observed a small decreasing gradient from inshore to offshore. Proteins were the main constituent of the BPC, followed by lipids and carbohydrates (Fig. 12, left). Their values did not change remarkably among stations with the exception of St. 7, characterised by the highest proteins content (1623 ± 25 µg C g_{dry}^{-1}; Table 3). The other components of the BPC (lipids, CHO-H_2O and CHO-EDTA) showed a slightly higher variability and no evident pattern was detected (Fig. 12, left). Along the Angitola channel, carbohydrates extracted in EDTA were higher than in the other stations (Table 3). Prokaryotic abundance in the sediment showed a great variability among stations, particularly along the Angitola channel (Fig. 12, right). The lowest density was measured

286 at St. 11 (0.70 ± 0.05 10^8 cells g_{dry}^{-1}), whereas the maximum at St. 7 (2.94 ± 0.38 10^8 cells g_{dry}^{-1}).
287 A strong variability was also observed along the northern sector, where a strong increase of the
288 prokaryotic abundance was recognized at St. 12.
289
290 *4.4 Physical parameters of CTD measurements*
291 CTD profiles were analyzed focusing on the temperature close to the bottom of each profile, i.e.
292 looking for signals of geothermal activity. The standard deviation evaluated for each profile at its
293 bottom and 5 m above gives no evident anomalous signal – thus ranging within the variability of a
294 significant statistical test. The lack of variability in temperature detection close the seafloor could
295 be partially justified by the distance of the CTD measurement from the seafloor (at least 10 m).
296
297
298 **5. Discussions**
299 The aim of this paper is to contribute with sub-surface offshore data and interpretations to identify
300 the possible seismogenic source of the 8 September 1905 earthquake, contributing to better
301 constrain its location and M_w, using a unique approach.
302 Evidence from MCS data analysis (Figs. 6 and 9) allowed us to identify three faults that
303 deform the deposits of the S. Eufemia basin: 1) the Angitola Fault (Fig. 6, Box); 2) the Polyphased
304 Fault in the central part of the gulf (Fig. 6); and 3) the S. Eufemia Fault (Fig. 9).
305 The Angitola fault is identifiable by its tectonic control on the straight trend of the Angitola
306 Channel, and by the steep and deep levees associated with a >150 m bathymetric offset (Fig. 6,
307 Box). Deformation rapidly decreases with depth and fades out before reaching the Messinian top
308 (Fig. 6). AF, therefore, is a shallow (if long) structural feature with no basin-wide tectonic role,
309 showing that it has no causative relationship with the 1905 earthquake or any earthquake at all.
310 The Polyphased Fault deforms the deeper sedimentary stack and the Messinian top, clearly
311 showing positive inversion features (Fig. 6). In the shallower stack, this fault is associated with

anticlines, and deformation is accommodated along several sub-parallel secondary faults buried below a thick chaotic body (Fig. 8). This fault system is long-lived, well organized through the pre-Messinian sequence and has affected the central part of the S. Eufemia basin. However, it does not extend through the upper part of the Plio-Quaternary deposits and therefore has no present-day tectonic activity. Like with the Angitola Fault, no relationship can be established between the Polyphased Fault and the 1905 earthquake.

The S. Eufemia Fault is an active normal fault, sub-parallel to the large normal faults that control the basins in the western Calabrian mainland (i.e., the Mesima and the Gioia Tauro basins). Its dip-slip kinematics appears to have been consistent at least since the late Miocene, as shown by the MCS profiles for the full sedimentary stack (Fig. 9, Box) and by Chirp data for its shallower section (Fig. 10). The S. Eufemia Fault is properly oriented with (1) fault plane solutions derived for earthquakes occurred offshore to the NW (Mulargia et al., 1984), and (2) current extensional tectonics of western Calabria (Westaway, 1993; Bordoni and Valensise, 1998; Monaco and Tortorici, 2000; Catalano et al., 2003; Pizzino et al., 2004; Ferranti et al., 2007). Moreover, this fault shows a 8-km-long and up to 3-m-high scarp (Fig. 5) associated with the cut-off of the fault plane rupture, located near shore. Such scarp occurs close to (1) the maximum damage area of the 1905 earthquake, and to (2) the coastal strip between Vibo Marina and Tropea, inundated by the tsunami associated with the 1905 earthquake (Guidoboni et al., 2007; Fig. 2). Although such seafloor rupture may not necessarily be the direct trigger of the tsunami associated with this event, it is possibly a favorable factor (NGDC/WDC, 2012). Biological data analysis provides some indications about the recent activity of the S. Eufemia Fault in terms of seafloor heterogeneity and fluids circulation, which could be associated with the fluid up-welling from deep sediments. The presence of active faulting could influence the water currents at a local scale, favoring the accumulation of organic matter at the seafloor (Danovaro et al., 2010 and references therein). Data from shallower stations show more labile compounds (Danovaro et al., 1998) as colloidal carbohydrates, which promote microbial activities, thus supporting high abundances as those

observed at St. 7 and St. 8 (Fig. 12, left; de Brouwer and Stal, 2001). On the other hand, moving offshore along the Angitola channel, the labile compounds probably decrease due to preferential use by prokaryotes. Although available, the prokaryotic community could be less supported by the refractory organic fraction, harder to degrade, and this could partially explain the limited abundances at the offshore stations. An exception is represented by St. 4, characterized by high prokaryotic density not supported by the high biopolymeric C content (Fig. 12). This anomaly could be explained considering that St. 4 is located at the border of the Angitola channel (Figs. 4 and 11), along which water enriched by organic matter can flow.

Along the southern transect, the high organic content at St. 8 suggests the presence of up-welling fluids, which could represent an alternative source of carbon and energy for the microbial community. Prokaryotes with particular metabolisms (as chemiosynthetic ones) could in fact be enhanced and their proliferation could support the other trophic levels explaining partially the high biopolymeric C values observed (Fig. 12, left). Even if not supported by the low organic matter content, also the high prokaryotic abundance at St. 12 (Fig. 12, right), located along the seafloor trace of the S. Eufemia Fault (Figs. 4 and 10, left), could be explained in part by the presence of deep fluids, not necessarily warm, up-welling along the fault plane, which act as a source of carbon (Fig. 12, left). Such hypothesis is in agreement with the small fluid escape detected on the Chirp profile (Fig. 10B).

Concerning the geometrical parameters of the S. Eufemia Fault, its measured length of only 13 km (Fig. 10A) and its total displacement of 460 m lead us to infer a (much) longer fault, at least for two simple reasons:

a) a stratigraphic one: the southwesterly strand of the S. Eufemia fault is buried below the Angitola channel system that completely masks any fault deformation clues; and

b) a tectonic one: all field and experimental observation of normal faults consistently show decreasing throw towards fault tips (for a reference: Ramsay and Huber, 1987), as suggested by the decreasing deformation toward the northeast (Figs. 10B, C, and D).

From the macroseismic M_w estimates ranging between 6.7 and 7.0 (Gruppo di Lavoro CPTI04, 2004; Guidoboni et al., 2007; Rovida et al., 2011), the expected fault length derived using empirical relationships by Wells and Coppersmith (1994) and Kanamori and Anderson (1975) should exceed our estimated 25 km, as suggested by field evidence for other Italian earthquakes of the same M_w range (see: Ward and Valensise, 1989; Pantosti and Valensise, 1990; Burrato and Valensise, 2008; Pino et al., 2009). It would, however, be close to the 20 to 30 km range inferred using Walsh and Watterson (1988) formulations (see em20 and em30 in Fig. 13A). On the other hand, instrumental estimates ranging from M 7.0 (Mulargia et al., 1984) to M 7.5 (Michelini et al., 2006) require up to a >>50 km expected fault length. Given the epicentral locations proposed by these authors and by Riuscetti and Schick (1975), such fault should lie entirely offshore, west of Capo Vaticano, causing a long-wave and long-term imprint on the geology offshore central Calabria, to-date not recognized on data. Based on the current set of knowledge and on the geological evidence in our data, we prefer a conservative approach, considering 6.8 to 7.0 as a fairly reliable estimate range (Fig. 13; Table 2). In fact, it is certainly true that poorly located moderate-size earthquakes are associated with uncertain M_w estimates, especially when a novel location can be constrained offshore by geological means (see an example in Fracassi et al., 2012).

Finally, although our data cover only the marine sector of the S. Eufemia Gulf, they fall in a broader seismotectonic context (Fig. 13) and shed some light on possible contradictions among the various seismogenic faults / source models previously proposed, so different from one another (Fig. 3, Table 1).

In chronological order, length (22 km) and dip direction (SE) of PE (Peruzza et al.; 1997) are consistent with our data, thus making PE an interesting source model, although lying essentially onland. MT (Monaco and Tortorici; 2000) dips to the NW and lies in part within our survey's boundaries but is not shown on our data. Therefore, MT is not likely to affect the inner Gulf, while it could affect the NW flank of the Capo Vaticano promontory, and would belong to an entirely distinct fault system. VP (Valensise and Pantosti; 2001b) is the longest possible source in the

390 literature (40 km). Our data show no evidence of this source, which however is interestingly sub-
391 parallel to the S. Eufemia Fault, with same dip direction, like PE.

392 CV (Piatanesi and Tinti, 2002) is essentially MT, although dipping at very high angle; given
393 its location, same considerations done for MT apply for CV. VV (Piatanesi and Tinti, 2002), a NW-
394 dipping high-angle normal fault, lies outside our survey's boundaries and we therefore cannot verify
395 its geometry and role. However, since its rupture would occur onland, one would likely need to
396 invoke other nearby phenomena to account for the tsunami, such as large submarine slides, which
397 our marine data do not show. We therefore doubt that VV can be considered as a viable
398 seismogenic source for the 1905 earthquake. On the other hand, MT/CV's location and geometry
399 seems to conflict with the S. Eufemia Fault, for which we gathered positive evidence from our data.

400 CT (Cucci and Tertulliani, 2010) is located away from the area of maximum damage of the
401 1905 earthquake, along a regional transverse structure. Maximum damage is expected to occur in
402 and near the hanging-wall of CT, which however is not the case here (major damage is located way
403 north of CT's foot-wall). Therefore, while we clearly have no geological data to discuss CT, we
404 doubt it can be associated with the 1905 earthquake.

405 Based on the above considerations, we believe that the S. Eufemia Fault redraws the
406 seismotectonic understanding of this sector of western Calabria (Fig. 13), and that it proves to be a
407 credible candidate as a seismogenic source model for the 1905 earthquake.

408

409

410 **6. Conclusions**

411 Uncertain epicentral location and M estimate of large historical earthquakes that have occurred at
412 sea yet caused major damage on-land often hamper the correct understanding of such destructive
413 events. In a region such as Calabria, with its numerous seismic crises and puzzling catastrophic
414 earthquakes that have occurred in a relatively narrow landmass, identifying the likely seismogenic
415 source that could be associated with the 8 September 1905 event is of key relevance to correctly

evaluate the seismogenic potential of this area and its seismic hazard. To contribute to this goal, we present a multidisciplinary study that brings together evidence from our data to shed new light on the seismo-tectonics of central-western Calabria.

Our geophysical data allowed us to identify three tectonic features in the Gulf: 1) the Angitola Fault, which deforms only shallower sediments; 2) the Polyphased Fault system, currently buried below a thick chaotic body; and 3) the N31°-striking S. Eufemia normal Fault, rupturing the shallow deposits for 13 km along-strike, that dips to the southeast and extends through the whole sedimentary stack up to the seabed. Among these structures, the S. Eufemia Fault is the only active one and compatible with the 1905 earthquake required features, i.e.: 1) expected fault size suitable for the macroseismic M_w range, 2) a 8-km-long seabed rupture, corresponding to the up-ward prolongation of the fault plane, compatible with the occurrence of a tsunami, 3) location fitting the distribution of the maximum damage area, and 4) geometry in agreement with the regional seismotectonic model of the Calabria block. In light of these factors, we maintain that the S. Eufemia Fault is the most credible seismogenic source for the 1905 earthquake, also against the critical review of source models proposed in the literature.

Recent activity of the S. Eufemia Fault is also witnessed by the fluid escapes detected close to the seafloor. Such evidence is also confirmed by the high Prokaryotes abundance and biopolymeric C content distribution that we tentatively explain with deep fluids, locally up-welling along the fault plane, acting as source of carbon.

Despite the undersized length of the rupture associated with the S. Eufemia Fault, cumulative displacement indicates that this fault is likely at least as long as the basin itself and spans along-strike the whole Gulf - possibly beyond into the mainland. Geomorphological survey, drainage basin evolution and displacement modeling are the premier tools of another on-going study to test our hypothesis against field and regional evidence, to understand how this major tectonic feature falls within the fault network described in previous studies.

Captions:

Figure 1 - A) Structural sketch of the Southern Apennines and Calabrian Arc, simplified by Catalano and Sulli (2006) and van Dijk et al. (2000); slip vectors from D'Agostino and Selvaggi (2004). Shaded relief modified © Google Earth, using data by SIO, NOAA, U.S, Navy, NGA, and GEBCO. Small red dots represent M_w>3 instrumental earthquakes recorded since 2000 up to-date, from INGV Seismic Bulletin (ISIDe: http://iside.rm.ingv.it). SM = Strait of Messina.TF = Tindari Fault; CBF = Cirò-Benevento Fault.

Figure 2 - Morpho-bathymetric map of the study area (from NOAA satellite data http://topex.ucsd.edu/WWW_html/mar_topo.html; contour interval: 50 m), showing intensities distribution (Mercalli-Cancani-Sieberg scale) caused by the 1905 earthquake and the seismogenic faults associated with it in the literature: 1) Capo Vaticano Fault (Monaco and Tortorici, 2000); 2) Vibo Valentia Fault (Piatanesi and Tinti, 2002); 3) Coccorino Fault Zone (Cucci and Tertulliani, 2006, 2010); 4) Angitola Fault (Peruzza et al., 1997; Valensise and Pantosti, 2001a); 5) Angitola Fault (Valensise and Pantosti, 2001b). Notice that the highest damage was reported on the northern flank of the Capo Vaticano Promontory. Yellow stars indicate the 1905 epicentral locations proposed by (S1) Riuscetti and Schick (1975), (S2) Camassi and Stucchi (1997), (S3) Boschi et al. (2000) and Guidoboni et al. (2007), (S4) Rizzo (1906), and (S5) Michelini et al. (2006). Blue waves indicate the tsunami effects recorded by contemporary observers (data from Tinti and Maramai, 1996).

Figure 3 – Source models of the 8 September 1905 earthquake derived from the literature, based on seismogenic faults in Fig. 2 (data in Tab. 1). Inset 1: conceptual model of geometry and parameters. Inset 2: list of source models and associated studies.

Figure 4 - Image of the high resolution morpho-bathymetric map. Thin yellow lines indicate the newly-acquired seismic dataset; white triangles show locations of the oceanographic and geo-biological measurements; the blue circle show location of the industrial Marisa well. The seismic profiles described later are shown by thick yellow lines. Grey shade: mainland

Figure 5 - High resolution morpho-bathymetric map, with a detail (inset). The white dashed line underlines the Angitola Channel (AC) trend; thick white arrows highlight the several minor incisions and slide. LMT, Lametia Terme; Br., Briatico.

Figure 6 – Time migrated seismic profile GSE10_05 located in the central part of the S. Eufemia Gulf; interpreted faults are indicated with dashed black lines. Box (left): the likely dip-slip fault affecting the Angitola channel is indicated as AF ? = Angitola Fault; the point where fault offsets is null (null point) is indicated with a black dot; SL indicates the southern levee. Inset: bathymetric map showing a sketch of the two faults location.

Figure 7 - Marisa well plotted on the nearest seismic profile, GSE10_02 (location in Fig. 4), running parallel to the fault plane.

Figure 8 -– Left: high resolution morpho-bathymetry of the area surrounding the Polyphased Fault (thick red line). Right: a detail of the upper part of the Polyphased Fault system deforming the central part of the S. Eufemia sedimentary basin (Fig. 6).

Figure 9 - Time migrated seismic profile GSE10-07 located close to the continental shelf (see location in Fig. 4). Faults are shown as dashed black lines; AC = Angitola Channel; white thick

491 arrows indicate gentle folds, while the black one indicates the drag fold. Inset: bathymetric map
492 showing a sketch of the normal fault location.
493
494 **Figure 10 –** A) high resolution morpho-bathymetric map showing the location of the S. Eufemia
495 Fault, including the segment recognized on the geophysical data (thick black line encircled by a thin
496 rectangle around the seafloor rupture) and the one derived from analytical relationships (dashed
497 black line). B) part of Chirp profile 39 crossing the outcropping fault plane. C) part of Chirp profile
498 52 crossing the fault plane and shallow sediments deformation. D) part of Chirp profile 71 crossing
499 the fault plane deforming shallow sediments without reaching the seafloor.
500
501 **Figure 11 -** Location map of biological samples (white triangles), whose analysis results are listed
502 in table 3. N tran. = Northern transect; AC tran. = Angitola Channel transect; S tran. = Southern
503 transect.
504
505 **Figure 12** – Left: Biopolymeric C content and its composition measured at the twelve stations,
506 grouped in the three transects. The arrows indicate the near shore to offshore direction. CHO-EDTA
507 = carbohydrates extracted in EDTA; CHO-H2O = colloidal carbohydrates. Right: prokaryotic
508 abundances measured at the twelve stations grouped in the three transects. The arrows indicate the
509 near shore to offshore direction.
510
511 **Figure 13** – A) sketch map including the Sant'Eufemia Fault (thick red box) seismogenic source
512 against: a) source models based on causative faults of the 8 September 1905 earthquake available in
513 the literature (see Fig. 2 and 3; Table 1), and b) Individual Seismogenic Sources from DISS 3.1.1
514 (DISS Working Group, 2010). The length of the two end members (em20 and em30) derived from
515 the Walsh and Watterson (1988) empirical relationship (20 and 30 km fault length, respectively).
516 Notice that em30 reaches into the mainland beyond the Gulf's extents. Among em20 and em30, we

517 adopted a conservative median length of 25 km. See parameters and explanations in Table 2. B)
518 morpho-structural map combining the satellite-derived bathymetry
519 (http://topex.ucsd.edu/WWW_html/mar_topo.html; contour interval: 50 m) and the main on-land
520 faults (modified after Monaco and Tortorici, 2000; Pizzino et al., 2004; Tansi et al., 2007) and the
521 offshore faults identified on our geophysical dataset.
522
523 **Table 1 -** Parameters for the source models causative of the 8 September 1905 earthquake available
524 in the literature (see also Fig. 2). IDs identify models taken from the following papers: PE =
525 Peruzza et al. (1997); VP = Valensise and Pantosti (2001b); MT = Monaco and Tortorici (2000);
526 CV = Capo Vaticano Fault, in Monaco and Tortorici (2000), parameters by Piatanesi and Tinti
527 (2002); VV = Vibo Valentia Fault, in Monaco and Tortorici (2000), parameters by Piatanesi and
528 Tinti (2002); CT = Cucci and Tertulliani (2010). Note that source model parameters were available
529 only for Peruzza et al. (1997) and for Piatanesi and Tinti (2002), while in most cases L (Length)
530 was deduced from mapped fault trace; we computed W (Width) and the remaining parameters using
531 empirical and analytical relationships. TD and BD are top and bottom depth, respectively; Sl is slip;
532 M_w (W&C) and M_w (K&A) are computed using formulations by Wells and Coppersmith (1994) and
533 Kanamori and Anderson (1975), respectively.
534
535 **Table 2** - Parameters for the source model deduced from the SE (S. Eufemia) Fault. First and
536 second row list the two end-members (20 and 30 km legnth, respectively); third row lists the source
537 with the median length (25 km), that we adopted in this study. ID identifies the source model. TD
538 and BD are top and bottom depth, respectively; Sl is Slip; M_w (W&C) and M_w (K&A) are computed
539 using formulations by Wells and Coppersmith (1994) and Kanamori and Anderson (1975),
540 respectively. L is Length inferred using cumulative displacement of the Miocene reflector, *sensu*
541 Walsh and Watterson (1988); W is Width computed using empirical and analytical relationships.
542 Dip is constrained using averaged Vp velocity and adjacent wells.

Table 3 - Values and standard deviation (SD) of the chemical and biological parameters. TN = Total Nitrogen; TC = Total Carbon; TOC = Total Organic Carbon; CHO-H_2O = colloidal carbohydrates; CHO-EDTA = carbohydrates extracted in EDTA.

Acknowledgements

We wish to thank OGS that supported the acquisition of the multidisciplinary dataset in the frame of the ISTEGE (Indagine Sismotettonica del TErremoto dell'8 Settembre 1905 (Mw 7.4) nel Golfo di Sant'Eufemia - offshore tirrenico calabrese) project. Special thanks are due to Drs. Vedrana Kovacevic and Giampiero Cossarini (OGS) who performed the temperature (CTD) data analysis, and to Drs. Gianluca Valensise and Salvatore Barba (INGV), and Dario Civile (OGS) for the fruitful scientific discussions. Finally, we wish to thank the R/V *OGS-Explora* technicians' team. Remarks by two anonymous referees and the Editor greatly enhanced this manuscript. Seismic data interpretation was managed using the Kingdom software (IHS, Global Inc.). This paper is ISMAR-CNR contribution.

References

Amodio-Morelli, L., Bonardi, G., Colonna, V., Dietrich, D., Giunta, G., Ippolito, F., Liguori, V., Lorenzoni, P., Paglionico, A., Perrone, V., Piccarreta, G., Russo, M., Scandone, P., Zanettin-Lorenzoni, E., and Zuppetta, A., 1976. L'Arco Calabro-Peloritano nell'orogene Appenninico-Maghrebide. Memorie della Società Geologica Italiana 17, 1-60.

Amoruso, A., Crescentini, L., and Scarpa R., 2002. Source parameters of the 1908 Messina Straits, Italy, earthquake from geodetic and seismic data. Journal of Geophysical Research: Solid Earth 107, B4. doi: 10.1029/2001JB000434.

569 Anzidei, M., Antonioli, F., Benini, A., Gervasi, A., and Guerra, I., 2012. Evidence of vertical
570 tectonic uplift at Briatico (Calabria, Italy) inferred from Roman age maritime archaeological
571 indicatore. Quaternary International, doi: 10.1016/j.quaint.2012.01.019.
572 Argnani, A., and Trincardi, F., 1988. Paola slope basin: evidence of regional contraction on the
573 eastern Tyrrhenian margin. Memorie della Società Geologica Italiana 44, 93-105.
574 Argnani, A., and Trincardi, F, 1993. Growth of a slope ridge and its control on sedimentation: Paola
575 slope basin (eastern Tyrrenian margin). Special Publications International Association of
576 Sedimentology 20, 467-480.
577 Baratta, M., 1906. Il grande terremoto calabro dell'8 settembre 1905. Atti della Societa Toscana di
578 Scienze Naturali, Memorie, 22.
579 Barone, M., Dominici, R., Muto, F., Critelli, S., 2008. Detrital modes in a Late Miocene wedge-top
580 basin, northeastern Calabria, Italy: compositional record of wedge-top partitioning. Journal of
581 Sedimentary Research 78, 693–711.
582 Basili, R., Valensise, G., Vannoli, P., Burrato, P., Fracassi, U., Mariano, S. and Tiberti, M.M., 2008.
583 The Database of Individual Seismogenic Sources (DISS), version 3: summarizing 20 years of
584 research on Italy's earthquake geology, Tectonophysics 453, 1/4, 20-43. doi:
585 10.1016/j.tecto.2007.04.014.
586 Bonardi, G., Cavazza, W., Perrone, V., and Rossi, S., 2001. Calabria-Peloritani Terrane and
587 Northern Ionian Sea. In: Martini L.P., Vai G.B. (Eds.), Anatomy of an Orogen: the Apennines
588 and adjacent Mediterranean Basins. Kluwer Academic Publication 287-306.
589 Bordoni, P., and G. Valensise, 1998. Deformation of the 125 ka marine terrace in Italy: tectonic
590 implications. In: I. Stewart e C. Vita Finzi (eds.), Late Quaternary coastal tectonics,
591 Geological Society Special Publications 146, 71-110.
592 Boschi, E., Guidoboni, E., Ferrari, G., Mariotti, D., Valensise, G., Gasperini, P. (Eds.), 2000.
593 Catalogue of strong Italian earthquakes from 461 B.C. to 1997. Annali di Geofisica 43, with
594 CD-Rom, 259 p.

595 Burrato, P., and Valensise, G. 2008. Rise and fall of a hypothesized seismic gap: source complexity
596 in the Mw 7.0 16 December 1857 Southern Italy earthquake. Bulletin of the Seismological
597 Society of America 98, 1, 139-148. doi: 10.1785/0120070094.
598 Calò, M., Dorbath, C., Luzio, D., Rotolo, S.G., and D'Anna, G., 2012. Seismic velocity structures
599 of southern Italy from tomographic imaging of the Ionian slab and petrological inferences.
600 Geophysical Journal International, doi: 10.1111/j.1365-246X.2012.05647.x.
601 Camassi, R., and Stucchi, M., 1997. NT4.1.1, un catalogo prametrico di terremoti di area italiana al
602 di sopra della soglia del danno – Gr. Naz. Difesa dai Terremoti, Rapp. Interno, Milano, 95 pp.
603 Castello, B., Selvaggi, G., Chiarabba, C., and Amato, A., 2006. CSI Catalogo della sismicità
604 italiana 1981-2002, versione 1.1, INGV-CNT, Roma, http://csi.rm.ingv.it/.
605 Catalano, S., G. De Guidi, C. Monaco, G. Tortorici, and L. Tortorici, 2003. Long-term behavior of
606 the late Quaternary normal faults in the Straits of Messina area (Calabrian arc): structural and
607 morphological constraints. Quaternary International 101-102, 81-91.
608 Catalano, R., and Sulli, A., 2006. Crustal image of the Ionian basin and accretionary wedge.
609 Bollettino di Geofisica Teorica eApplicata 47, 3, 343-374.
610 Cibic, T., Acquavita, A., Aleffi, F., Bettoso, N., Blasutto, O., De Vittor, C., Falconi, C., Falomo, J.,
611 Faresi, L., Predonzani, S., Tamberlich, F., Fonda Umani, S., 2008. Integrated approach to
612 sediment pollution: A case study in the Gulf of Trieste. Marine Pollution Bulletin 56, 1650-
613 1667.
614 Cifelli, F., Mattei, M., and Rossetti, F., 2007. Tectonic evolution of arcuate mountain belts on top of
615 a retreating subduction slab: The example of the Calabrian Arc. Journal of Geophysical
616 Research 112, B09101, doi: 10.1029/2006JB004848.
617 Cucci, L., and Tertulliani, A., 2006. I terrazzi marini nell'area di Capo Vaticano (arco calabro): solo
618 un record di sollevamento regionale o anche di deformazione cosismica? Il Quaternario 19,
619 89-101.

620 Cucci, L., and Tertulliani, A., 2010. The Capo Vaticano (Calabria) coastal terraces and the 1905 M7
621 earthquake: the geomorphological segnature of the regional uplift and coseismic slip in
622 southern Italy. Terra Nova 22, 5, 378-389. doi: 10.1111/j.1365-3121.2010.00961.x.
623 D'Agostino, N., D'Anastasio, E., Gervasi, A., Guerra, I., Nedimović, M.R., Seeber, L., and Steckler,
624 M., 2011. Forearc extension and slow rollback of the Calabrian Arc from GPS measurements.
625 Geophysical Research Letters 38, L17304, doi: 10.1029/2011GL048270
626 D'Agostino, N., and Selvaggi, G., 2004. Crustal motion along the Eurasia-Nubia plate boundary in
627 the Calabrian Arc and Sicily and active extension in the Messina Straits from GPS
628 measurements. Journal of Geophysical Research 109, B11402, doi:10.1029/2004JB002998.
629 Danovaro, R., Company, J.B., Corinaldesi, C., D'Onghia, G., Galil, B., Gambi, C., Gooday, A.J.,
630 Lampadariou, N., Luna, G.M., Morigi, C., Olu, K., Polymenakou, P., Ramirez-Llodra, E.,
631 Sabbatini, A., Sardà, F., Sibuet, M., Tselepides, A., 2010. Deep-sea biodiversity in the
632 Mediterranean Sea: the known, the unknown, and the unknowable. PLoS ONE 5, 8, e11832:
633 1-25. doi: 10.1371/journal.pone.0011832.
634 Danovaro, R., Marrale, D., Della Croce, N., Dell'Anno, A., Fabiano, M., 1998. Heterotrophic
635 nanoflagellates, bacteria and labile organic compounds in continental shelf and deep-sea
636 sediments of the eastern Mediterranean. Microbial Ecology 35 (3-4), 244-255.
637 De Brouwer, J.F., and Stal, L.J., 2001. Short-term dynamics in microphytobenthos distribution and
638 associated extrecelluler carbohydrates in surface sediments of an intertidal mudflat. Marine
639 Ecology Progress Series 218, 33-44.
640 Del Ben, A., Barnaba, C., Taboga, A., 2008. Strike-slip systems as the main tectonic features in the
641 Plio-Quaternary kinematics of the Calabrian Arc. Marine Geophysical Research 29, 1–12, doi:
642 10.1007/s11001-007-9041-6.
643 Devoti, R., Esposito, A., Pietrantonio, G., Pisani, A.R., Riguzzi, F., 2011. Evidence of large scale
644 deformation patterns from GPS data in the Italian subduction boundary. Earth and Planetary
645 Science Letters 311 (3–4), 230-241, doi: 10.1016/j.epsl.2011.09.034.

646 DISS Working Group, 2010. Database of Individual Seismogenic Sources (DISS), Version 3.1.1: A
647 compilation of potential sources for earthquakes larger than M 5.5 in Italy and surrounding
648 areas. http://diss.rm.ingv.it/diss/, © INGV 2010 - Istituto Nazionale di Geofisica e
649 Vulcanologia - All rights reserved.
650 Ferranti, L., Monaco, C., Antonioli, F., Maschio, L., Kershaw, S. and Verrubbi, V., 2007. The
651 contribution of regional uplift and coseismic slip to the vertical crustal motion in the Messina
652 Straits, southern Italy: evidence from raised Late Holocene shorelines. Journal of Geophysical
653 Research 112, B06401, doi: 10.1029/2006JB004473.
654 Fracassi, U., Di Bucci, D., Ridente, D., Trincardi, F., and Valensise, G., 2012. Recasting Historical
655 Earthquakes in Coastal Areas (Gargano Promontory, Italy): Insights From Marine
656 Paleoseismology, Bulletin of the Seismological Society of America 102, 1, 1-17. doi:
657 10.1785/0120110001.
658 Gasparini, C., Iannacone, G., Scandone, P., and Scarpa, R., 1982. Seismotectonics of the Calabrian
659 Arc. Tectonophysics 82, 267–286.
660 Gruppo di Lavoro CPTI, 2004. Catalogo Parametrico dei Terremoti Italiani, versione 2004
661 (CPTI04). INGV, Bologna, http://emidius.mi.ingv.it/CPTI/.
662 Guidoboni, E., and J. E. Ebel, 2009. Earthquakes and Tsunamis in the Past. Cambridge Univ. Press,
663 Cambridge, 590 p.
664 Guidoboni, E., Ferrari, G., Mariotti, D., Comastri, A., Tarabusi, G., and Valensise, G., 2007.
665 CFTI4Med, Catalogue of Strong Earthquakes in Italy (461 B.C.-1997) and Mediterranean
666 Area (760 B.C.-1500). INGV-SGA. Available from http://storing.ingv.it/cfti4med/.
667 Kanamori, H., and Anderson, D.L., 1975. Theoretical basis of some empirical relations in
668 seismology. Bulletin of the Seismological Society of America 65, 5, 1073-1095.
669 Knott, S.D., and E. Turco, 1991. Late Cenozoic kinematics of the Calabrian arc, southern Italy,
670 Tectonics 10 (6), 1164-1172.

671 Loreto, M.F., Zgur, F., Facchin, L., Fracassi, U., Pettenati, F., Tomini, I., Burca, M., Diviacco, P.,
672 Sauli, C., Cossarini, G., De Vittor, C., Sandron, D., and the Explora technicians team, 2012. In
673 Search of New Imaging For Historical Earthquakes: A New Geophysical Survey Offshore
674 Western Calabria (Southern Tyrrhenian Sea, Italy), Bollettino di Geofisica Teoreorica e
675 Applicata 53. doi: 10.4430/bgta0046.
676 Lunau, M., Lemke, A., Walther, K., Martens-Habbena, W., Simon, M., 2005. An improved method
677 for counting bacteria from sediments and turbid environments by epifluorescence microscopy.
678 Environmental Microbiology 7, 7, 961-968.
679 Malinverno, A., and Ryan, W.B.F., 1986. Extension in the Tyrrhenian Sea and shortening in the
680 Apennines as result of arc migration driven by sinking of the lithosphere. Tectonics 5, 227-
681 245.
682 Martini, M., and Scarpa, R., 1982. Italian earthquakes since 1900. Proc. E. Fermi Summer School in
683 Geophysics, Varenna, Springer-Verlag.
684 Mattei, M., F. Cifelli, and N. D'Agostino, 2007. The evolution of the Calabria Arc: Evidence from
685 paleomagnetic and GPS observations, Earth and Planetary Science Letters 263, 259–274. doi:
686 10.1016/j.epsl.2007.08.034.
687 Michelini, A., Lomax A., Nardi A., and Rossi A., 2006. La localizzazione del terremoto della
688 Calabria dell'8 settembre 1905 da dati strumentali. In: Guerra I. and Savaglio A. (eds.), "8
689 settembre 1905, terremoto in Calabria", Università della Calabria, 225-240.
690 Milia, A., Turco, E., Pierantoni, P.P., and Schettino, A., 2009. Four-dimensional tectono-
691 stratigraphic evolution of the Southern peri-Tyrrhenian Basins (Margin of Calabria, Italy).
692 Tectonophysics 476, 41-56. doi: 10.1016/j.tecto.2009.02.030
693 Monaco, C., and Tortorici, L., 2000. Active faulting in the Calabrian arc and eastern Sicily. Journal
694 of Geodynamics 29, 407-424.
695 Mulargia, F., Balsi, P., Achilli, V., Broccio, F., 1984. Recent crustal deformaitons and tectonics of
696 the Messina Strait area. Geophysical Journal International 76, 369-386.

National Geophysical Data Center / World Data Center (NGDC/WDC), 2012. Global Historical Tsunami Database, Boulder, CO, USA, available at http://www.ngdc.noaa.gov/hazard/tsu_db.shtml

Nieuwenhuize, J., Maas, Y.E.M., Middelburg, J.J., 1994. Rapid analysis of organic carbon and nitrogen in particulate materials. Marine Chemistry 45, 217-224.

Pantosti, D., and Valensise, G., 1990. Faulting mechanism and complexity of the 23 November, 1980, Campania-Lucania earthquake inferred form surface observations. Journal of Geophysical Research 95, B10, 15319-15341.

Patacca, F., Sartori, R., Scandone, P., 1990. Tyrrhenian basin and Apenninic arcs: kinematic relations since Late Tortonian times. Memorie Società Geologica Italiana 45, 425–451.

Patacca, F., Sartori, R., Scandone, P., 1993. Tyrrhenian basin and Apennines. Kinematic evolution and related dynamic constraints. In: Boschi, E., Mantovani, E., Morelli, A. (Eds.), Recent Evolution and Seismicity of the Mediterranean Region. Kluwer Academic Publishers, Dordrecht, Netherlands, pp. 161–171.

Patacca, E., Scandone, P., 2004. The Plio-Pleistocene thrust belt – foredeep system in the Southern Apennines and Sicily (Italy). In: Crescenti, U., D'Offizi, S., Merlini, S., Lacchi, L. (Eds.), Geology of Italy. Soc. Geol. It., Roma, 93-129.

Pella, E. and Colombo, B., 1973. Study of carbon, hydrogen and nitrogen determination by combustion-gas chromatography. Microchimica Acta 5, 697-719.

Pepe, F., Sulli, A., Bertotti, G., and Cella, F., 2010. Architecture and Neogene to Recent evolution of the western Calabrian continental margin: An upper plate perspective to the Ionian subduction system, central Mediterranean. Tectonics 29, TC3007. doi: 10.1029/2009TC002599.

Peruzza, L., Pantosti, D., Slejko, D., Valensise, G., 1997. Testing a new hybrid approach to seismic hazard assessment: an application to the Calabrian Arc (Southern Italy). Naturala Hazards 14, 113-126.

723 Piatanesi, A., and Tinti, S., 2002. Numerical modelling of the September 8, 1905 Calabrian
724 (southern Italy) tsunami. Geophysical. Journal International 150, 271-284. doi:
725 10.1046/j.1365-246X.2002.01700.x.
726 Pino, N.A., Piatanesi A., Valensise G., and Boschi E., 2009. The 28 December 1908 Messina
727 Straits Earthquake (Mw 7.1): A Great Earthquake throughout a Century of Seismology.
728 Seismological Research Letters 80, 2, 243-259. doi: 10.1785/gssrl.80.2.243.
729 Pizzino, L., Burrato, P., Quattrocchi, F., and Valensise, G., 2004. Geochemical signatures of large
730 active faults: the example of the 5 February 1783, Calabrian earthquake (southern Italy).
731 Journal of Seismology 8, 3, 363-380. doi: 10.1023/B:JOSE.0000038455.56343.e7.
732 Postpischl, D., 1985. Catalogo dei terremoti italiani dall'anno 1000 al 1980. Consiglio Nazionale
733 delle Ricerche, Progetto Finalizzato Geodinamica, Graficoop, Bologna, 239 pp.
734 Ramsay, J.G., and Huber, M.I., 1987. The techniques of modern structural geology. Vol. 2: Folds
735 and Fractures, Academic Press, London, 700 p.
736 Ravenschlag, K., Sahm, K., Knoblauch, C., Jørgensen, B.B., and Amann, R., 2000. Community
737 structure, cellular rRNA content and activity of sulfate-reducing bacteria in marine arctic
738 sediments. Applied and Environmental Microbiology 66(8), 3592-3602.
739 Riuscetti, M., and Schick, R., 1975. Earthquakes and tectonics in Southern Italy. Bollettino di
740 Geofisica Teorica e Applicata 17, 59-78.
741 Rizzo, G.B., 1906. Sulla velocità di propagazione delle onde sismiche del terremoto della Calabria
742 del giorno 8 Settembre 1905. C. Clausen Ed., 46 pp.
743 Rotondi, R., 2010. Bayesian nonparametric inference for earthquake recurrence time distributions in
744 different tectonic regimes. Journal of Geophysical Research: Solid Earth 115, B01302. doi:
745 10.1029/2008JB006272.
746 Rovida, A., Camassi, R., Gasperini, P., Stucchi, M. (eds.), 2011. CPTI11, the 2011 version of the
747 Parametric Catalogue of Italian Earthquakes. Milano, Bologna, http://emidius.mi.ingv.it/CPTI.

748 Sartori, R., 2003. The Tyrrhenian back-arc basin and subduction of the Ionian lithospere. Episodes
749 26, 3, 217-221.
750 Sharp, J.H., 1974. Improved analysis for" particulate" organic carbon and nitrogen from seawater.
751 Limnology and Oceanography, 984-989.
752 Tansi, C., Muto, F., Critelli, S., and Iovine, G., 2007. Neogene-Quaternary strike-slip tectonics in
753 the central Calabrian Arc (southern Italy). Journal of Geodynamics 43 (3), 393-414.
754 Tinti, S., and Maramai, A., 1996. Catalogue of tsunamis generated in Italy and in Côte d'Azur,
755 France: a step towards a unified catalogue of tsunamis in Europe. Annali di Geofisica
756 XXXIX, 6, 1253-1299.
757 Tertulliani, A., and Cucci, L., 2008. Fenomeni associati al terremoto della Calabria del 1905.
758 Quaderni di Geosifica, ISSN 1590-2595, No. 60.
759 Tertulliani, A., and Cucci, L., 2009. Clues to the identification of a seismogenic source from
760 environmental effects: the case of the 1905 Calabria (Southern Italy) earthquake. Natural
761 Hazards Earth System Sci., 9, 1787-1803, doi: 10.5194/nhess-9-1787-2009.
762 Tiberti, M.M., Fracassi, U., and Valensise, G., 2006. Il quadro sismotettonico del grande terremoto
763 del 1905, in: Guerra I. and Savaglio A. (eds.), "8 Settembre 1905: Terremoto in Calabria",
764 Università della Calabria, 181-205.
765 Trincardi, F., Corregiari, A., Field, M.E., and Normark, W.R., 1995. Turbidite deposition from
766 multiple sources: Quaternary Paola Basin (eastern Tyrrenian Sea). Journal of Sedimentary
767 Research 65, 469-483.
768 Valensise, G., 1988. Low angle normal faulting during the 1908, Messina, earthquake revealed by
769 geodetic data analysis (abstract), Eos Trans., AGU, 69(44), F1433, Fall Meet. Suppl.
770 Valensise, G., and D. Pantosti, 2001a. Seismogenic faulting, moment release patterns and seismic
771 hazard along the central and southern Apennines and the Calabrian arc. In: G. B. Vai and I. P.
772 Martini (Eds.), Anatomy of an orogen: the Apennines and adjacent Mediterranean basins.
773 Kluwer Academic Publishers, Dordrecht, 2001, 495-512.

774 Valensise, G., and Pantosti, D., 2001b. The investigation of potential earthquake sources in
775 peninsular Italy: A review. Journal of Seismology 5, 3, 287-306, doi:
776 10.1023/A:1011463223440.
777 van Dijk, J.P., 1991. Basin dynamics and sequence stratigraphy in the Calabrian Arc Central
778 Mediterranean); records and pathways of the Crotone Basin. Geologie en Mijnbouw 70, 187-
779 201.
780 van Dijk, J.P., 1992. Late Neogene Fore-arc Basin Evolution in the Calabrian Arc (Central
781 Mediterranean); Tectonic Sequence Stratigraphy and Dynamic Geohistory. With Special
782 Reference to the Geology of Central Calabria. Geologica Ultraiectina 92, 288 pp.
783 van Dijk, J.P., Bello, M., Brancaleoni, G.P., Cantarella, G., Costa, V., Frixa, A., Golfetto, F.,
784 Merlini, S., Riva, M., Toricelli, S., Toscano, C., and Zerilli, A., 2000. A new structural model
785 for the northern sector of the Calabrian Arc. Tectonophysics 324, 267-320.
786 Vannucci, G., and Gasperini, G., 2004. The new release of the Database of Earthquake Mechanisms
787 of the Mediterranean Area (EMMA version 2). Annals of Geophysics 47, 1, with CD-Rom.
788 VIDEPI, 2012. Visibilità dei dati afferenti all'attività di esplorazione petrolifera in Italia. © 2009-
789 2012, Progetto ViDEPI - Ministero dello Sviluppo Economico UNMIG - Società Geologica
790 Italiana - Assomineraria, http://www.videpi.com.
791 Walsh, J.J., and Watterson, J., 1988. Analysis of the relationship between displacements and
792 dimensions of faults. Journal of Structural Geology 10, 3, 239-247.
793 Ward, S.N., and Valensise, G., 1989. Fault parameters and slip distribution of the 1915, Avezzano,
794 Italy earthquake derived from geodetic observations. Bulletin of the Seismological Society of
795 America 79, 690-710.
796 Wells, D., and Coppersmith, K., 1994. New empirical relationship among magnitude, rupture
797 length, rupture width, rupture area and surface displacement. Bullettin of Seismological
798 Society of America 84, 974-1002.

799 Westaway, R., 1992. Seismic moment summation for historical earthquakes in Italy: tectonic
800 implications. Journal of Geophysical Research 97, 15.437-15.464
801 Westaway, R., 1993. Quaternary uplift of Southern Italy. Journal of Geophysical Research 98, B12,
802 741-772.

Figure 1

Click here to download high resolution image

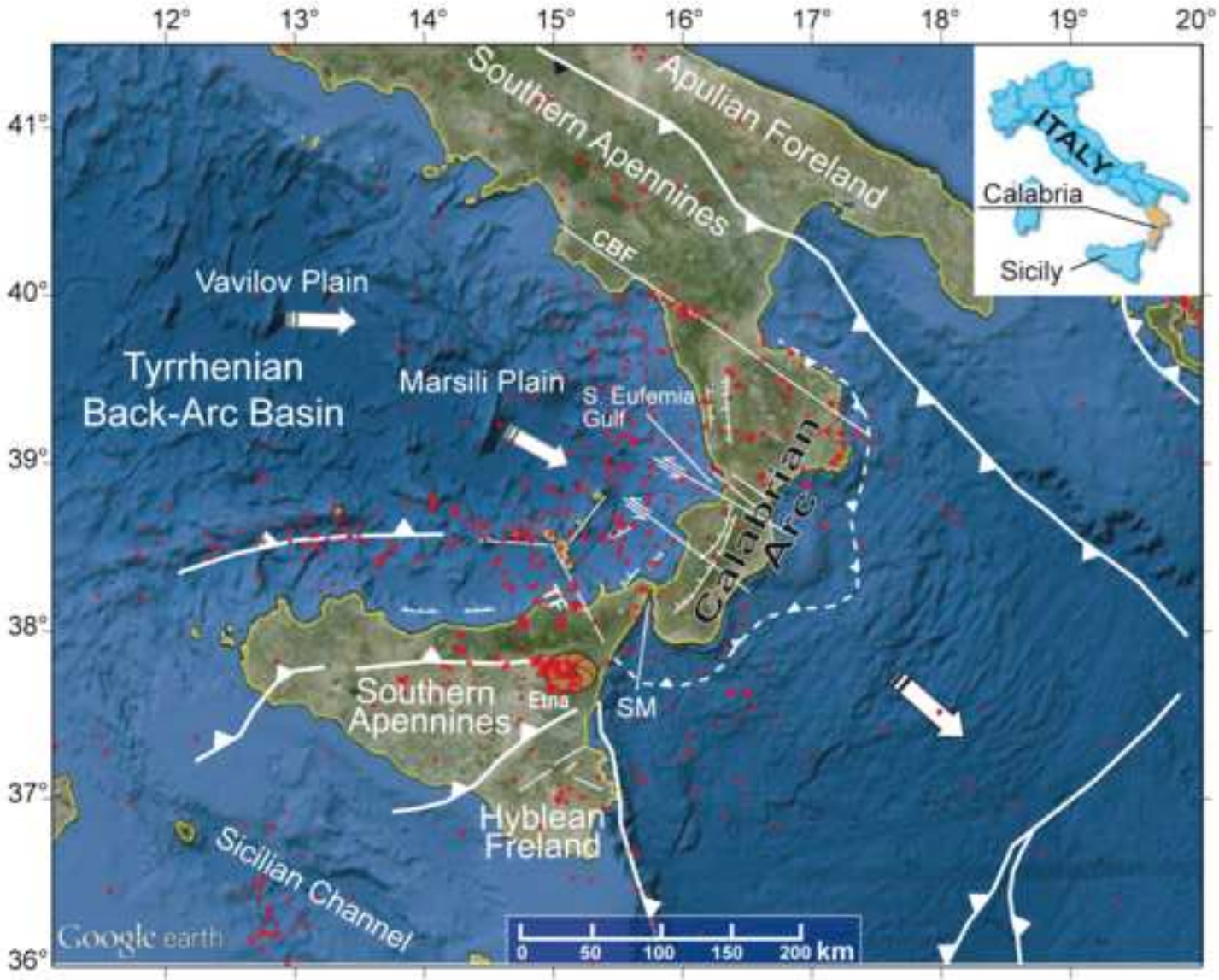

Figure 2

Click here to download high resolution image

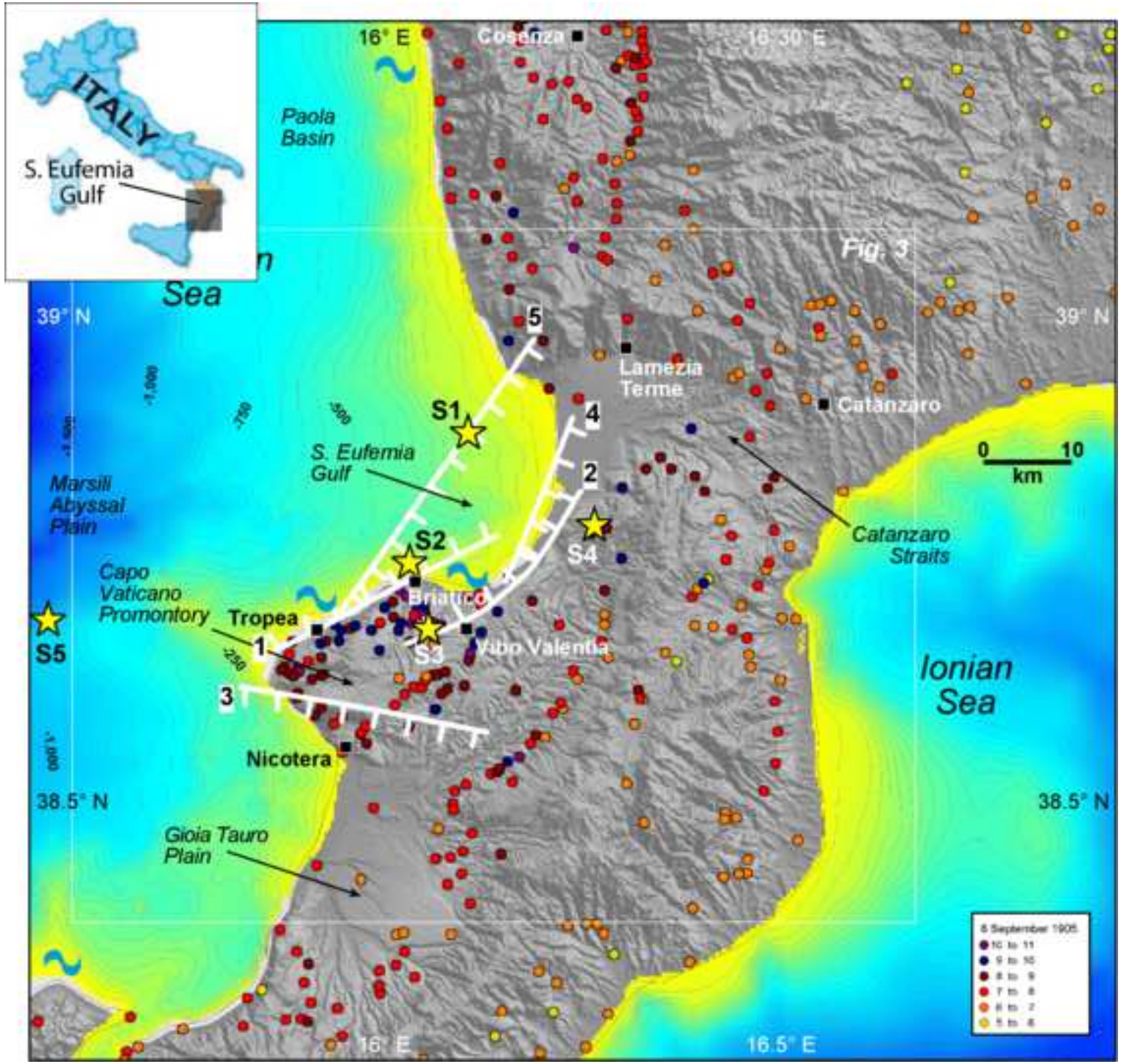

Figure 3 format TIFF

Click here to download high resolution image

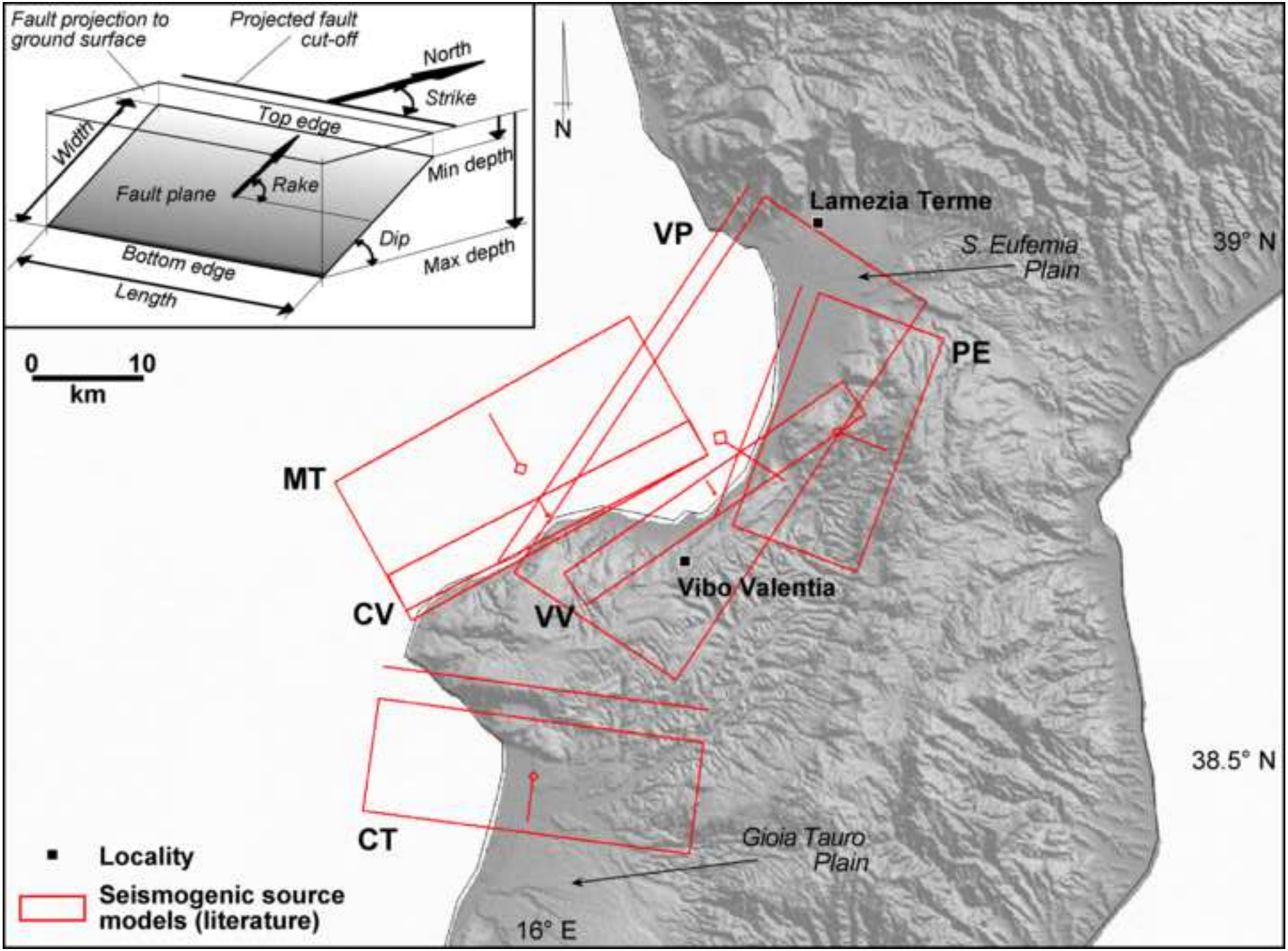

Figure 4 TIFF format
Click here to download high resolution image

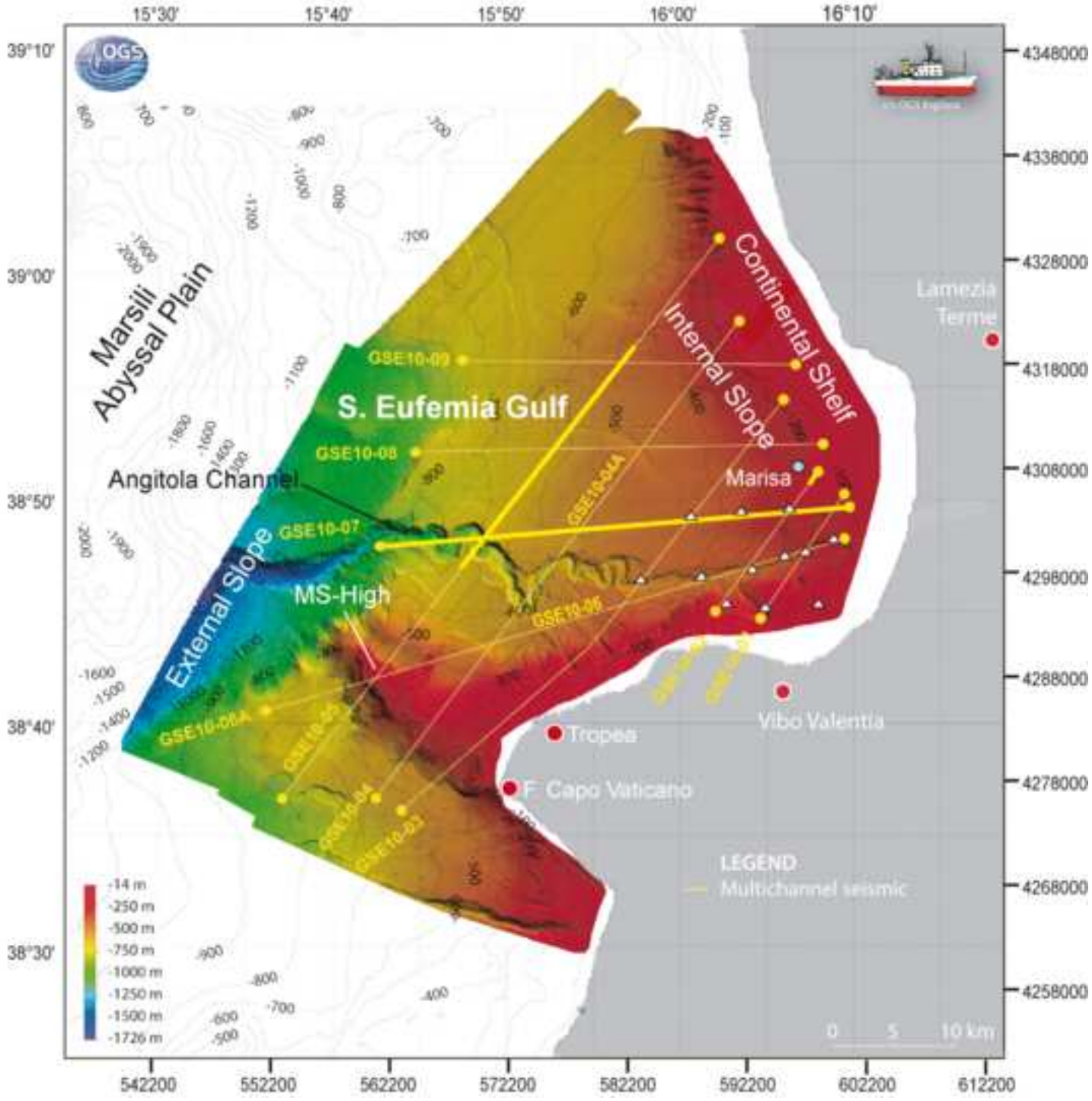

Figure 5 TIFF format
Click here to download high resolution image

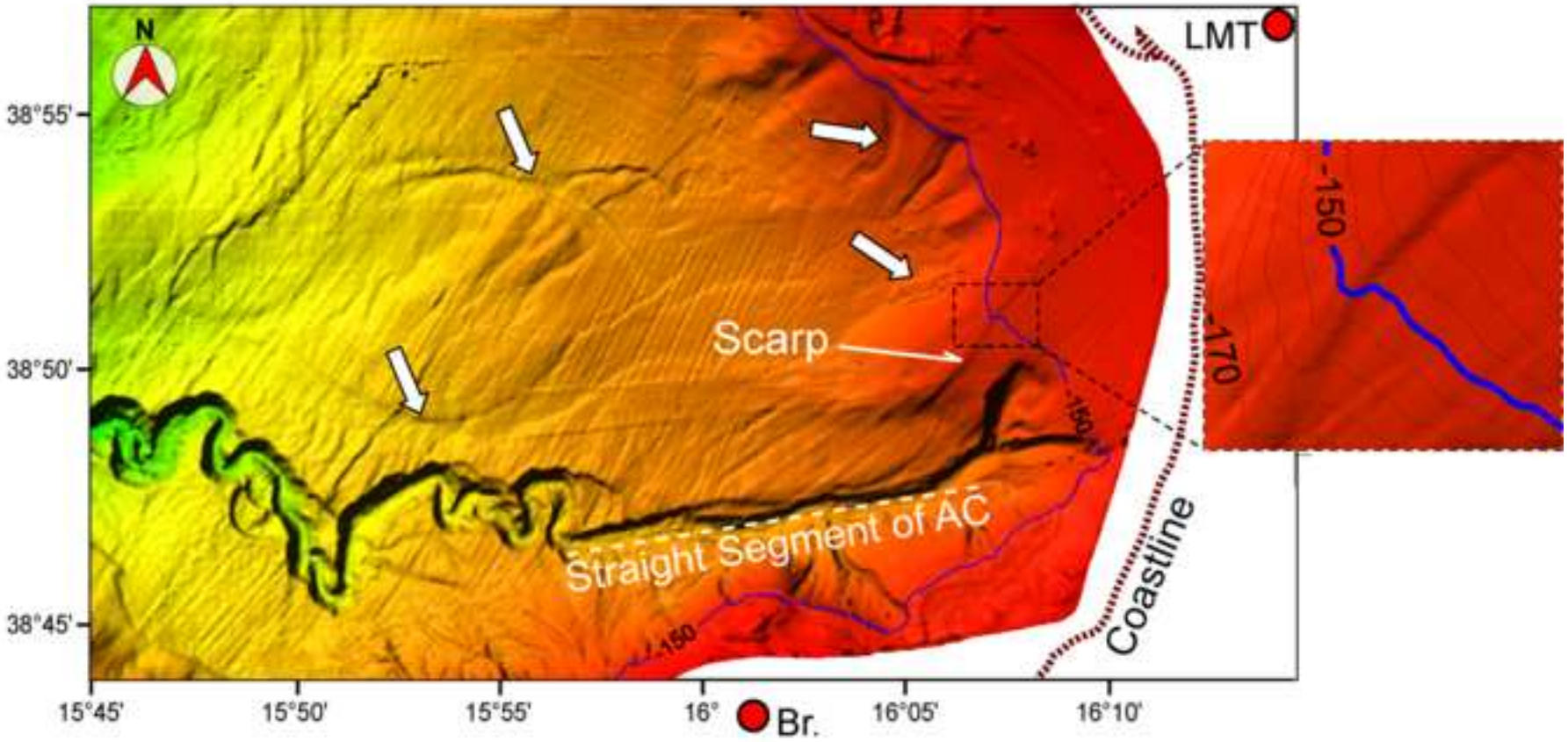

Figure 6 TIFF format

Click here to download high resolution image

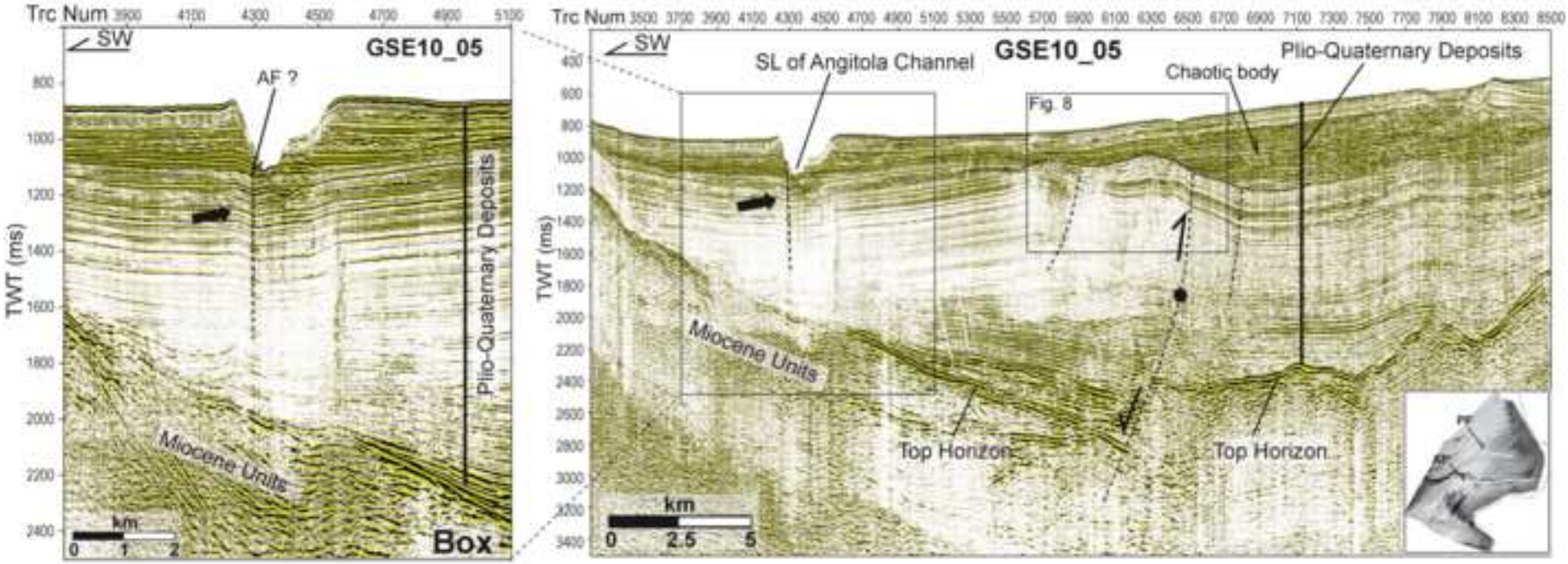

Figure 7 TIFF format
Click here to download high resolution image

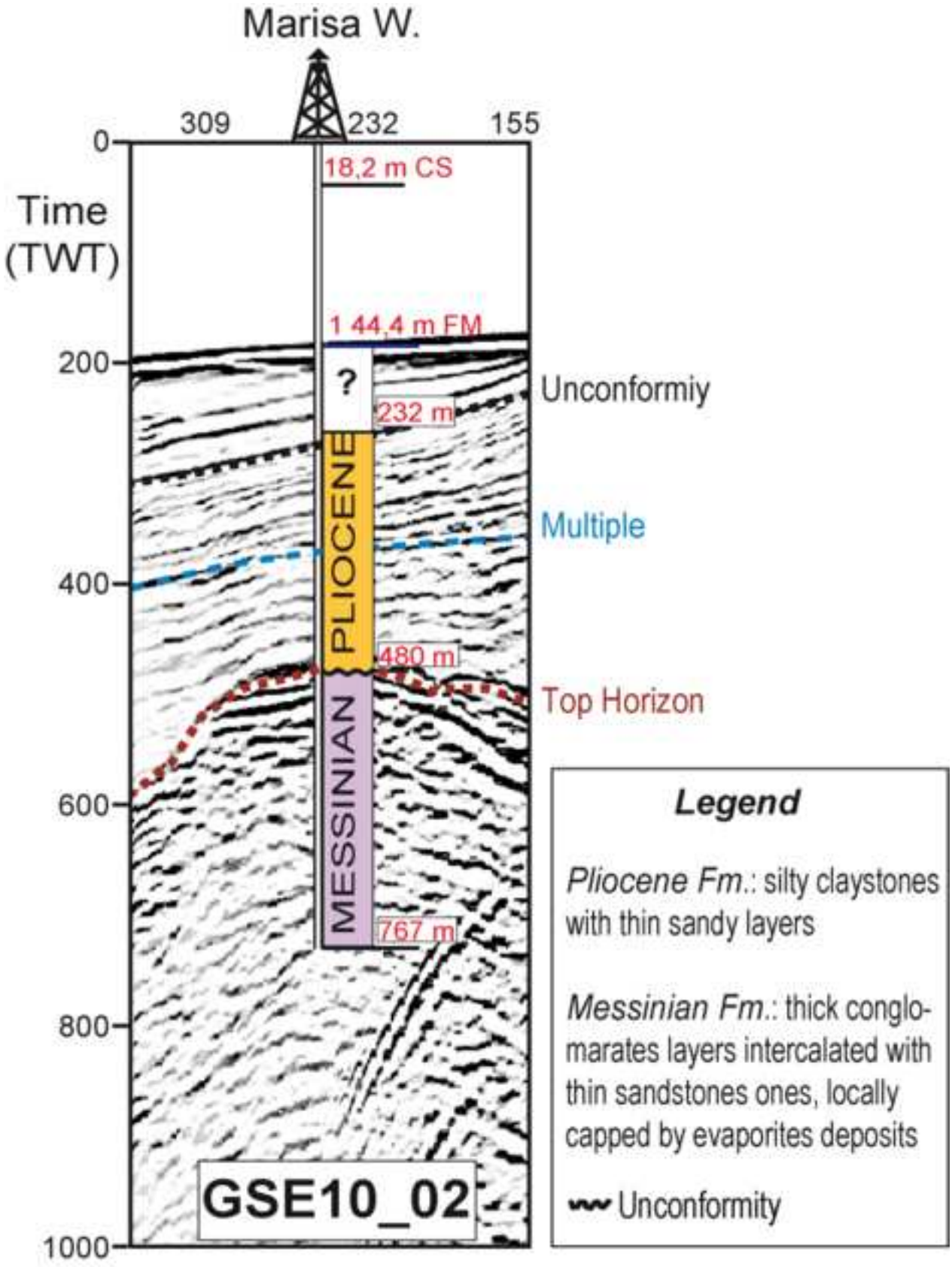

Figure 8 TIFF format

Click here to download high resolution image

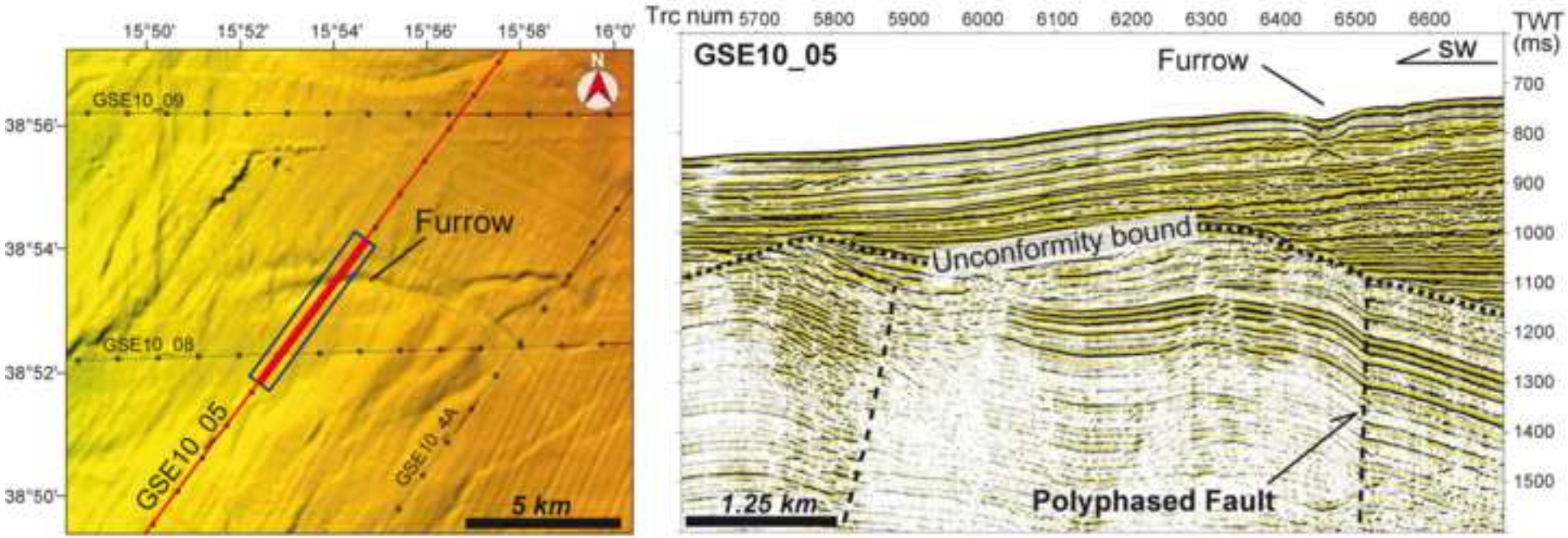

Figure 9 TIFF format

Click here to download high resolution image

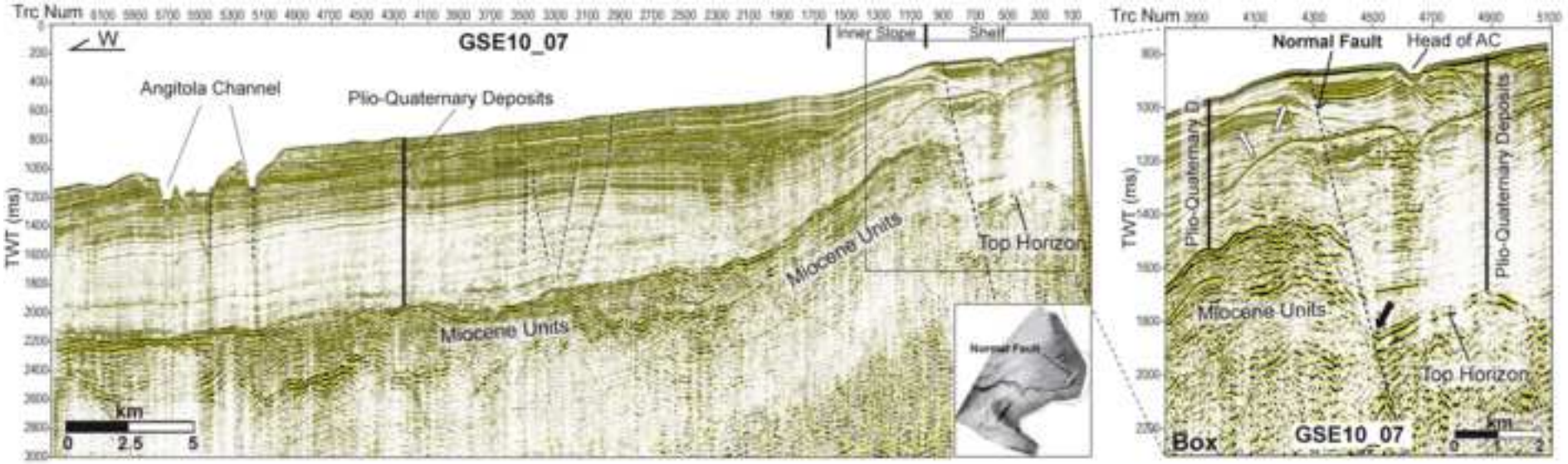

Figure 10 TIFF format

Click here to download high resolution image

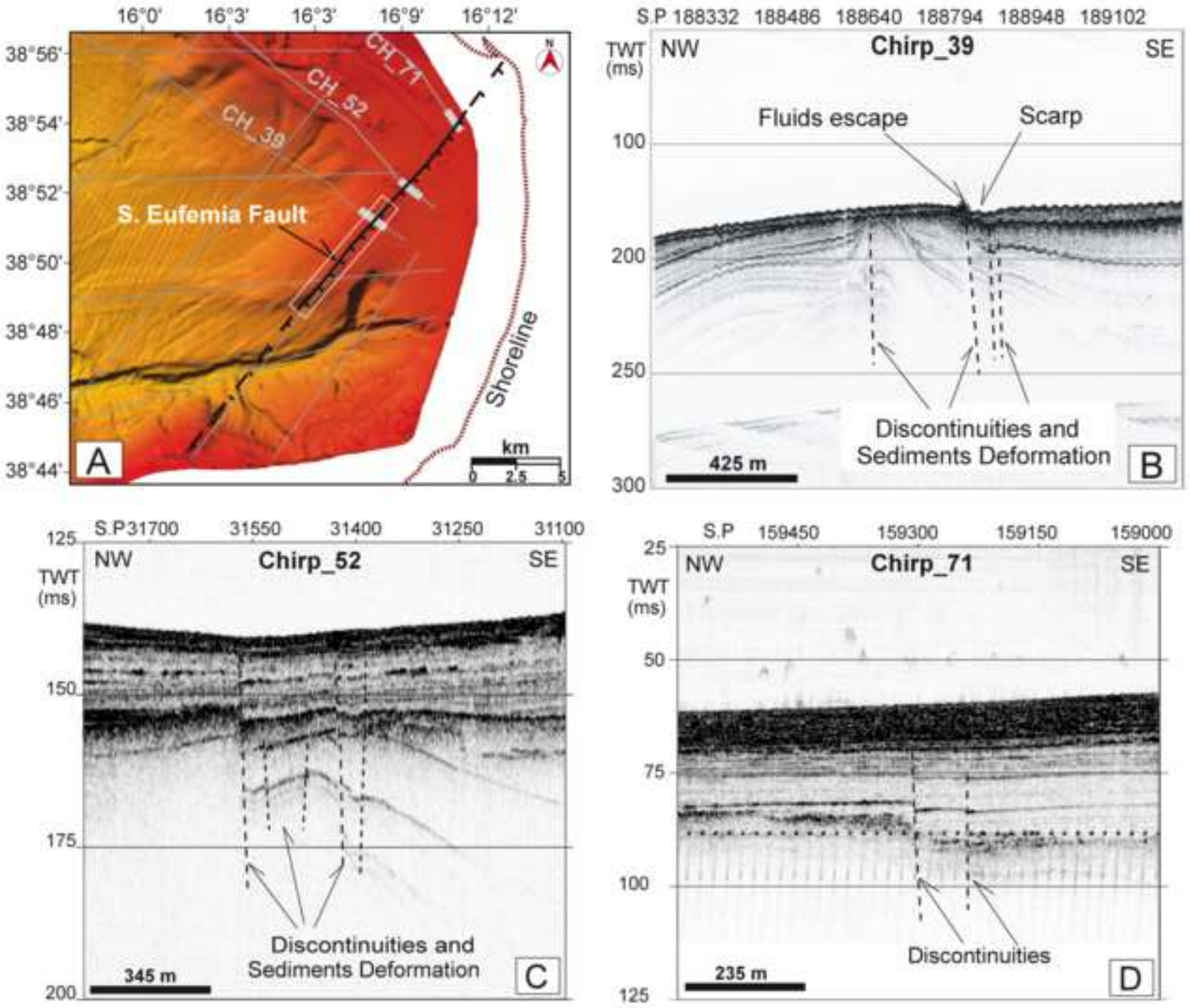

Figure 11 TIFF format
Click here to download high resolution image

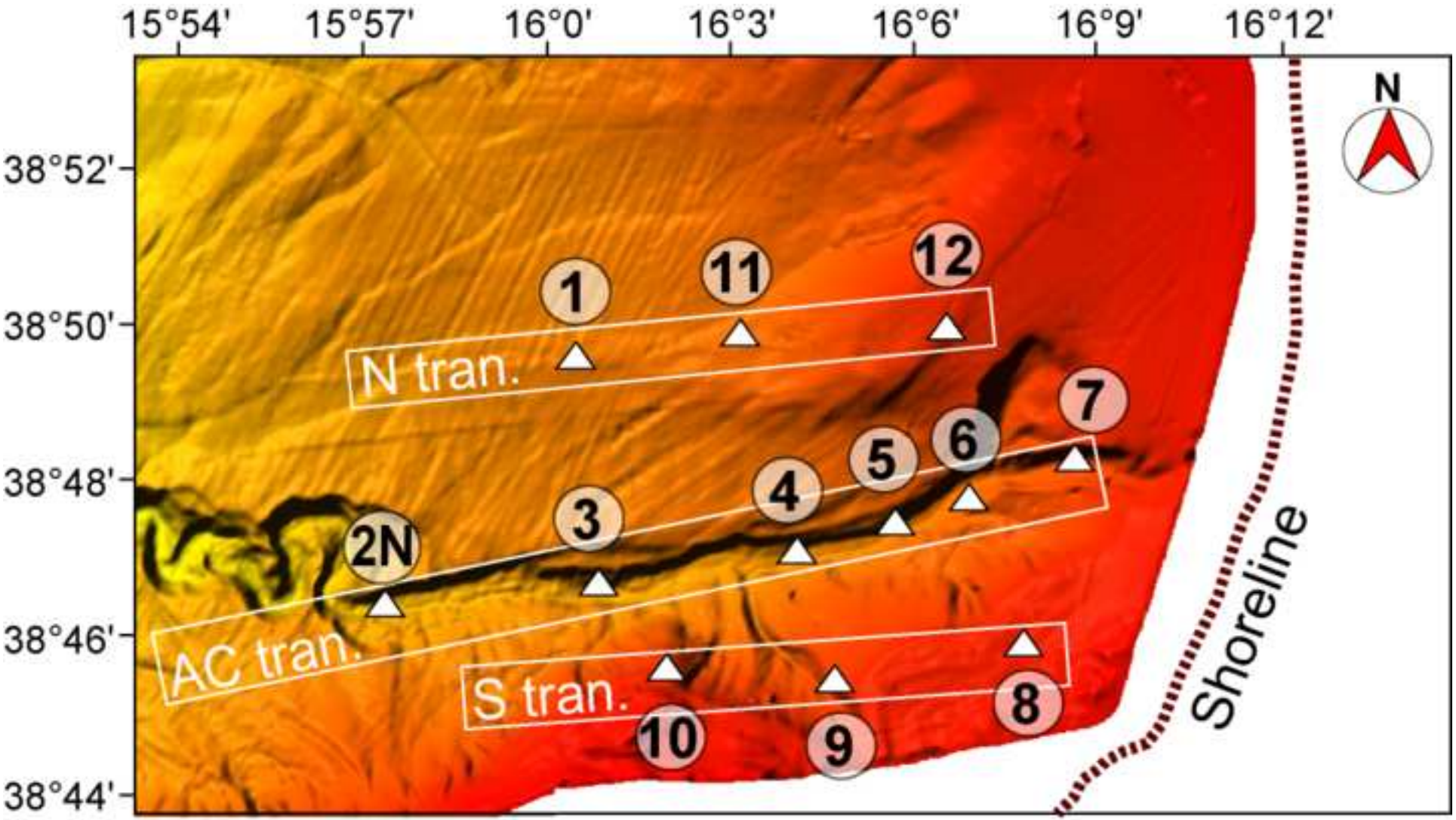

Figure 12 TIFF format
Click here to download high resolution image

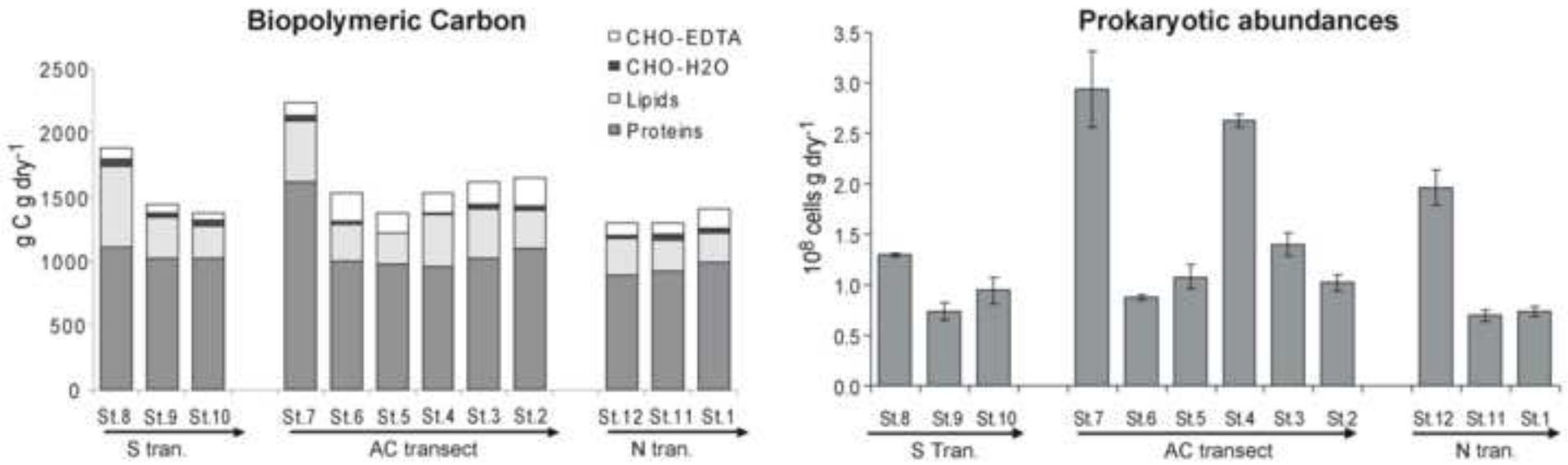

Figure 13 TIFF format

Click here to download high resolution image

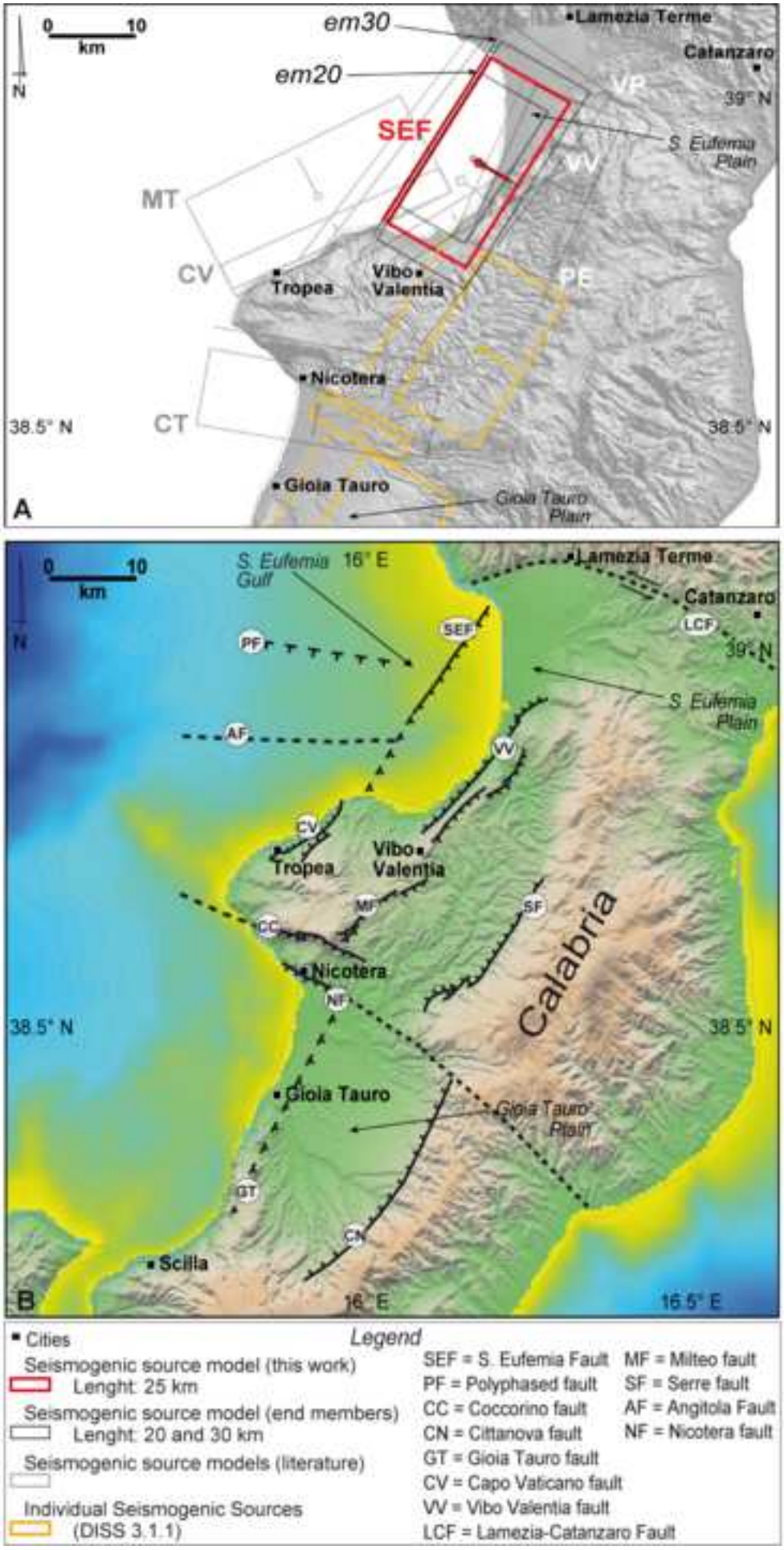

Table 1 format TIFF

Click here to download high resolution image

ID	Strike	Dip	Rake	L (km)	W (km)	TD (km)	BD (km)	SI (m)	M_w (W&C)	M_w (K&A)	M_0 (Nm)
PE	23	30	270	22	13.5	1	7.8	1	6.5	6.6	8,91E+18
VP	36	30	270	40	19.8	1	10.9	2	6.9	7.1	4,75E+19
MT	243	30	270	30	16.2	0	8.1	1.5	6.7	6.8	2,19E+19
CV	245	80	270	30	20	0	19.7	2.5	6.8	7.0	4,50E+19
VV	238	80	270	30	20	0	19.7	2.5	6.8	7.0	4,50E+19
CT	100	60	270	29	20	5	22.3	0.84	6.7	6.7	1,46E+19

Table 2 TIFF format

Click here to download high resolution image

ID	Strike	Dip	Rake	L (km)	W (km)	TD (km)	BD (km)	SI (m)	M_w (W&C)	M_w (K&A)	M_0 (Nm)
em20	31	38	270	20	12.2	0.5	8	1.5	6.4	6.6	1.10E+19
em30	31	38	270	30	16.2	0.5	10.5	2.5	6.7	7	3.65E+19
SEF	31	38	270	25	14.4	0.5	11.2	2	6.5	6.8	2,16E+19

Table 3 TIFF format

Click here to download high resolution image

St.	TN mg N g^{-1}	TC mg C g^{-1}	TOC mg C g^{-1}	Proteins µg C g_{dry}^{-1}	Lipids µg C g_{dry}^{-1}	CHO-H_2O µg C g_{dry}^{-1}	CHO-EDTA µg C g_{dry}^{-1}	Picobenthos $*10^8$ cells g_{dry}^{-1}
8	0.89 ± 0.04	21.16 ± 0.08	8.20 ± 0.09	1112.83 ± 28.43	625.72 ± 78.20	54.90 ± 1.52	81.86 ± 5.22	1.30 ± 0.02
9	0.82 ± 0.02	20.96 ± 0.25	7.71 ± 0.02	1021.28 ± 32.19	320.83 ± 20.44	33.72 ± 1.17	66.85 ± 3.46	0.74 ± 0.08
10	0.66 ± 0.01	18.13 ± 0.18	6.55 ± 0.22	1026.82 ± 21.29	251.23 ± 15.47	43.42 ± 1.29	60.69 ± 5.75	0.95 ± 0.13
7	0.85 ± 0.01	20.40 ± 0.04	7.56 ± 0.04	1623.05 ± 24.91	467.62 ± 19.68	45.02 ± 1.29	101.66 ± 1.97	2.94 ± 0.38
6	0.74 ± 0.03	18.74 ± 0.06	6.80 ± 0.07	997.54 ± 49.35	289.27 ± 11.97	22.19 ± 1.31	214.42 ± 3.56	0.87 ± 0.02
5	0.68 ± 0.01	18.21 ± 0.04	6.84 ± 0.16	982.58 ± 11.32	228.88 ± 24.30	14.25 ± 1.26	146.53 ± 8.31	1.08 ± 0.12
4	0.83 ± 0.04	20.83 ± 0.14	7.24 ± 0.09	959.87 ± 4.58	403.76 ± 14.62	13.63 ± 1.46	144.48 ± 7.54	2.62 ± 0.06
3	0.73 ± 0.02	20.66 ± 0.08	6.66 ± 0.13	1024.25 ± 28.74	391.54 ± 7.87	25.83 ± 2.42	180.17 ± 6.01	1.40 ± 0.12
2N	0.77 ± 0.02	20.18 ± 0.07	6.78 ± 0.04	1094.89 ± 19.82	298.75 ± 7.86	35.12 ± 4.05	217.77 ± 12.13	1.02 ± 0.08
12	0.79 ± 0.01	19.91 ± 0.09	6.19 ± 0.12	887.88 ± 18.21	285.75 ± 20.10	28.27 ± 2.38	102.24 ± 1.42	1.96 ± 0.18
11	0.78 ± 0.04	19.32 ± 0.07	6.22 ± 0.03	919.75 ± 17.41	242.34 ± 3.67	46.03 ± 2.24	97.63 ± 2.36	0.70 ± 0.05
1	0.74 ± 0.01	19.58 ± 0.03	6.20 ± 0.06	992.99 ± 6.73	229.93 ± 13.48	23.75 ± 1.39	160.26 ± 11.72	0.73 ± 0.05

Values and standard deviation (SD) of the chemical and biological parameters. TN = Total Nitrogen; TC = Total Carbon; TOC = Total Organic Carbon; CHO-H_2O = colloidal carbohydrates; CHO-EDTA = carbohydrates extracted in EDTA.